ANALYSING MOVEMENT OF CENTROID OF CONVEYANCE OF A BRAIDED RIVER : AN ATTEMPT TO IDENTIFY THE CHANNEL MIGRATION OF THE BRAHMAPUTRA RIVER IN BANGLADESH

by:

SUHARYANTO

A Thesis

Submitted to the Faculty of Graduate Studies in Partial

Fulfillment of the Requirements for the Degree of

Master of Science

DEPARTMENT OF CIVIL ENGINEERING

UNIVERSITY OF MANITOBA

WINNIPEG, MANITOBA

ISBN 0-315-77725-7

Canada

ANALYZING MOVEMENT OF CENTROID OF CONVEYANCE OF A BRAIDED RIVER: AN ATTEMPT TO IDENTIFY THE CHANNEL MIGRATION OF THE BRAHMAPUTRA RIVER IN BANGLADESH

BY

SUHARYANTO

A Thesis submitted to the Faculty of Graduate Studies of the University of Manitoba in partial fulfillment of the requirements for the degree of

MASTER OF SCIENCE

Abstract

The objective of the study is to analyse the movement of the centroid of conveyance of the Brahmaputra River, which is a braided river, in an attempt to capture the general tendency of the river movement as a whole. For each river cross section, which is comprised of several sub-channels or braids, the velocity distribution is calculated using a finite element method of the Galerkin type. The distribution of the conveyance is obtained from this velocity distribution by applying Manning's equation. The centroid of the conveyance of the whole cross section is then calculated by applying the first moment of the distribution of conveyance about a pre-determined reference point (in this case the east bank). The method is designed to overcome problems of negative marginal conveyance encountered in monitoring cumulative conveyance across a cross section in earlier studies of channel migration of the Brahmaputra River. The analysis is performed on thirty three cross section locations with six to seven years of records for each location. During the period of study, the centroidal movement determined in this manner does not shows any general trend of migration of the Brahmaputra River, although there are an erratic sub-channel movements within the river belt.

ACKNOWLEDGEMENT

I would like to express my sincere gratitude to my advisor, Professor I. C. Goulter, for his valuable guidance, encouragement, and moral support throughout my study at the University of Manitoba and this thesis preparation.

I am proud to extend my thanks to Professor C. Booy, Professor L. P. Stene, and Professor B. Lence for their suggestions and comments.

I would also like to express my gratitude to Mr. O. Simbolon who provided the opportunity for the financial support from HEDP (Higher Education Development Project) Phase I.

I am specially indebted to Mr. Ansari Khan for providing me valuable data and helpful guidance. I would like also to express my sincere gratitude to Mr. Paul Jacobs for his valuable comments. Sincere thanks go to my fellow graduate students in water resources at the University of Manitoba for being my sincere friends and encouraging my work. I would also like to express my gratitude to all my colleagues in the Indonesia Student Group, their families and many others for their help and friendship.

My sincere thanks and deep appreciation goes to my mother, my brothers, and my sisters for their understanding throughout my studies.

Contents

List of Tables

List of Figures

Chapter 1

INTRODUCTION

The Brahmaputra River in Bangladesh has long attracted world wide attention because of its vastness and its destructive power. The river has an average width of 6 km, ranging in some locations up to 15 km wide. The river experiences yearly flooding during which water level is overtoping its flood plain and inundated the highly populated and intensely cultivated area along the river. River bank erosion is another serious problem of the river. The river bank erosion mostly occurs during the subsiding limb of the flood when flowage of subsurface water from the bank formations occurs. During this period and the low flow period after the flood, sediment load is deposited to form bars as the carrying capacity of the river decreases. The river seeks a steeper gradient by deepening into river bed to maintain its carrying capacity. It was observed that the location of the thalweg wanders back and forth in the river belt even during a single flood cycle (Coleman, 1969). The location of the river bank which is approached by this thalweg likely to have a very steep slope. As a result, this bank is susceptible to bank erosion.

This study attempts to identify a general trend of the river bank erosion and migration. Knowledge of trends in river bank erosion will assist the process of planning and development of the river floodplain. The trend of river bank erosion will be evaluated by analysing the movement of the

centroid of flow conveyance over time.

This study is organized in five chapters. The first chapter explains the characteristics of the Brahmaputra River. A literature reviews on researches related to the Brahmaputra River is presented in Chapter 2. Chapter 3 describes the methodology used in this study. Chapter 4 discusses the results of the study. In the last chapter, conclusions and recommendations are made.

1.1 General Description of the River.

The Brahmaputra River originates in the northernmost ranges of the Himalayas in Tibet. As shown in Figure 1.1, it traverses a distance of 2,897 km (1,800 miles) through China, India, and Bangladesh before it reaches the Bay of Bengal.

At its origin, the river is known as Tsangpo (the Purifier). Near Dadiya, where the main channel of the river, known as the Dihang, enters India, the river receives two major tributaries called Dibang and Lauhitya. The river then takes the name of Brahmaputra, the Son of the Creator. The river subsequently flows through the Assam valley of eastern India. From here it flows around the spurs of the Garo Hills near Goalpara of Assam to enter Bangladesh, and flows southward for 270 km through the Garo-Rajmahal gap before its confluence with the Ganges near Aricha.

The Brahmaputra River receives the major portion of its flow from the snowmelt of the Himalayas and other mountainous areas in the region during the spring season. Heavy rainfall in India and Bangladesh during the monsoon also contributes a large amount of discharge to the river. The river, which acts as the main drainage channel of the area, receives dis-

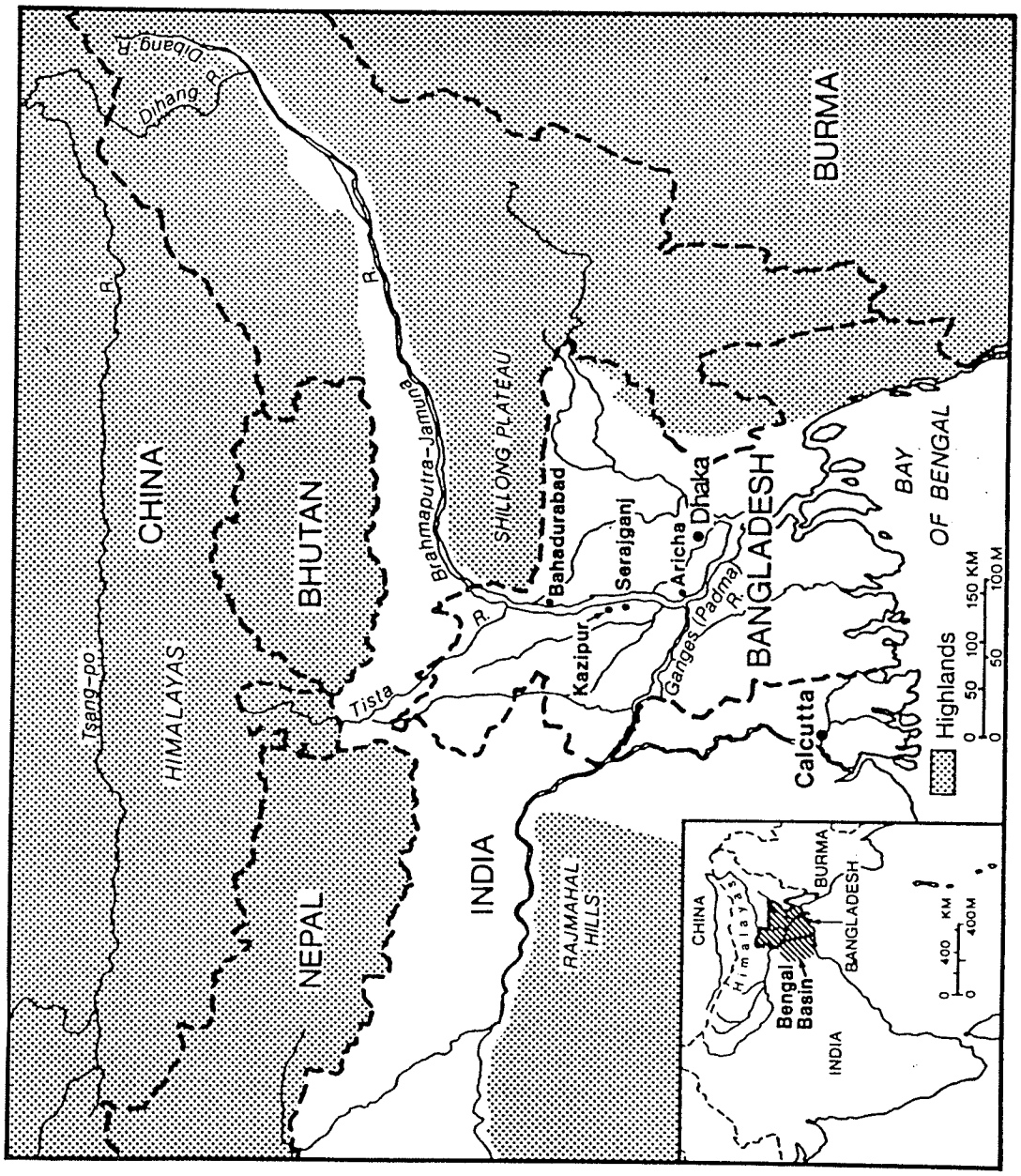

Figure 1.1: Location of the Brahmaputra River System. (after Chowdhury, 1988)

charges from numerous tributary channels. It also has a number of distributary channels. In 1830, one of its distributaries, which flowed southward, suddenly became the main channel. The old abandoned river course is now known as the Old Brahmaputra (see Figure 1.2). The name of the new main channel changes to Jamuna after its bifurcation with the Old Brahmaputra. In this study, Jamuna is used interchangeably with the name Brahmaputra to refer to the river reach extending between Chilmari in the north and Aricha in the south. The location of Chilmari and Aricha on the river are shown in Figure 1.2. This region is the section of the river used to demonstrate the approach proposed in this study.

1.2 Location of The Study

The river reaches of the Brahmaputra River examined in this study are all located within the country of Bangladesh, which is itself situated between latitude 20^0 35" N and 26^0 75" N and longitude 88^0 03" E and 92^0 75" E.

Bangladesh is a major portion of the Bengal Basin in which the Brahmaputra-Jamuna floodplain is located. The other part of the Bengal Basin lies within the Indian territory of West Bengal. In the north, the Bengal Basin is bordered by the Shillong Hills, or Assam Plateau, which rises to 1,372 m to 1,829 m above sea level. The peninsular shield of India, known as the Rajmahal Hills, with an elevation range between 152 m to 144 m above sea level, borders the Bengal Basin to the northwest and west. The Chittagong-Tripura hills, which reach 610 m above sea level, form the eastern boundary. The south boundary is open towards The Bay of Bengal

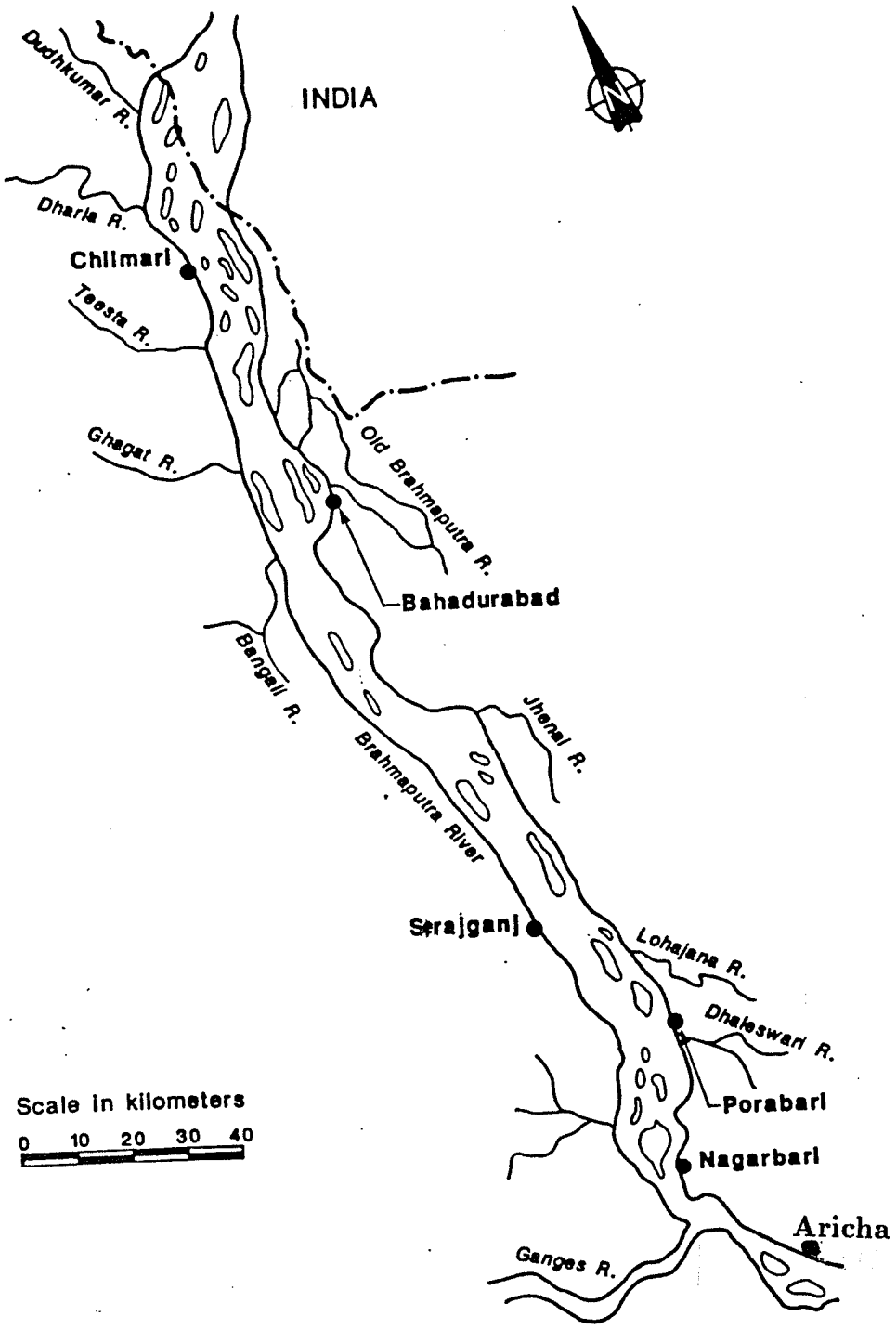

Figure 1.2: Detail of the River Reach under Investigation. (after Goulter and Dubois, 1988)

1.3 Characteristics of The Brahmaputra-Jamuna River

1.3.1 Morphology

The Brahmaputra-Jamuna river is a braided river with characteristic multiple channels, unstable cross-section, and highly variable discharge and sediment load. In the years immediately following the major avulsion of 1830, the river was initially sinuous. The river had become braided by 1867 due partly to the increase of discharge diverted from the old Brahmaputra to this new course (Bristow, 1987). Abundant sediment load and erodible flood plain conditions accentuate the braided form of the river (Coleman, 1969).

The river itself is characterized by multiple channels which are separated by high banks of sand shoals, or islands (known locally as chars). These 'islands' are very unstable and when eroded may cause several sub-channels to join, and new chars to form, resulting in a new division of the main channel into multiple braids.

1.3.2 Water Discharge

Reflecting its vast drainage area river upstream of Aricha (224,000 sq. miles or 528,176 sq. km), the river carries a very large discharge. As noted earlier, the large discharges result from snowmelt in the mountainous regions during the spring, and abundant rainfall during the summer monsoon (June to September) throughout the upper valley areas of Aruncha, Assam, and Meghalaya states of Indian territory.

The water discharge of the river is characterised by a very high variation and multi-peak hydrographs. Based on water level records and discharge

measurements taken since 1949 and 1956, respectively, at Bahadurabad station, the maximum discharge observed on the Brahmaputra-Jamuna river was estimated at 91,000 cubic meter per second (cumec) and occurred on the 6th of August, 1974. The minimum discharge was 2,860 cumec, observed in March, 1971 (Khan, 1988). An example of an annual hydrograph of the river showing this high variation of the discharge is shown in Figure 1.3. Figure 1.4 shows the spatial variation of rainfall over the catchment area of the Brahmaputra-Jamuna river. This spatial variation and the various lags associated with rainfall in different sections of the mountains contributes also to the high variation of discharge evident in Figure 1.3. As the river flow comes from two different sources, there are generally at least two peaks in the annual hydrograph of the river (Coleman, 1969). The first peak, if any, occurs during the mid of June. This flood is characterized by an extremely rapid rise. The second peak ussually occurs during the late of July to the early of August. Generally, this flood may last for a month. The third peak generally occurs during the early of September.

1.3.3 Sediment Load

Available data on bed load are scarce. Measurements of suspended load of the Brahmaputra-Jamuna river are not conducted on a daily basis, but with the frequency of collection being in the range of one to five days a month. These measurements are not conducted during low flow months. Therefore, the data on the suspended and bed load are incomplete, and thus are not particularly representative. The available data do, however, give a rough figure of the magnitude of the sediment discharge in the Brahmaputra- Jamuna River. Based on the data collected by the Water Development Board

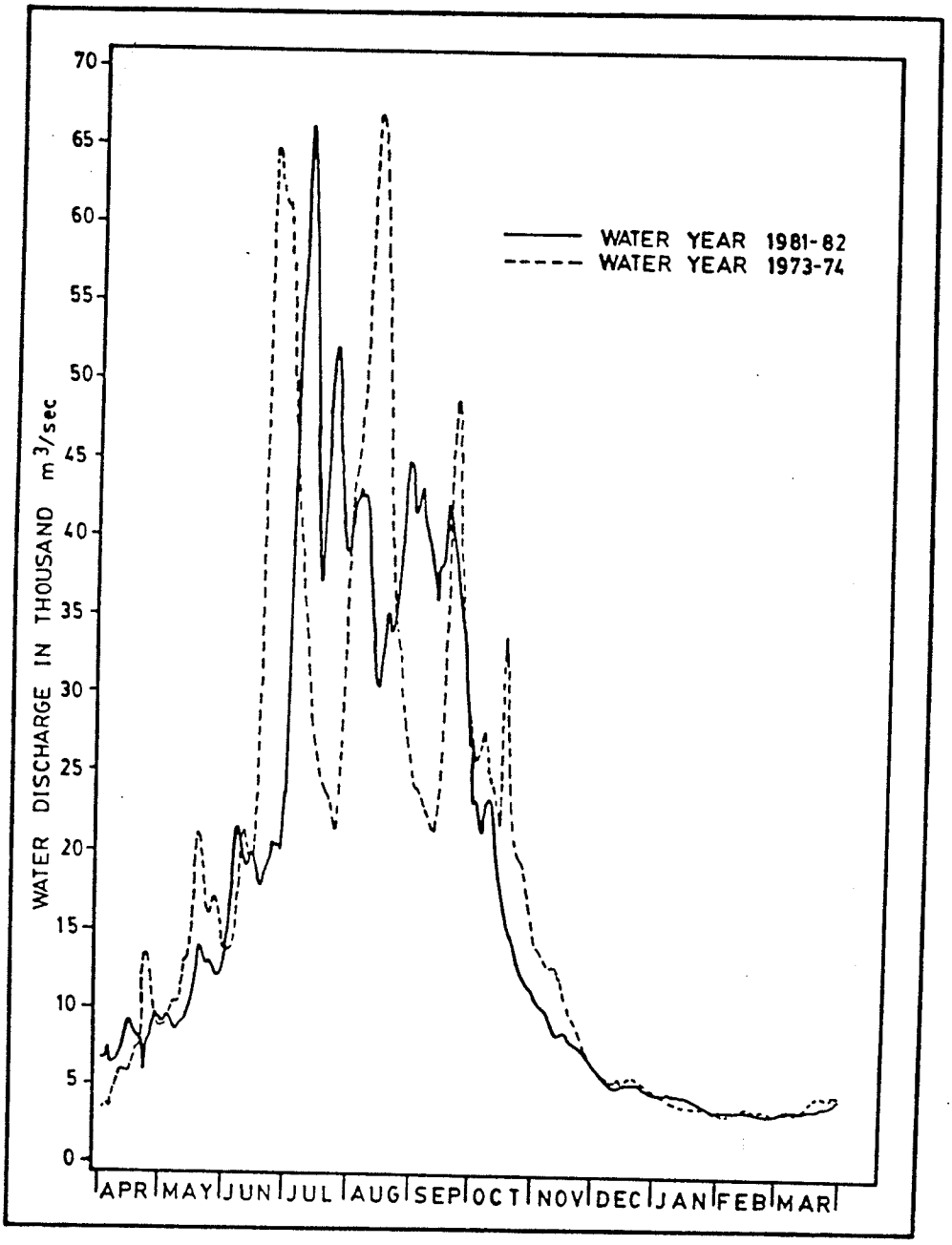

Figure 1.3: Annual Cycle of Hydrographs Showing the High Variation and Multiple Peaks. (after Khan, 1988)

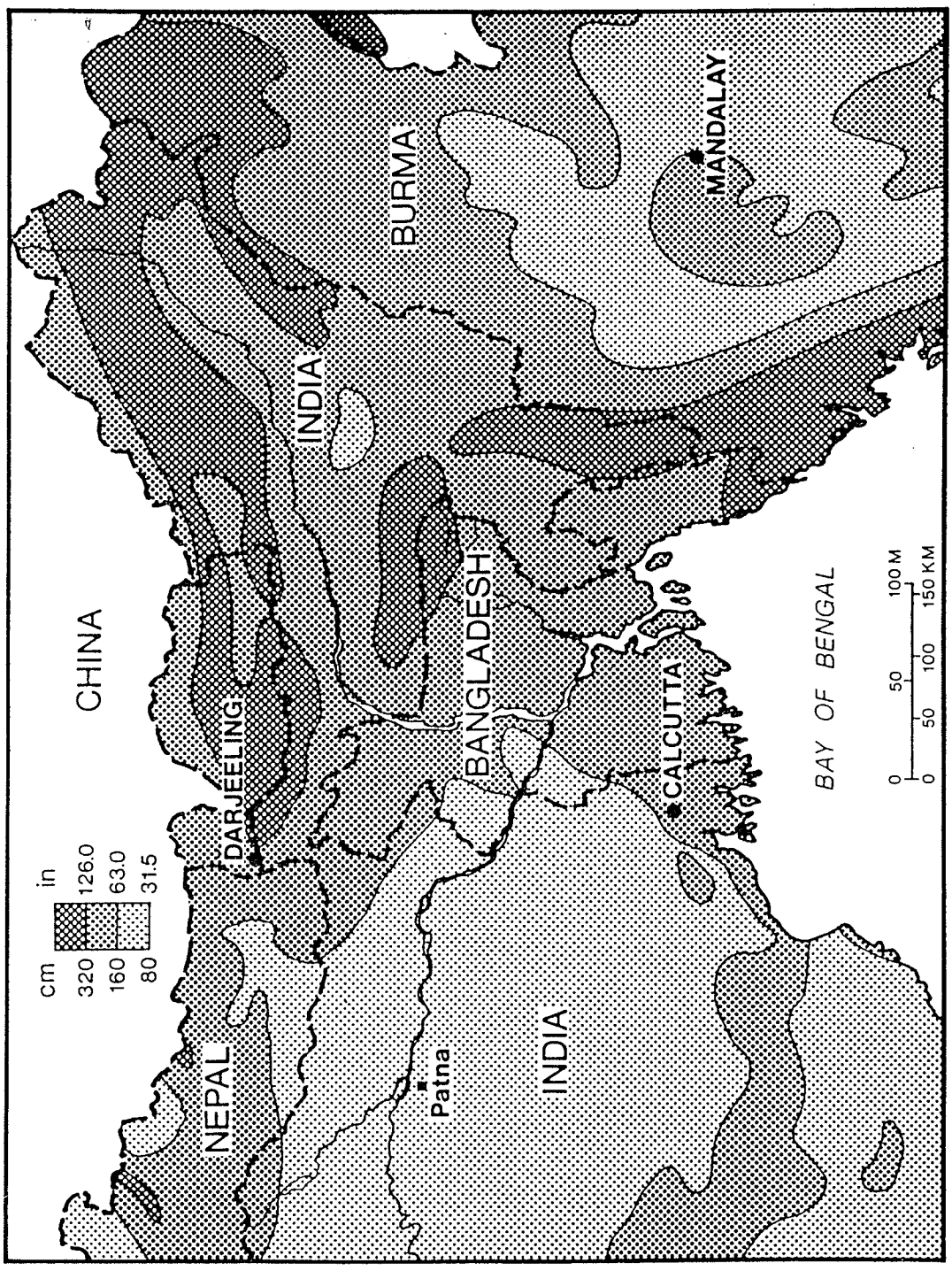

Figure 1.4: Distribution of Annual Rainfall over the Catchment of the Brahmaputra River (after Chowdhury, 1988).

of the Government of Bangladesh in the period 1976-1984, the average suspended sediment load during the low flow period ranges from 20,000 tons per day (in December, 1982) to 195,000 tons per day (in November, 1977) (Chowdhury, 1988). During the summer monsoon, the suspended sediment load can rise to 96,000 tons per day (in May, 1981) to 1,470,000 tons per day (in August, 1977). The estimated month-by-month variation in sediment load can be seen on Figure 1.5. These data show the expected result that suspended sediment load during high flow periods is far greater than that occurring during low flow periods.

Currently, measurements of suspended sediment and bed material are taken at stations Serajganj, Bahadurabad, and Nagarbari (The locations of these stations are shown on Figure 1.2). The data from Serajganj show that 70 to 90 percent of the suspended sediments are silt and clay. The remaining portion is fine and very fine sand. The bed material at Serajganj is characterized by 95 percent of fine sand, with neglible coarse sand, silt, and clay (Latif, 1969). The median size of the bed material reported by different agencies has no common value, although there is agreement that the bed material is composed of fine to medium sand. Coleman (1969) reported that the median size is in the range of 0.34 mm (fine sand) to 0.03 mm (silt). The estimated Manning's roughness coefficients at different locations of the river are 0.022 at Nagarbari, 0.018 at Serajganj, 0.021 at Garbargaon, and 0.035 at Bahadurabad (BWDB, 1978).

1.3.4 Slope

The water surface slope of the Brahmaputra-Jamuna river is very flat. Coleman (1969) reported that the flood surface water slope is only 0.000066 or

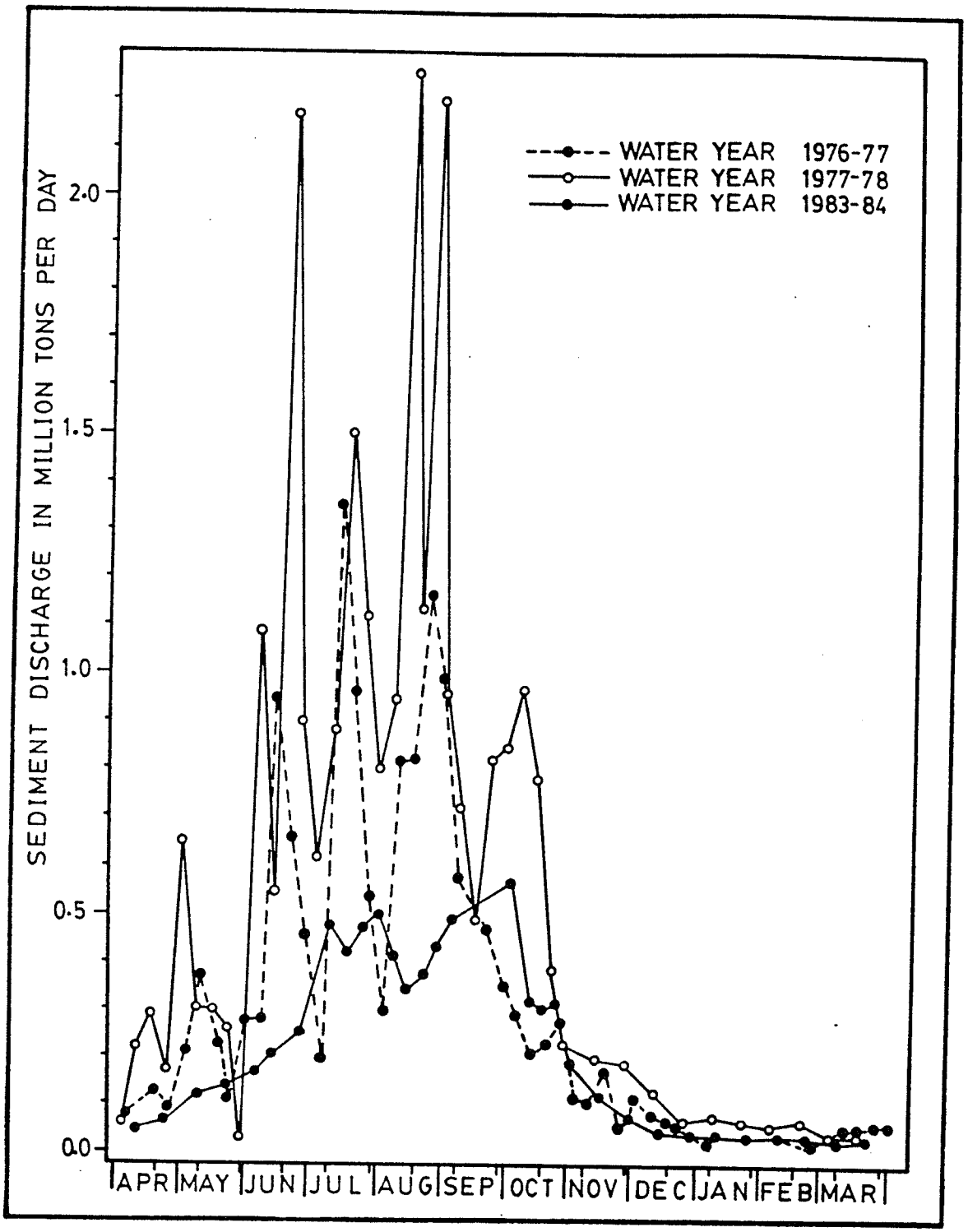

Figure 1.5: Monthly Variation of Daily Suspended Load for Selected Years. (after Khan, 1988)

0.066 m/km. Analysis of recent data (1970-1984) shows that the longitudinal slope of the low water surface varies from 0.000105 to 0.000053, with an average of 0.0000819 or 0.0819 m/km (Khan, 1988). In general, the water surface slope of the Brahmaputra-Jamuna river ranges from 0.000055 to 0.000093 (0.055 to 0.093 m/km) during high flow periods and from 0.000053 to 0.000089 (0.053 to 0.089 m/km) during low flow seasons (BWDB, 1978).

1.3.5 Erosion and Deposition

A major distinction of a braided river, relative to other types of river, is its unstable bed. A braided river is generally very unstable with the instability generally being attributed to its high variation in discharge, abundant sediment load, easily erodible bed and bank material, and steep slope (Knighton, 1984 quoted by Chowdhury, 1988). In the Brahmaputra River, which flows on alluvial deposits, the large amount of discharge and heavy sediment load especially influence the river instability (Coleman, 1969).

As noted in Section 1.3, the discharge of the Brahmaputra-Jamuna river has a very high degree of variation, with the overall discharge itself being high. This high value of discharge is a source of energy of the water flow which, in high flow conditions, causes the river banks to erode. The major process of bank line erosion in the Brahmaputra River, however, is mostly a result of either by liquefaction and flowage or by shear failure (Coleman, 1969). During flood periods the river banks are experiencing greater pressure, which forces the water into the bank formation. When the flood subsides, less pressure is exerted onto the bank. This situation causes the subsurface water of the bank material to flow into the channel

carrying non-cohesive material. Shear failure of the bank was found to be very common in the Brahmaputra River. This failure is mainly caused by undermining of the natural levee and oversteepening of the river bank as the thalweg approaches the bank lines (Coleman, 1969). Additionally, during low flow conditions, the sediment load in the flow tends to be deposited along the banks of the river and within the channel itself. This latter effect, coupled with the abundant sediment load in the river, results in the formation of chars, which later can change in their sizes, shapes, and locations. The formation of these chars can cause the flow to deflect, resulting in bank erosion. The formation of chars in the middle and along the banks of the channel during low flow, and the erosion of the banks and chars during the high flows and the subsiding flows, causes dramatic changes in the cross section geometry.

The slope of the river, which is very flat, would not seem sufficient to support this braided type of river. However, slope is not the only factor influencing the type of the river. The stream power of the river, which is defined as the expenditure of potential energy of the river, has proved to be more dominant in determining the river channel pattern (Chang, 1977). It is postulated that the river continuously changes toward the most efficient geometric cross section to attain a minimum rate of energy to overcome flow resistance (Chang, 1977). Further, he states that, in alluvial streams, this minimun stream power usually means minimum rate of sediment load. The Brahmaputra river, therefore, experiences changes to attain its most effective cross section and the minimum total energy expenditures. As for a given sediment concentration, unit stream power, defined as total energy expeditures per unit weight of water (Yang, 1976), is robust over a wide

range of stream velocity, depth, and slope, Yang (1976) concluded that unit stream power should be the dominant factor in sediment transport mechanism. Thus, unit stream power would also act as a more important factor influencing the Brahmaputra River pattern, rather than slope, as the river carries abundant of sediment load.

1.4 Objective of the Study

As the Brahmaputra-Jamuna River is a braided river, the processes of erosion and deposition in the river, and therefore migration of the river itself, are quite complex. A simplified approach to capturing the overall tendency in direction of movement of the multiple braids (sub-channels) and of the overall channel therefore appears neccessary.

The objective of the study is to develop a means of monitoring the movement of the centroid of conveyance of the channel as a whole and to use the results as an indicator of general tendency of movement of the individual braids in the channel. From these results an attempt is made to ascertain in which direction, if any, the complete channel at a particular location tends to migrate. The rationale in using this flow conveyance is that the flow conveyance reflects the amount of water that can be conveyed by the channel with a certain condition. It reflects up the influence of resistance of the channel boundary, energy gradient, hydraulic properties and the geometry of the channel. A greater value of flow conveyance indicates that more water is flowing through that sub-channel, and therefore, there may be more risk of bank erosion and sub-channel migration. As the Brahmaputra River has multiple channels, the use of centroid of this flow conveyance of the whole cross section would be able to indicate which bank, if any,

is erosion more pronounce. Knowing which bank is more susceptible to erosion, however, does not mean that the other bank would not experience erosion because both banklines of a braided river may experience erosion or deposition simultaneously (Stene, 1988).

1.5 Available Data

Water level records for the Brahmaputra-Jamuna river since 1949 are available at a few stations. Other data, such as hydrological records of water discharge and sediment material, geomorphic data containing temporary locations of the banklines and the thalwegs over time, and geologic data are available for periods since the 1960's. Data from satellite imagery in the form of photographic and digital images of the river reaches are also available.

Data on daily water discharge have been collected from Bahadurabad, Chilmari, Serajganj, and Nagarbari stations since 1965. The locations of these stations are shown in Figure 1.6. Data on daily water levels are available for longer periods at Chilmari, Bahadurabad, Kazipur, Porabari, Serajganj, and Nagarbari. Daily water level data are also available at several other stations on the tributaries and distributaries of the main river.

Data on sediment discharge are more scarce than data on discharge or water level. The record of suspended loads during flood seasons is available from stations such as Serajganj and Nagarbari.

Data on the cross sections of the river are available from 1976 to 1983 (excluding 1982) at the 33 locations shown in Figure 1.7.

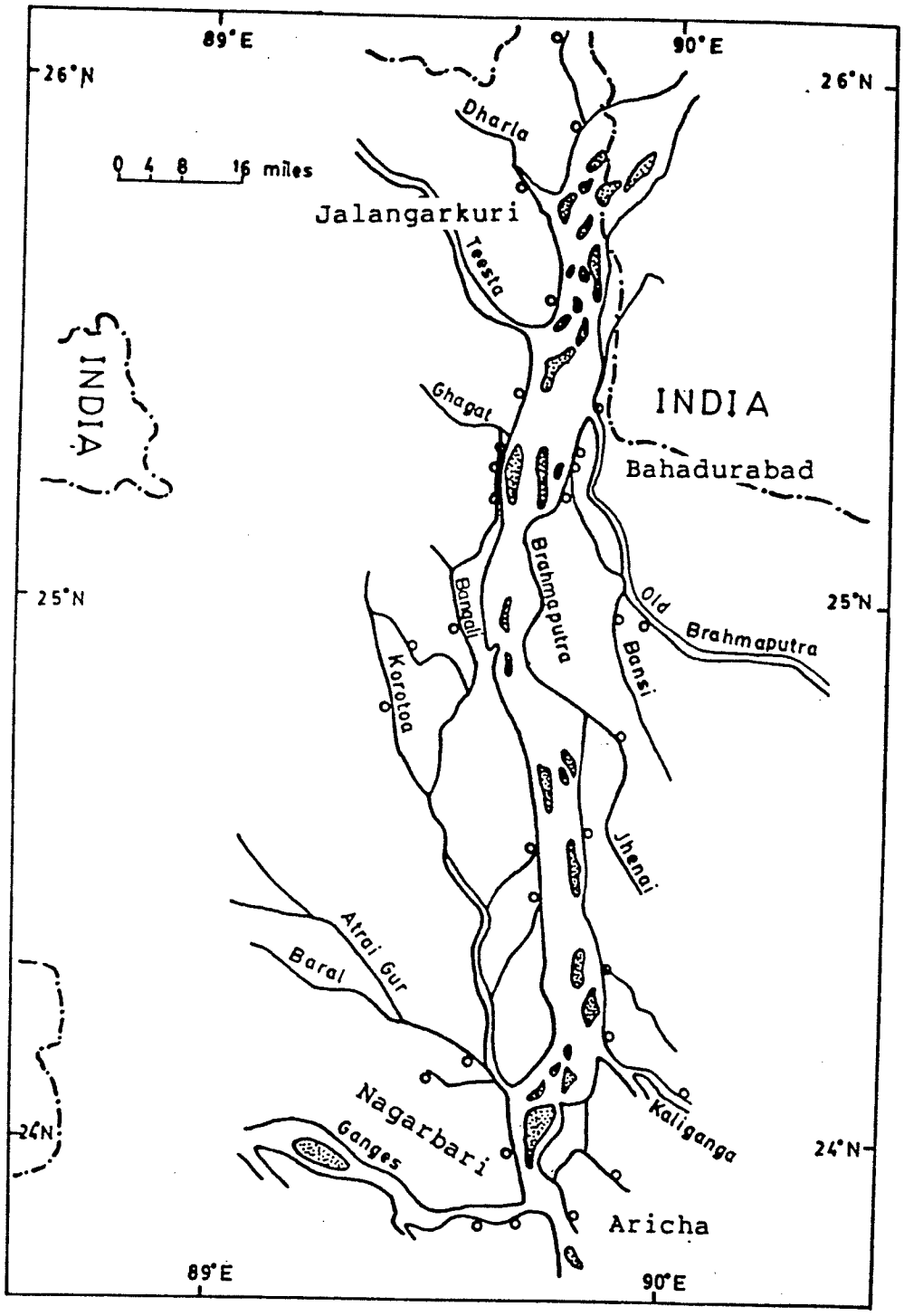

Figure 1.6: Locations of the Water Level and Water Discharge Stations. (after Khan, 1988)

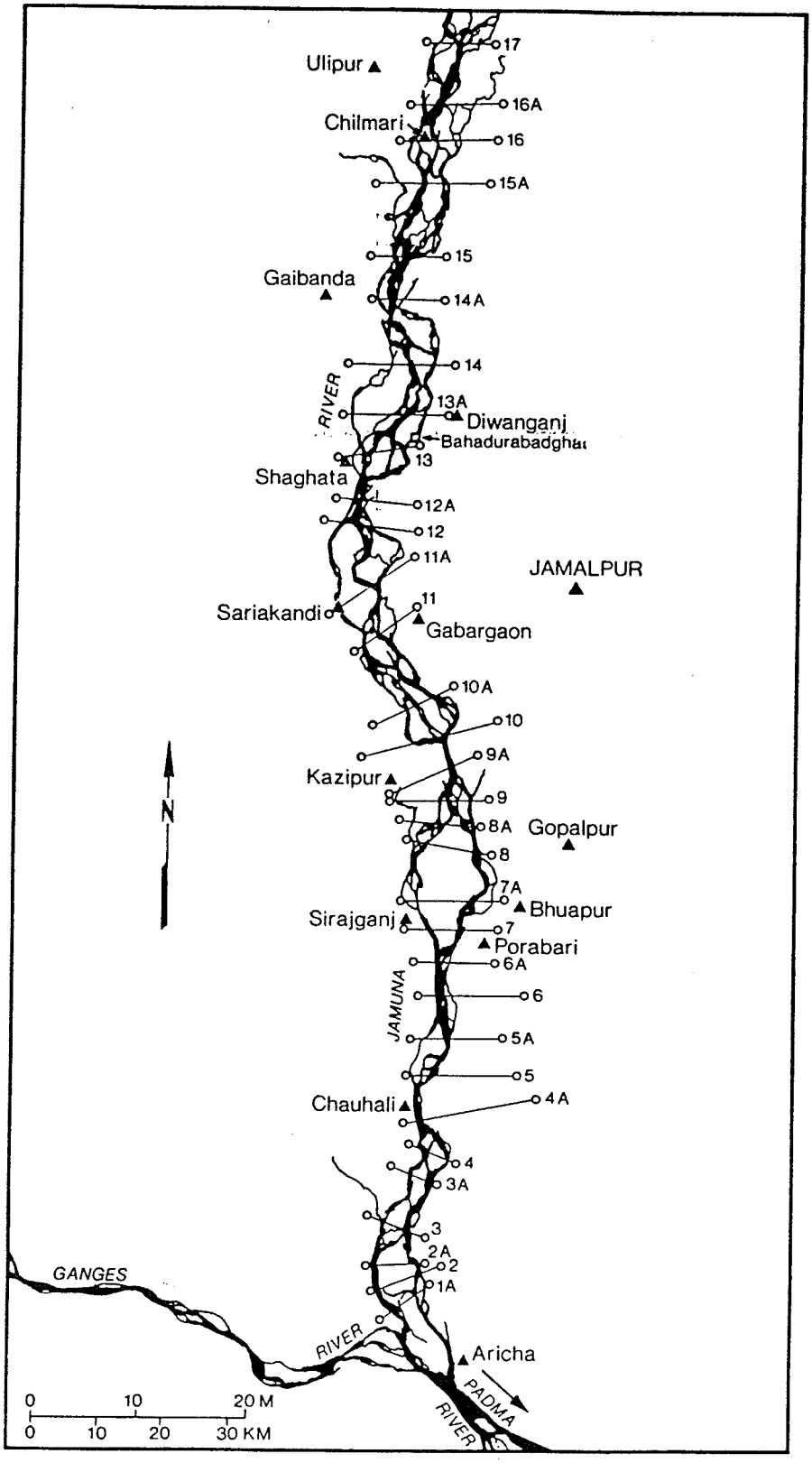

Figure 1.7: Locations of the Thirty Three Cross Section Measurements. (after Stene, 1988)

Chapter 2

LITERATURE REVIEW

Considerable research on meandering rivers has been undertaken in the last few decades. This research has lead to a reasonable understanding of the process of meandering, which has in turn made it possible to assess the behaviour of a meandering river with fairly satisfactory results. (See for example Yen, 1970; Andrews, 1982; and Graf, 1984). On the other hand, relatively little success has been achieved in understanding the processes of, and therefore, satisfacty prediction of, the behaviour of braided rivers. Most attempts in studying braided rivers are usually based on relating observed characteristics of the braids with hydraulic properties of the flow. Furthermore, because the studies are generally region specific (See for example Mosley, 1982), study of braided rivers still lacks generality thereby limiting the extent to which the results can be applied to other locations. Additionally, most, if not all, braided rivers studied in previous research are not comparable in scale to that of the Brahmaputra River.

A major and comprehensive study on the Brahmaputra River in Bangladesh has been reported by Coleman (1969), who noted that, while the long term tendency of the Ganges river migration is in an eastward direction, the Brahmaputra River is actually migrating westward. These long term migration tendencies appear to be predominantly controlled by major faults or fractures within the earth's crust (Coleman, 1969). However, the

short term movements of the Brahmaputra River, within its overall tendency to migrate west, are quite erratic with movements both to the east and west with rates as high as 792.5 m (2,600 ft.) per year being not uncommon.

The thalweg of the river during a flood cycle has been reported to migrate back and forth in an irregular fashion (Coleman, 1969). During the rising stage, the thalweg movement is gradual and has large amplitude, on the order of 914 m (3,000 ft.). The most erratic pattern of thalweg movement occurs during the falling stage. Over a period of a few days, the main currents have been reported to move up to 1000 m back and forth across the channel (Coleman, 1969).

Coleman (1969) also hyphothesized that there must be an intimate relationship between the variation of the current direction, rapid bankline movement, channel width, and the thalweg migration. Following the pioneering work by Coleman (1969), Bristow (1987) provided a more in depth understanding of the processes of depositon within the channel and of actual river migration. In his study, Bristow classified the braids of the Brahmaputra River into three hierarchies. The first-order channel is the channel between the outermost banklines. This first order channel is comprised of several second-order channels, while the second order channels themselves are made up of a number of third order channels. Studying a series of the river maps from year 1830 to 1984, Bristow (1987) observed that the first order channel moves back and forth within a 15 km wide belt with minor net migration to the west. Meanwhile, the second order channels, as observed from Landsat images from 1972 to 1978, experience switching and lateral migration at a rate of 1 km per year (Bristow, 1987). Although ero-

sion and deposition of bank lines might be predicted to occur alternatively, Khan (1988) noted that there was a general trend for the west bank line to migrate westward at an average rate of 120 m per year, while the east bank line did not show any trend in either direction.

Although these previous studies address the general trend of the river migration, there is still no effective means of predicting the 'next' movement of the channel. Recent work by Khan (1988) attempted to develop a practical approach to this prediction using bank line position data extracted from Landsat images as the variable in a statistical model. From the data of Landsat images for years 1973, and from 1976 to 1985, the river reaches were divided into equally spaced sections and the locations of both bank lines along the river reaches measured. The space and time variations of the bank line position were then used in a statistical analysis. The resulting model is a combination of a Transfer Function model and a Noise model, with the parameters of the Transfer Function model showing a significant relationship with mean discharge. The model was capable of predicting one year ahead whether bank movement would occur and in which direction, at the 95 % confidence level.

Other approaches which have analyzed the characteristics of the cross section over time were reported by Burger et al. (1988), Goulter and Dubois (1988) and Stene (1988). Burger et al. (1988) studied the cross section changes by analysing the form of the cumulative conveyance function across a section. Using cross section data from 1965 to 1986 from several selected location, their study shows that the river does not experience a consistent horizontal displacement. Goulter and Dubois (1988), with more emphasis on the approach in assessing the change in the Brahmaputra River, use

movement of the centroid of flow area and the change of its flow area over time to identify the lateral migration of the river. Demonstrated on six cross section locations with data from 1976-1983, it shows that there is no definite pattern of the river migration. In the same year, Stene (1988) studied the change of the river width and depth of the river over the thirty three cross section measurements. Analysing the cross section data from 1976 - 1983, he found that the river experienced persistent increase in its width on the majority of cross sections with an average of 1100 m. During this seven years period, the successive year comparison shows that 20 to 26 cross sections experience width increase, while the minority (7 to 13) show a width decrease. This study suggests that there may be a lateral migration of the river. However, it should be noted that bank line erosion persist on both banks (Stene, 1988). Using the same data, analysis of the channel deepening process indicates that the dominant activity of the river was channel degradation, although an individual cross section shows an alternate degradation and aggradation in the successive year. This fact supports an indication that the bed sediment is in pulses or wavelike motion (Stene, 1988).

Chapter 3

ANALYSIS

3.1 Methodology

The principle of the proposed methodology developed herein is to calculate the centroid of conveyance of a cross section. First, a velocity distribution of the flow over a cross section is calculated by solving the the Navier Stokes Equation. Consider a body of water flowing in the z direction depicted in Figure 3.1. The governing equation of this flow mechanism is the Navier Stokes equation. The z component of this equation is :

$$\rho\frac{\partial w}{\partial t}+\rho(u\frac{\partial w}{\partial x}+v\frac{\partial w}{\partial y}+w\frac{\partial w}{\partial z})=\rho f_z-\frac{\partial p}{\partial z}+\mu(\frac{\partial^2 w}{\partial x^2}+\frac{\partial^2 w}{\partial y^2}+\frac{\partial^2 w}{\partial z^2}) \tag{3.1}$$

where:

ρ	:	mass density of water.
x, y	:	cartesian coordinates in x and y axis, and perpendicular to the longitudinal axis, respectively.
z	:	z axis along the longitudinal axis of the river.
u, v, w	:	velocity along the $x, y$and z axis, respectively.
μ	:	dynamic viscosity coefficient.
f_z	:	external forces acting on the body of water in the direction of z axis $(= g\sin\theta)$.
g	:	gravitational acceleration.

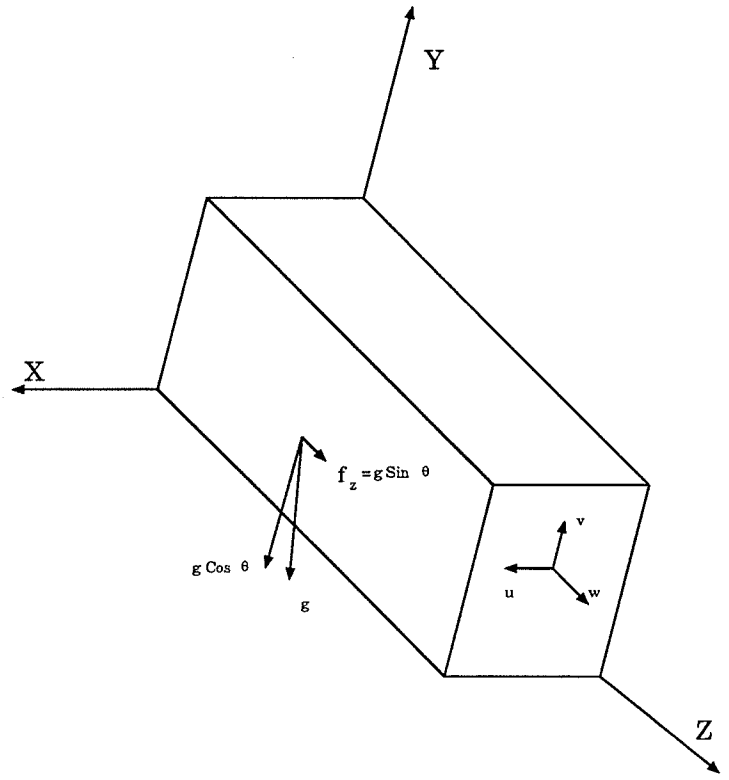

Figure 3.1: Sketch of A Flowing Body of Water.

$\frac{dp}{dz}$: pressure gradient along the longitudinal axis.

The application of this full equation requires a large amount of data which is not presently available. Considering that the only available data is yearly cross section measurements at a discrete location with an arbitrary interval between 2 km to 12 km, averaging 6 km interval, the following assumptions have to be made in order to apply Equation (3.1).

The time variation term, $\frac{\partial w}{\partial t}$, of Equation (3.1) dictates the need to have a much closer time interval of cross section measurement. This data is required because the geometry of a cross section of the river is likely to change dramatically even during a single flood season. Other data on the associated water discharge, energy gradient, and water surface velocity would also

be required. While those data are still lacking, the $\frac{\partial w}{\partial t}$ term is, therefore, neglected in this study.

The external force, f_z, acting on this body of water is mainly the gravitational acceleration. The longitudinal component of this force, $g \sin\theta$, can be ignored as the bed slope of the Brahmaputra River is very flat. With the same reason, the flow would be appropriately assumed as a uniform flow, i.e. $\frac{\partial w}{\partial z} = 0$. This assumption implies that there is no longitudinal velocity acceleration ($\frac{\partial^2 w}{\partial z^2} = 0$) as well.

The velocity components of u and v would also be neglected for this moment. The inclusion of these components dictates the need to have a very closely spaced cross section measurement. Without these data, the effect of three dimensional flow mechanisms would not be appropriately modelled as it can not take into account the influence of an immediately upstream and downstream condition of the cross section under consideration, and there would be no flow interaction between sub-channels. In the Brahmaputra River with its inherent braided channel, and therefore, its high spatial variation on the cross section geometry, it would need very closely spaced cross section measurement data even in the simplest three dimensional model in order not to overlook a local change on cross section geometry.

It is realised that the above assumptions oversimplify the flow mechanism. However, as the available data do not support the application of the full form of Equation (3.1), the use of this simplified equation would still be valuable in assisting an understanding of the river migration processes addressed in this study and in illustrating the application of Finite Element Method to this problem. The application of the full form of Navier-Stokes equation with the consideration of the y and x components is warranted

when the data are available. The application the full form of the Navier-Stokes equation would require complete set of data on the boundary conditions in one location such as data on velocity distribution, discharge hydrograph, cross section measurement, energy slope, and turbulence coefficient.

With the above assumptions, Equation (3.1) reduces to:

$$\frac{\partial^2 w}{\partial x^2} + \frac{\partial^2 w}{\partial y^2} = \frac{1}{\mu}\frac{\partial p}{\partial z} \tag{3.2}$$

In the turbulent flow such as prevails in natural channels μ would represent the summation of molecular viscosity, μ_l, and turbulent viscosity, μ_t. While the molecular viscosity depends on the type of fluid, the turbulent viscosity is a function of the flow and distance from the boundary wall. In natural flow, the turbulent viscosity is always several orders magnitude higher than the molecular viscosity and the laminar sub-layer is extremely thin. In this condition, the influence of molecular viscosity is negligible, and the flow is completely turbulent.

Therefore, Equation (3.2) becomes Equation (3.3), where μ_t stands for the turbulent or mixing viscosity. It is realized that the assumption of a constant turbulent viscosity involves serious simplification which, however, seems acceptable for this preliminary investigation.

$$\frac{\partial^2 w}{\partial x^2} + \frac{\partial^2 w}{\partial y^2} = \frac{1}{\mu_t}\frac{\partial p}{\partial z} \tag{3.3}$$

For an open channel flow, the pressure gradient can be assumed equal to the energy gradient of the flow. As the slope of the Brahmaputra River is very flat, even during high flow periods, this term can be assumed equal to the slope of water surface profile. This slope is further assumed to be the same throughout the all reaches of the study area. This assumption is

considered justifiable because Equation (3.3) is particularly a two dimensional equation. If this two dimensional equation is applied to a certain location with a known value of slope, the resulting equation will be a Poisson's equation in which the right hand side of the resulting equation will be a constant value. The change on the value of the right hand side of the Poisson's equation would only shift up or down the solution domain, and not changing the distribution of the solution domain. As this study is interested in the distribution of the velocity over a cross section, therefore, the assumption that the right hand side of Equation (3.3) is the same, equal to c, throughout the entire study reaches would not have serious effect on the analysis. Equation (3.3) reduces to:

$$\frac{\partial^2 w}{\partial x^2} + \frac{\partial^2 w}{\partial y^2} = c \tag{3.4}$$

Due to irregularities of the problem domain, an analytical solution of Equation (3.3) is not simple. Therefore, a numerical solution, finite difference or finite element method, should be used. Application of finite difference method is less suitable as, for a very irregular problem domain, a geometric representation of this domain is difficult to be achieved unless interpolations along the boundary are applied. In this case, it is likely that some nodes of the proposed grid would not located right on the the boundary. An example of this situation is shown in Figure 3.2. As the nodes $0, 3$, and 4 are not on the boundary line, an interpolation from the known boundary values at nodes 1 and 2 should be performed. One general interpolation function of Equation (3.4) is shown in Equation (3.5) with the neglected term in the order of $(\Delta x^3, \Delta y^3)$ (Garg, 1976). When a large number of these interpolations have to be performed, as in case of a very irregular cross section geometry, the associated interpolation errors itself

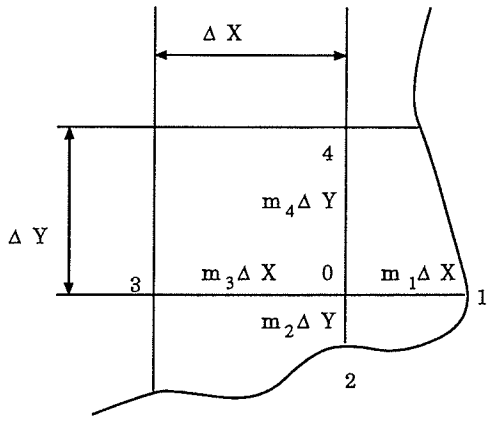

Figure 3.2: An example of Finite Difference Grid Close to the Boundary.

may become noticable.

$$\frac{2}{m_1(m_1+m_3)}\frac{\phi_1}{\Delta x^2}+\frac{2}{m_2(m_2+m_4)}\frac{\phi_2}{\Delta y^2}+\frac{2}{m_3(m_1+m_3)}\frac{\phi_3}{\Delta x^2}+\frac{2}{m_4(m_2+m_4)}\frac{\phi_4}{\Delta y^2}-(\frac{2}{\Delta x^2 m_1 m_3}+\frac{2}{\Delta y^2 m_2 m_4})=c \tag{3.5}$$

In this study, therefore, the solution is obtained by using the finite element method which is favourable in an irregular problem domain. In the finite element method, the solution domain is discretized into interconnected elements which, in this case, are right triangles. A sketch of this discretization is shown in Figure 3.3.

Therefore, the nodes composing these interconnected triangles are aligned in vertical lines. The velocity for each of the nodes located on the same vertical line are then averaged to get the averaged velocity at each vertical strip.

The conveyance of each vertical strip can then be calculated by applying Manning's equation to the average velocity in that strip as follows. In this study, the flow conveyance is defined as:

$$C = AR^{2/3} \tag{3.6}$$

where C is the flow conveyance, A the flow area, R the hydraulic radius. Arrangement of the Manning's formula will result in:

$$R^{2/3} = \frac{wn}{S_0^{1/2}} \tag{3.7}$$

where n is Manning's roughness coefficient, and S_0 the channel slope. Thus the flow conveyance can be calculated using the following formula.

$$C = \frac{wn}{S_0^{1/2}} A \tag{3.8}$$

The conveyance of a strip can then be calculated using the following equation.

$$C_{ijt} = \frac{\bar{w}_{ijt} n}{S_0^{1/2}} A_i \tag{3.9}$$

where $\bar{w}_{ijt}$ and C_{ijt} are the vertically-averaged longitudinal velocity and the conveyance of the vertical strip i of section j in time period t, respectively. A_i is the flow area of that vertical strip, i.e. the half flow area to the right and to the left, respectively, of the vertical line i (see Figure 3.3).

The location of the centroid of the conveyance of cross section j as a whole in time period t, relative to some reference point on the left (east) bank of the river, is then calculated by :

$$CC_{jt} = \frac{\sum_{i=1}^{m} C_{ijt} X_{ijt}}{\sum_{i=1}^{m} C_{ijt}} \tag{3.10}$$

where :

CC_{jt} : distance from the left (east) bank of centroid of conveyance of cross section j in time period t.

X_{ijt} : horizontal distance of the center of the vertical strip i of a cross section j in time period t from a datum (east bank).

m : number of vertical strips across the section.

The application of the above methodology to the thirty three locations of cross section, each with six to seven years of records, gives the variation of the centroid of conveyance of the river reaches under investigation over those times and spaces.

Evaluation of the proposed methodology is conducted by a comparison of the results of this method with an earlier method for assessing movement of the conveyance and with the time and space variation of the thalweg positions.

The main difference between the proposed method and the earlier method lies in the principles involved in the calculation of conveyance of each vertical strip. In the earlier method (Burger et al. 1988), the conveyance at each vertical strip is calculated by applying Manning's equation under the assumption that the wetted perimeter of that strip is that portion of the perimeter located at the boundary between the fluid and the channel. Furthermore, the strip under consideration is assumed as an individual (distinct) portion, not interconnected with its adjacent strips. These two assumptions cause calculation error, which is accumulated in the values of conveyance for strips at the far end of the cross section. In particular, at the last vertical strip across a cross section, the calculated conveyance can be negative as shown on Figure 3.4.

This figure shows the existence of negative flow conveyance of a rectangular cross section with the width equal to 10 m, and divided into 10 vertical strips. This negative value results from the accumulation of errors associated with the calculation of the elemental conveyance. It is suspected, therefore, the wider the channel, the larger the error will be. As the Brahmaputra River is a very wide river with the width/depth ratio in

the order of 1000, it is necessary to use an approach which will not result in negative values of flow conveyance.

Goulter and Dubois (1988) studied the movement of the centroid of the cross section area to identify the migration. However, as noted by those authors, the shortcoming of that method is the assumption that the flow area of a cross section, rather than conveyance, is trully representative of the flow capacity. The use of this flow area would not be able to account for the flow mechanism as it does not take into account the role of channel slope, bed roughness, hydraulic radius, and wetted perimeter of the flow. The incorporation of the above properties suggest the investigation of the movement of the centroid of flow conveyance. This flow conveyance reflects the amount of water that can be conveyed by a channel, and thus, reflects the influence of the above hydraulic properties.

In the proposed method, instead of treating each vertical strip individually, a vertical strip is considered as an interconnected portion of the flow. Thus, the proposed method will give a better value of the location of the centroid of conveyance than the Burger et al. (1988) approach.

Thalweg position, which is used as another means of indicating channel migration by Coleman (1969), is also used to evaluate the results from this methodology.

3.2 Water Elevation

As noted earlier the Brahmaputra River has wide variation in its discharge, and therefore, also its water level. This variation indicates the need to use a significant water level above which the influence of the rest of cross section will be assumed negligible. The cross section below this water level is

considered to have significant influence on the channel formation process. In single channels, this water level has been generally assumed as bankfull water level, which is being associated with bankfull discharge. In braided river, however, this water level may not be associated with bankfull discharge, which has been generally known as a channel forming discharge of a single channel (Harvey, 1969; and Pickup and Warner, 1976), as there has no sufficient evident indicates that the bankfull discharge of braided rivers has the same characteristics as that of single channels. This water elevation would only be considered as an elevation above which the influence of the rest of cross section is insignificant.

In this study, this water elevation is identified by the use of the available cross section measurement. Harvey (1969) and Pickup and Warner (1976) defined bankfull water level of a single channel as the stage at which the width/depth ratio (W/D) of a cross section reaches a minimum. The stage corresponding to a distinct change in the relationship of cross section area to its top width may also indicate the bankfull stage. These methods are primarily developed for single channel. Analysing 20 streams in north western New South Wales, Riley (1972) concluded that bankfull water level of single channels indicated by width/depth ratio of rectangular cross sections is close to the actual bankfull elevation. This fact indicates that the use of width/depth ratio would be best for nearly rectangular channels, which have an almost vertical channel walls. While the Brahmaputra River has generally an almost vertical bank, the application of this width/depth ratio may indicate an elevation below which the the cross section has significant influence in the channel process.

In this study, the water elevation, therefore, is determined by analysing

both the relationship between the W/D ratio and the water level, and the plot of the flow area versus top width. Examples of these plots are shown in Figures 3.5 and 3.6, respectively.

In Figure 3.5, the portion of the graph which should be considered in determining the minimum value of W/D ratio is that above elevation 0. This criterion is required because, at water elevations below 0, the cross section is not a valid representation of the whole cross section. In the section of the graph with elevations above 0, there are two significant points that are possible candidates for as the minimum W/D ratio for this cross section. The first occurs at an elevation of about + 0.75 m, with the second at elevation + 7.0 m. Additional information such as that in Figure 3.6, may show which one of these two candidate points is more appropriate for consideration as the water elevation. As Figure 3.6 shows that an abrupt change in the relationship between the flow area and top width occurs at the second point, the bankfull water level for this cross section is assigned to the second point (Elevation + 7.0 m). The water elevations for all cross sections under investigation can be determined in the similar manner. The values of these water elevations adopted from this analysis are summarised in Table 3.1.

For the cross sections which are coincident with those studied by Goulter and Dubois (1988), a comparison of the water levels, defined as a cut-off elevation in the study by Goulter and Dubois (1988) can be conducted. The cut-off elevations used by Goulter and Dubois (1988) are shown on Table 3.2. The locations of the cross sections in their study are those sections close to Serajganj (cross sections J6, J6-A, and J7) and those in the viccinity of Bahadurabad (cross sections J13, J13-A, and J14). The water elevations

used in this study are generally higher than those cut-off elevations. Based on the time variation of water level at Bahadurabad station, shown in Figure 3.7, the cut-off elevations are approximately equal to mean annual water level, while the water elevations used in this study are higher than mean annual water level with about 30% probability of being equelled or exceeded. Frequency curves of water level using data from 1976 to 1982 at stations Bahadurabad, Serajganj, and Porabari are shown in Figure 3.8. It is not possible, however, to evaluate the probability of exceedence of these water elevations for each location of cross section measurement because not all locations have water level measurement.

It is worthwhile to note that these water elevations are likely to occur simultaneously as indicated by the time plot of water levels at station Bahadurabad, Serajganj, and Porabari. This plot (Figure 3.9) indicates a simultaneous rise and fall of water levels at those three stations.

3.3 Finite Element Method

As an analytical solution of Equation (3.4) for an irregular domain is not known, a finite element solution is used (Koutitas, 1983; Brebbia and Ferrante, 1983). In this method, the solution domain is conceived as an ensemble of interconnected elements. The solution in each element is obtained by introducing field variables, which are valid within each element, and the base (shape) function as a function of field variables. This base function is then multiplied by the values of each field variable at each node to get the approximate function of the solution in that element. This approximate function is called a field function. This field function can be solved by using variational calculus, or the method of weighted residuals which will result

Table 3.1: Values of Water Elevation Used in the Study.

Cross Section Number	Station	Water Level (m)	Cross Section Number	Station	Water Level (m)
1	J-1	7.00	18	J-9 A	14.00
2	J-1 A	7.00	19	J-10	14.00
3	J-2	7.00	20	J-10 A	14.00
4	J-2 A	7.00	21	J-11	16.00
5	J-3	8.00	22	J-11 A	17.00
6	J-3 A	9.00	23	J-12	17.00
7	J-4	9.00	24	J-12 A	17.50
8	J-4 A	9.00	25	J-13	17.50
9	J-5	9.50	26	J-13 A	18.00
10	J-5 A	9.50	27	J-14	19.00
11	J-6	9.50	28	J-14 A	20.00
12	J-6 A	11.00	29	J-15	20.00
13	J-7	12.00	30	J-15 A	22.00
14	J-7 A	12.00	31	J-16	22.00
15	J-8	13.00	32	J-16 A	22.00
16	J-8 A	13.00	33	J-17	24.00
17	J-9	13.50			

Table 3.2: Values of Water Elevation Used in the Study by Goulter and Dubois (1988).

Cross Section Number	Station	Water Level (m)	Cross Section Number	Station	Water Level (m)
1	J-6 A	9.14	4	J-13	15.20
2	J-7	9.14	5	J-13 A	15.20
3	J-7 A	9.14	6	J-14	15.20

in an algebraic equation. The solution of the whole domain is obtained by assembling the field functions of the whole elements and solving the complete set of equations simultaneously. The application of variational method can be applied to only simple problem, while the weighted residuals method embraces a wider scope of problems that can be solved. The weighted residuals method is applicable both in linear and non-linear problem. Among several approaches of weighted residuals method, the Galerkin method has more general application. Therefore, the Galerkin method is used in this study.

3.4 Galerkin Method

Instead of several methods of weighted residuals approaches, the Galerkin method is used in this analysis. This choice is mainly because, in the principle, the Galerkin method is trying to make residuals orthogonal to members of the complete set of functions. The base function is usually a member of the complete set of functions. It is understood as a property of a complete set of functions that a piecewise continuous function, such as the residuals, can be orthogonal to each and every member only if the function is identically equal to zero (Finlayson and Scriven, 1967). Therefore, by making

the residuals orthogonal to the members of a complete system of functions, it causes the residuals to vanish. One way to ensure this orthogonality is by using the base functions as the weighting functions such as in Equation (3.17). Detailed explanation on the performance of the Galerkin over other weighted residuals method can be found in the paper by Finlayson and Scriven (1967).

An illustration of the Galerkin method is shown below. Consider a two dimensional problem domain of a Poisson's equation and with its boundaries as shown in Figure 3.10.

$$\frac{\partial^2\phi}{\partial x^2} + \frac{\partial^2\phi}{\partial y^2} = c \text{ in } \Omega \tag{3.11}$$

The boundaries of the problem domain are: the first boundary in which the variable ϕ is equal to a known value ($\overline{\phi}$) and the second boundary which indicates a known flux into or out of the problem domain. These boundaries are expressed mathematically as :

$$\phi = \overline{\phi} \text{ on } \Gamma_1 \tag{3.12}$$

$$q = \frac{\partial\phi}{\partial n} = \frac{\partial\phi}{\partial x}n_x + \frac{\partial\phi}{\partial y}n_y = \overline{q} \text{ on } \Gamma_2 \tag{3.13}$$

As the field function is an approximation, there will be errors ϵ_1, ϵ_2 and ϵ_3 corresponding to errors at each node of the problem domain Ω, at every point of the boundary domain Γ_1 and at every node of the boundary domain Γ_2, respectively. Therefore, Equations (3.11) to (3.13) becomes:

$$\frac{\partial^2\phi}{\partial x^2} + \frac{\partial^2\phi}{\partial y^2} - c = \epsilon_1 \neq 0 \tag{3.14}$$

$$\overline{\phi} - \phi = \epsilon_2 \neq 0 \tag{3.15}$$

$$\overline{q} - \frac{\partial\phi}{\partial x}n_x - \frac{\partial\phi}{\partial y}n_y = \overline{q} - q = \epsilon_3 \neq 0 \tag{3.16}$$

An improvement in the solution is obtained by minimization of the errors, a process which is conducted for the whole domain as the matrix formulation of an element can not be solved individually. The error minimization for the whole domain is expressed as :

$$\int_{\Omega} \epsilon_1 w_{1,i} d\Omega + \int_{\Gamma_1} \epsilon_2 w_{2,i} d\Gamma_1 + \int_{\Gamma_2} \epsilon_3 w_{3,i} d\Gamma_2 = 0 \tag{3.17}$$

where $w_{1,i}$, $w_{2,i}$ and $w_{3,i}$ are three different types of weighting distribution functions. In the galerkin method, the weighting functions are assumed equal to the base function. The above expression represents a set of simultaneous equations which theoretically allow an approximate solution of ϕ to be found. A detailed explanation of the matrix formulation of this solution strategy is explained in Appendix A.

3.5 Discretization Strategies

The discretization of the problem domain sometimes is not a straightforward step. This step involves the choice of the shape and the size of elements, the node numbering, and the ease in which external boundary values are incorporated. The shape and the size of elements affects the accuracy of the calculation. In principle, these two factors should allow a close representation of the problem domain, geometrically and physically. In a two dimensional problem domain, for example, the mosaic of the ensemble of these elements should approximate the geometric form and the size of the problem domain. Physically, at the place where unknown variables are expected to have steep gradients, smaller elements should be used to reflect every noticeable change in the unknown variables. In this study, the discretized domain is made as close as possible to the shape of a cross section

under consideration. The total area of the elements calculated using the data of the nodes coordinates should be a close approximation of the total area of the corresponding cross section.

Node numbering also influences the accuracy and the time required for the computation process. In an extreme condition, when the nodes are numbered inconsistently and thus their values are scattered, the resulting matrix for the system equations will be sparse. In this situation the cells of the matrix with values different from zero will be scattered throughout, and not banded along the diagonal of the matrix. This situation causes a less accurate and efficient solution. To reduce the sparsity of the matrix of the system, the nodes are numbered consecutively along the shorter side. For example, in a wide cross section where its depth is relatively very small compared to its width, the numbering will proceed along its depth.

Finally, this discretization should be able to incorporate the possibility of a change in the external boundary conditions. Each node should be located as close as possible to the location where there may be an external boundary in the future. This strategy reduces the need to interpolate an external boundary condition should it become the part of the system.

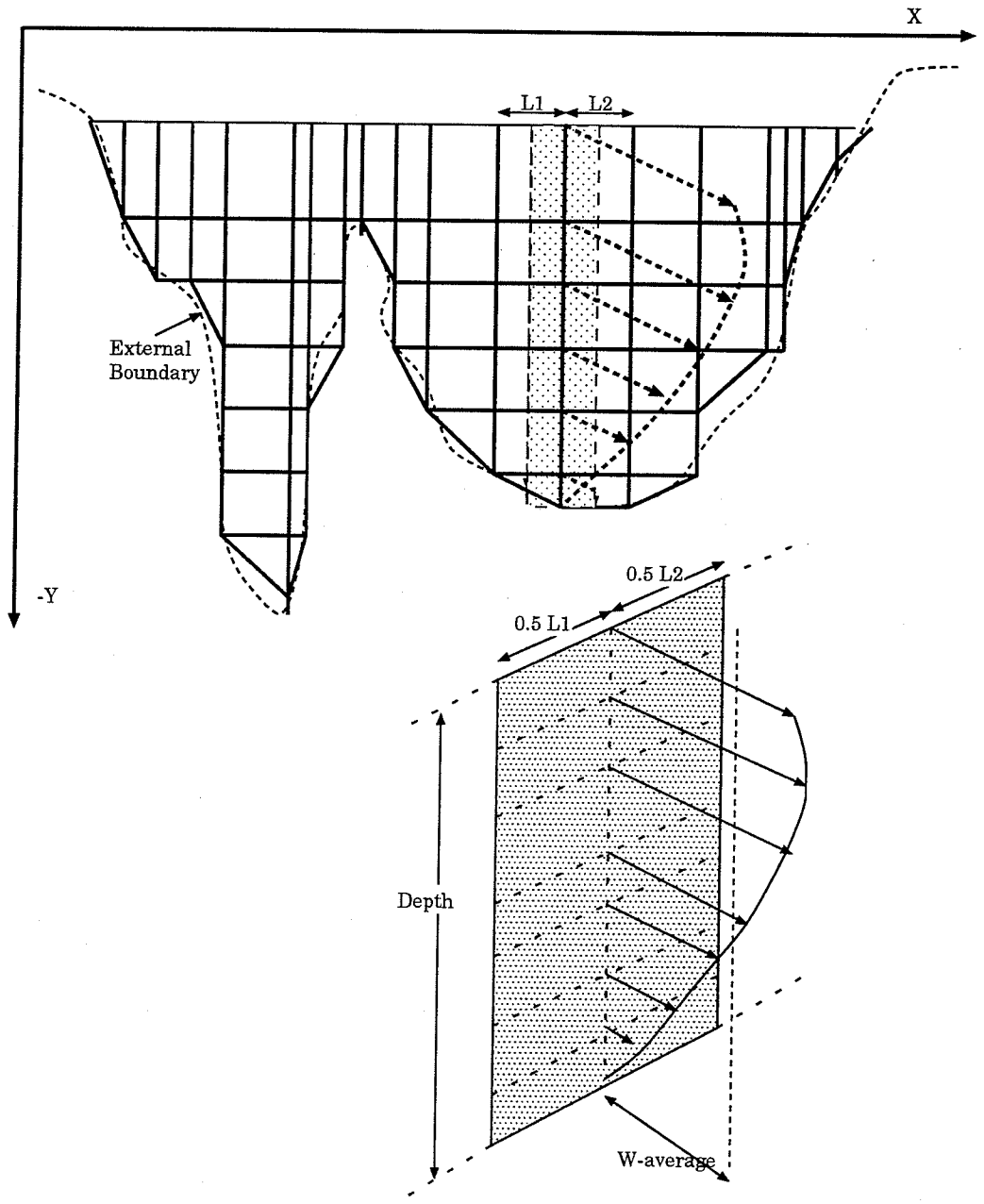

Figure 3.3: An example of a Discretized Domain.

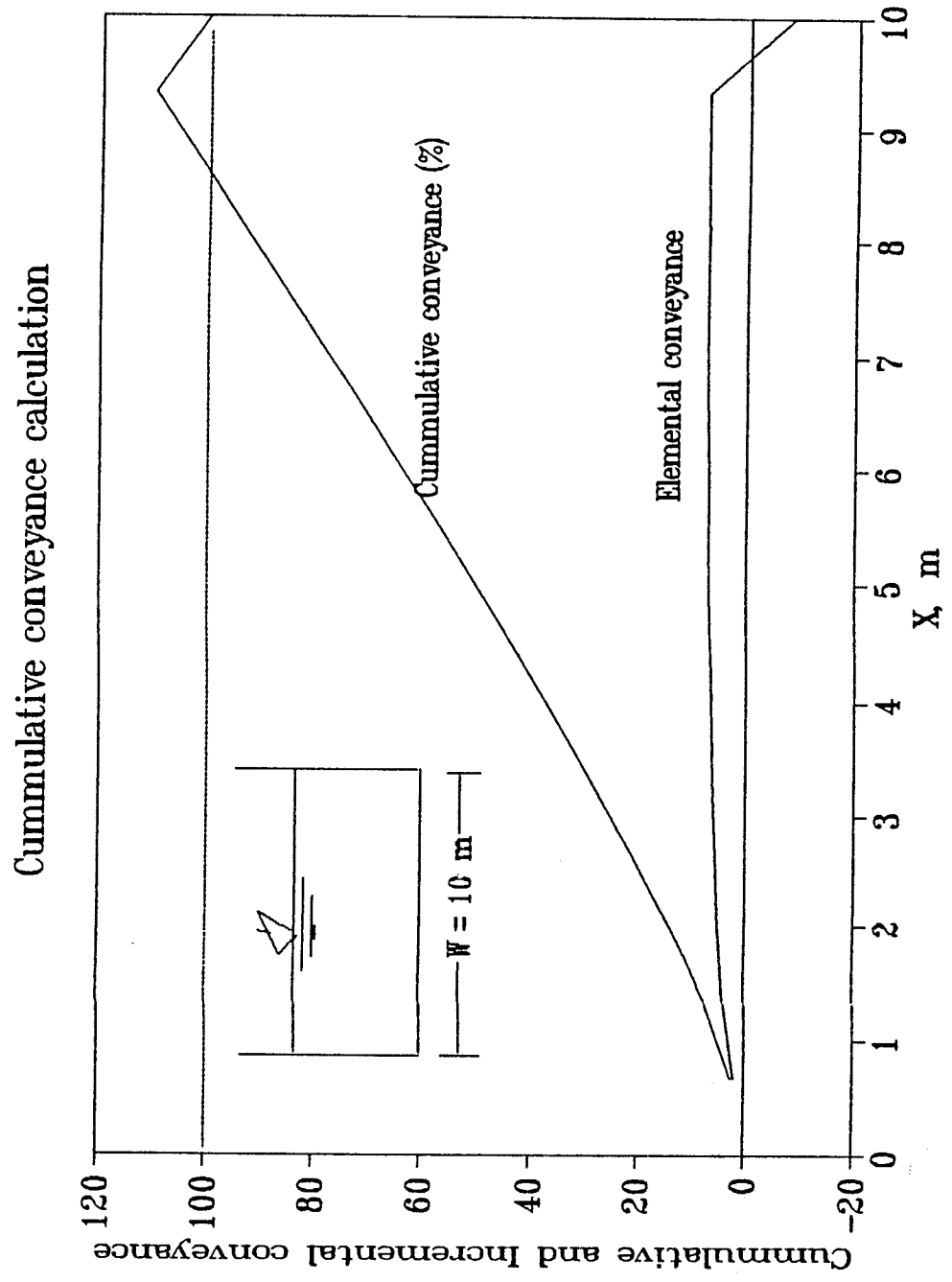

Figure 3.4: The Existence of Negative Conveyance at the Far End of a Rectangular Cross Section.

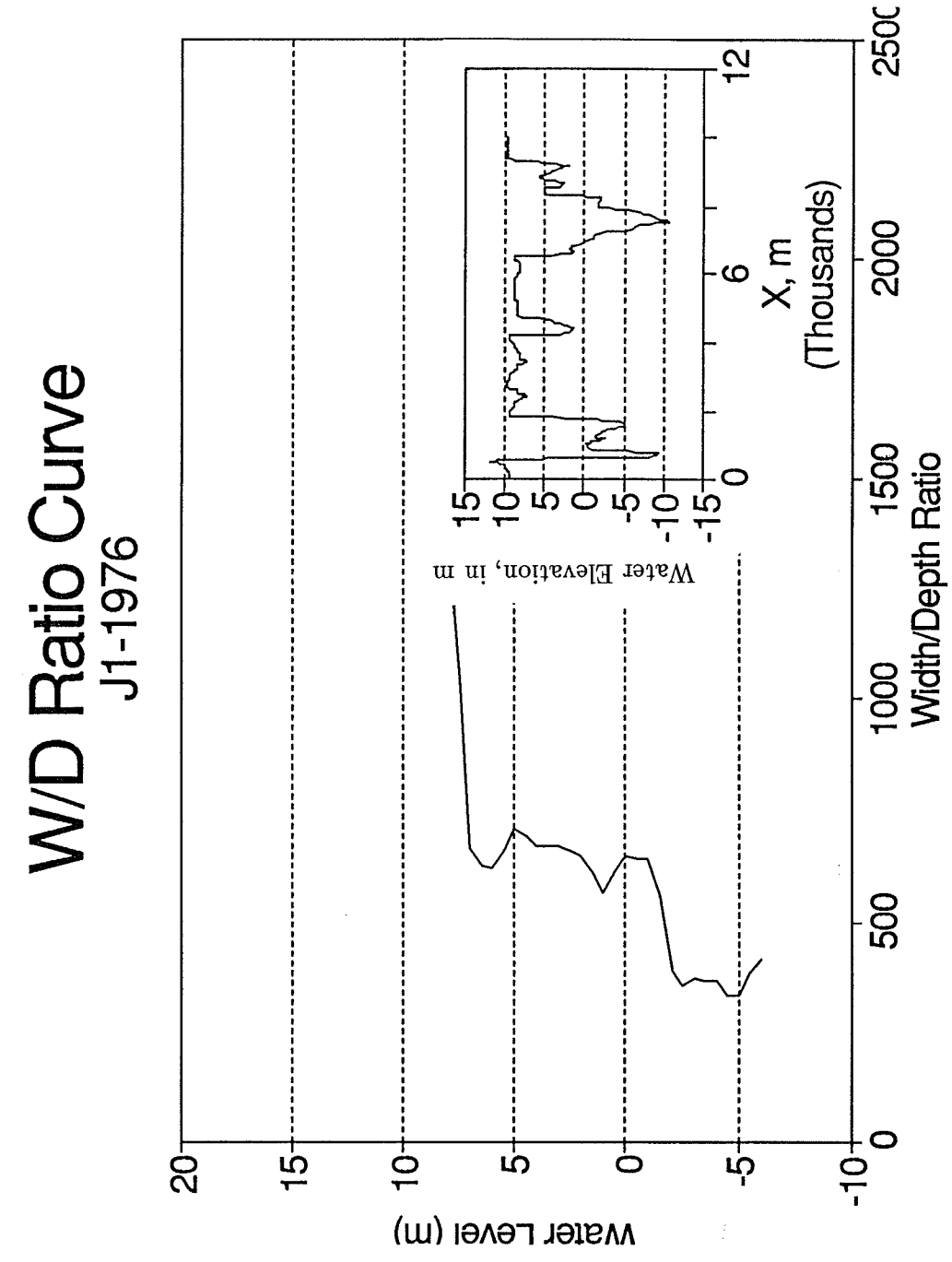

Figure 3.5: An Example of the Plot between Width/Depth Ratio and Water Level.

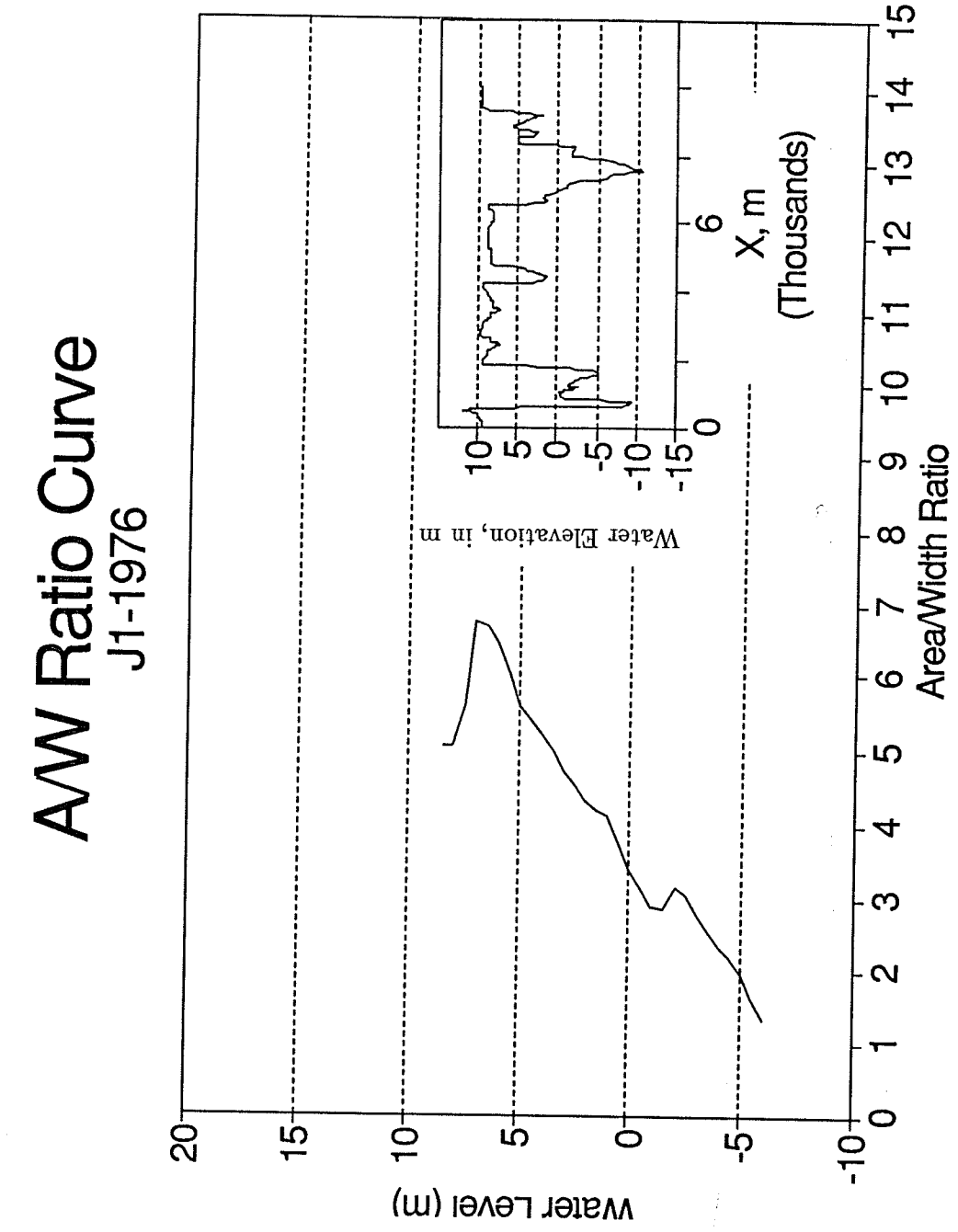

Figure 3.6: An Example of the Plot between the Flow Area and its Top Width.

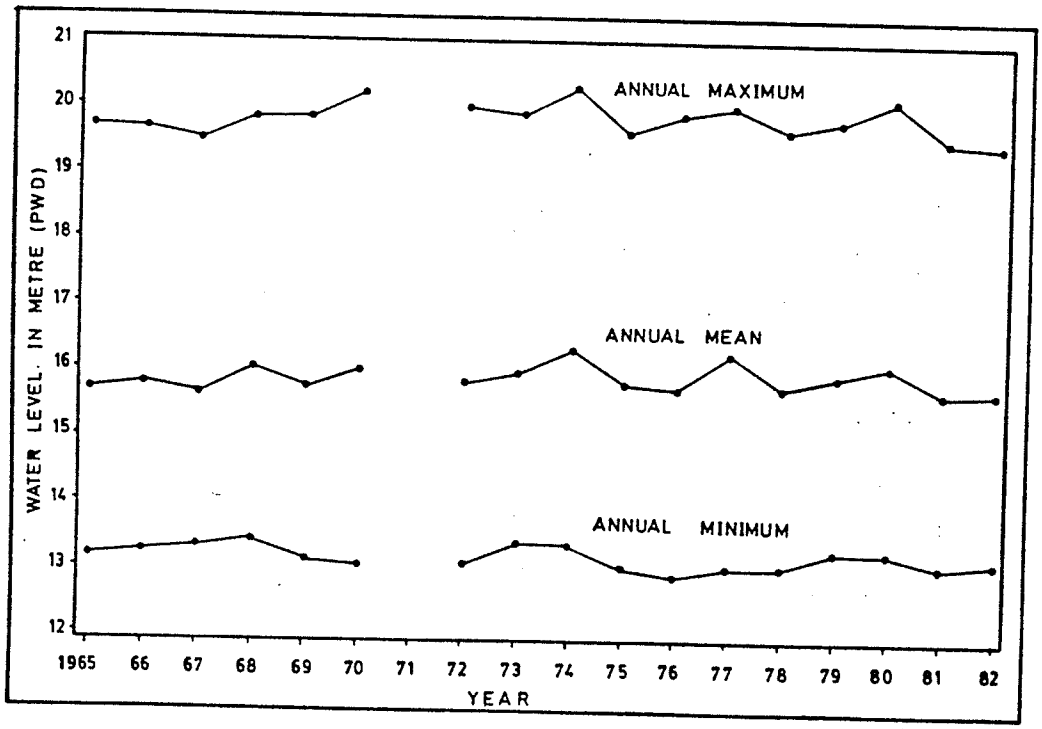

Figure 3.7: Time Variation of Water Level at Bahadurabad Station. (after Khan, 1988)

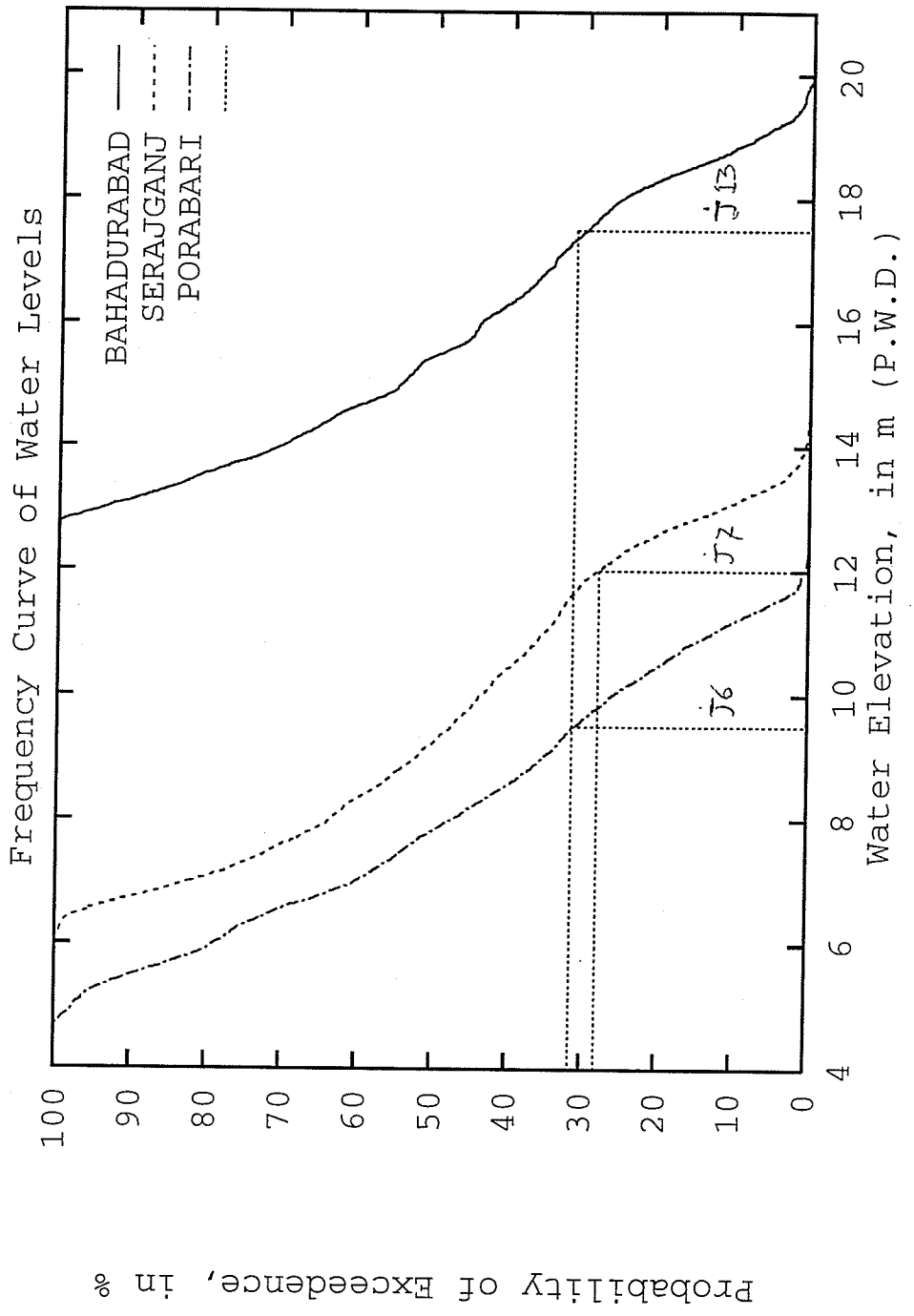

Figure 3.8: Frequency Curve of Water Levels at Bahadurabad, Serajganj, and Porabari Stations.

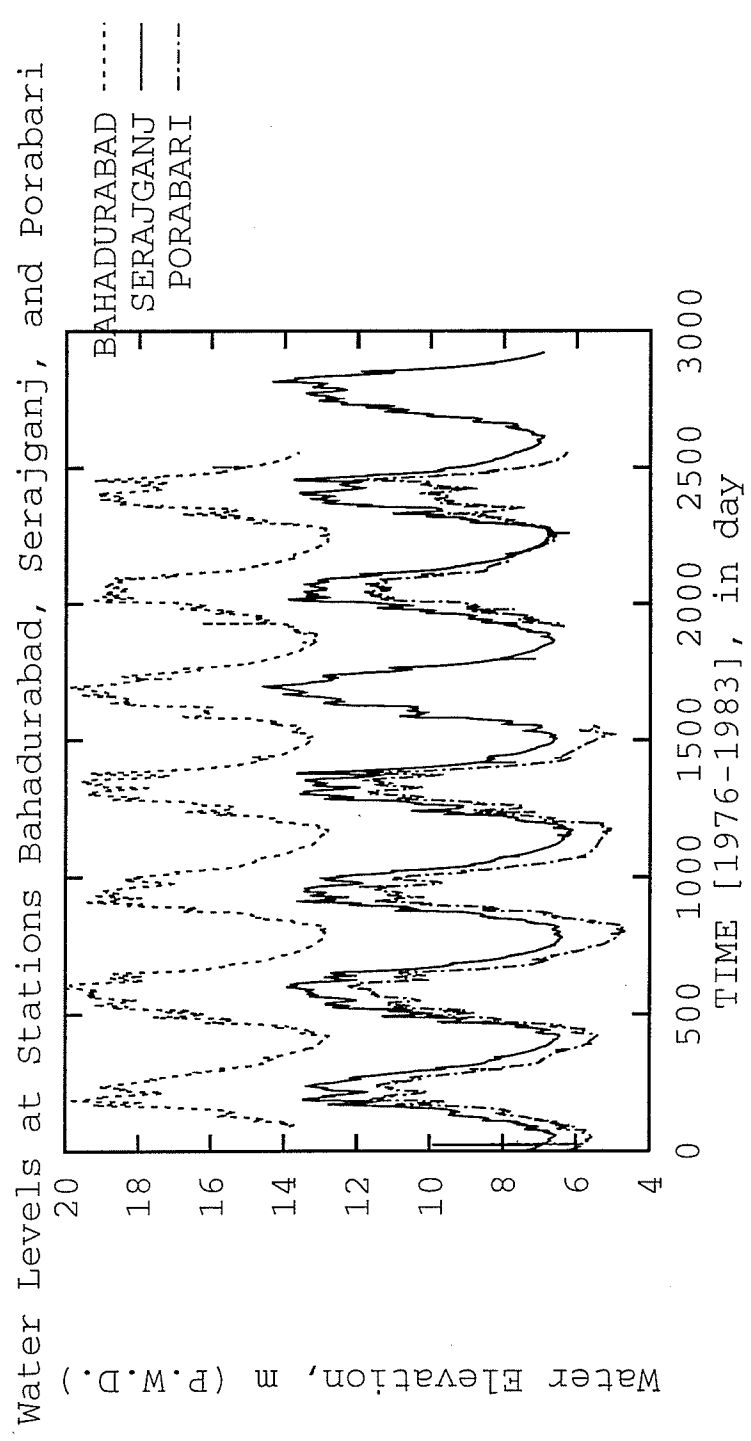

Figure 3.9: Water Levels at Stations Bahadurabad, Serajganj, and Porabari.

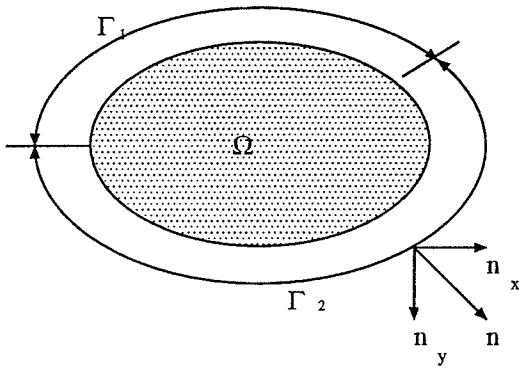

Figure 3.10: An example of a problem domain.

Chapter 4

RESULTS OF THE STUDY

A FORTRAN program outlined in Brebbia and Ferrante (1983) was used as the basis form in implementing the Finite Element method in this study. A slight modification of this program is performed to allow the solution of the Poisson's equation and the calculation of the location of centroid of flow conveyance.

The program is organized as follows (see Figure 4.1). First, it reads a data input. The data input contains information on the number of nodes, the number of elements, the number of nodes on the boundary, node numbers and their coordinates, element numbers and the nodes composing each element (called as element connectivity data), and node numbers on the boundary along with their boundary values. As an illustration, an example of a discretized cross section is shown in Figure 4.2. In this example, there are 109 nodes, 167 elements, and 35 nodes on the external boundary. The nodes on the external boundary are those nodes which circumscribe the discretized cross section excluding those nodes on the free surface of that section. In this study, the nodes on the external boundary represent the physical boundary separating the body of water from the land forming the channel. Therefore, those nodes are prescribed as having zero velocity.

Evaluation of each element matrix, step 2 in Figure 4.1, is performed by applying Equation (A.19). Application of Equation (A.19) to the first

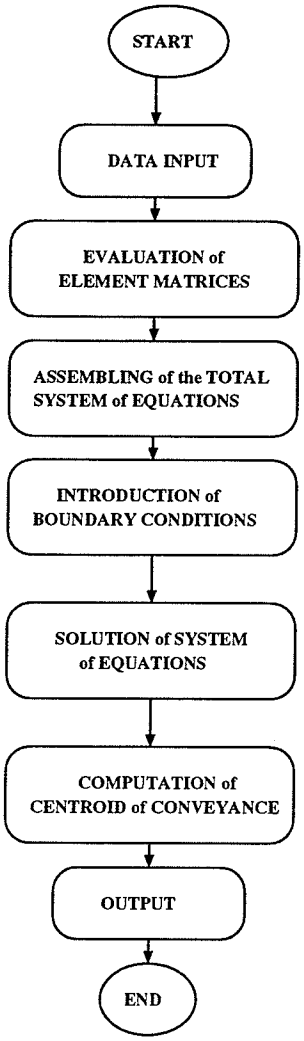

Figure 4.1: A Main Flow Chart of the Finite Element Analysis

element in Figure 4.2, for example, will give:

$$\begin{bmatrix} k_{11}^1 & k_{12}^1 & k_{17}^1 \\ k_{21}^1 & k_{22}^1 & k_{27}^1 \\ k_{71}^1 & k_{72}^1 & k_{77}^1 \end{bmatrix} \begin{Bmatrix} \phi_1 \\ \phi_2 \\ \phi_7 \end{Bmatrix} = \begin{Bmatrix} P_1^1 \\ P_2^1 \\ P_7^1 \end{Bmatrix} \tag{4.1}$$

Once all elements have been evaluated, all element matrices are to be assembled to form a total system of equations (step 3 in Figure 4.1). This step involves summation of all contributions from the interconnected ele-

ments. Suppose that we want to assemble the first and the second element matrices. The second element matrix is:

$$\begin{bmatrix} k_{22}^2 & k_{27}^2 & k_{28}^2 \\ k_{72}^2 & k_{77}^2 & k_{78}^2 \\ k_{82}^2 & k_{87}^2 & k_{88}^2 \end{bmatrix} \begin{Bmatrix} \phi_2 \\ \phi_7 \\ \phi_8 \end{Bmatrix} = \begin{Bmatrix} P_2^2 \\ P_7^2 \\ P_8^2 \end{Bmatrix} \tag{4.2}$$

The summation between these two matrices will result in:

$$\begin{bmatrix} k_{11}^1 & k_{12}^1 & \dots & k_{17}^1 & 0 & \dots \\ k_{21}^1 & k_{22}^1 + k_{22}^2 & \dots & k_{27}^1 + k_{27}^2 & k_{28}^2 & \dots \\ \vdots & \vdots & \ddots & \vdots & \vdots & \vdots \\ k_{71}^1 & k_{72}^1 + k_{72}^2 & \dots & k_{77}^1 + k_{77}^2 & k_{78}^2 & \dots \\ 0 & k_{82}^2 & \dots & k_{87}^2 & k_{88}^2 & \dots \\ \vdots & \vdots & \ddots & \vdots & \vdots & \vdots \end{bmatrix} \begin{Bmatrix} \phi_1 \\ \phi_2 \\ \vdots \\ \phi_7 \\ \phi_8 \\ \vdots \end{Bmatrix} = \begin{Bmatrix} P_1^1 \\ P_2^1 + P_2^2 \\ \vdots \\ P_7^1 + P_7^2 \\ P_8^2 \\ \vdots \end{Bmatrix} \tag{4.3}$$

When this summation is conducted for all elements, the system of equations is developed. The external boundary conditions are then introduced to the resulting total system of equations (step 4 in Figure 4.1). Once the total system of equations with the prescribed boundary conditions has been obtained, the solution of this system matrix can be obtained using any standard procedures to solve a set of simultaneous equations (step 5 in Figure 4.1). In this study it uses Gauss elimination and back subtitution.

The output of this solution is longitudinal velocity at each node. The calculation of the location of centroid of flow conveyance can then be performed using Equation 3.9 and 3.10 (step 6 in Figure 4.1).

The results of the analysis for the thirty three cross sections is listed in Table 4.1. This table shows the location (specified as a distance from the east bank) of the centroid of flow conveyance. Throughout the discussion, the values listed in this table are referred as CFEM (centroid of flow

Conveyance using the Finite Element Method). Another program was also written to calculate the location (again specified as a distance from the east bank) of the centroid of flow conveyance and flow area using the earlier methodologies introduced by Burger et al. (1988) and Goulter and Dubois (1988), respectively. The results of these analyses are listed in Tables 4.2 and 4.3, respectively. The values listed in Table 4.2 are referred as CCM (centroid of flow Conveyance using Conventional Method), while those in Table 4.3 as ACM (centroid of flow Area using Conventional Method). The locations of thalweg position are also listed in Table 4.4.

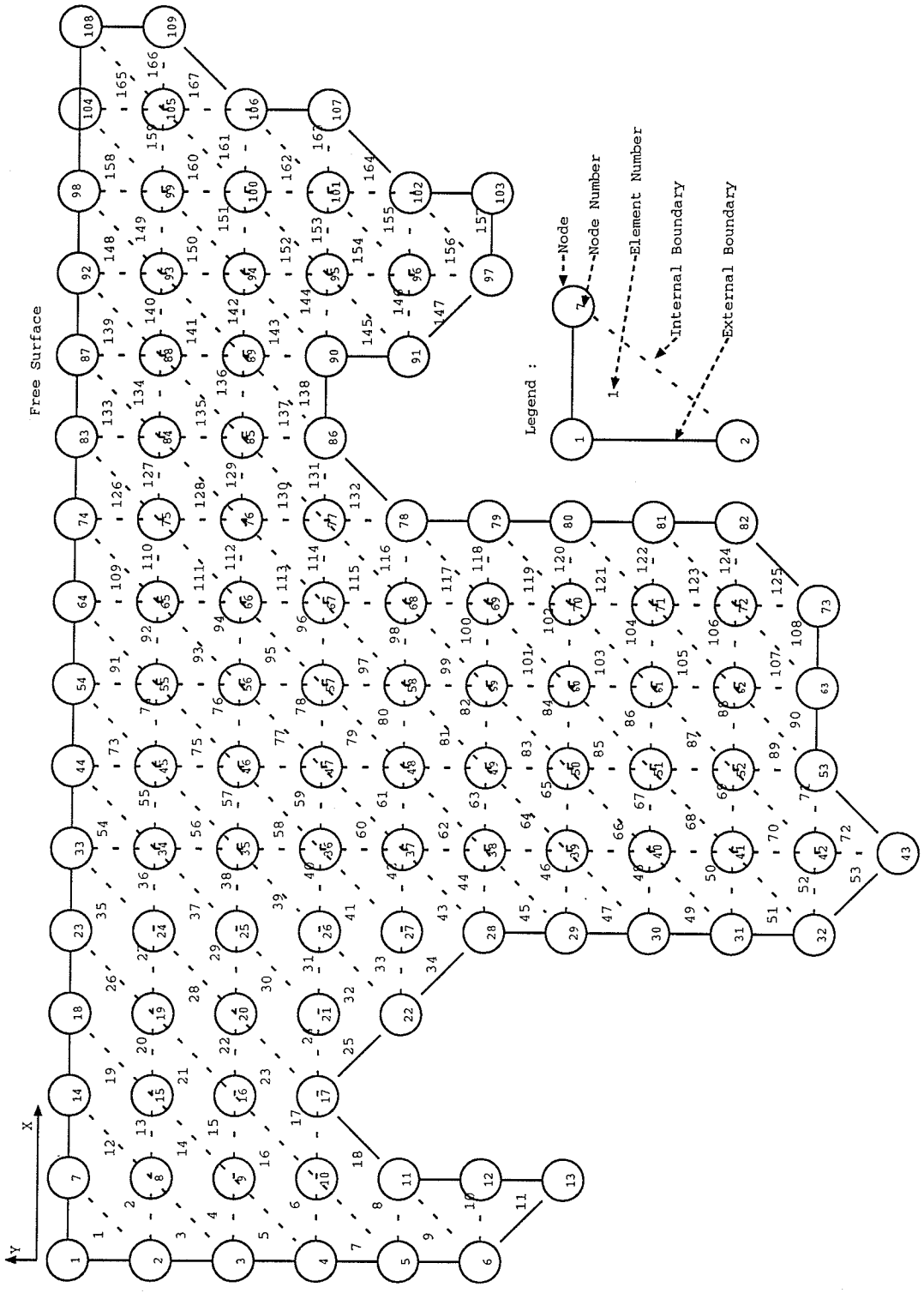

Figure 4.2: An Example of Discretization of a Hypothetical Cross Section

Table 4.1: Location of Centroid of Conveyance using Finite Element Method, CFEM.

Cross Section Number	Distance from the Left Bank in metres						
	Year						
	1976	1977	1978	1979	1980	1981	1983
J-1	5913.96	3842.86	4424.17	4567.05	4259.99	3985.35	6265.96
J-1A	3976.51	5888.61	5586.82	4488.12	4486.08	3946.89	6244.16
J-2	7898.54	8227.02	6798.72	7332.38	6140.77	6930.81	6486.38
J-2A	3755.94	3396.49	4793.89	4183.58	5741.75	6523.84	7503.71
J-3	4904.85	5956.35	4473.05	5629.34	6660.92	5724.57	3828.62
J-3A	2221.40	1476.24	1843.92	926.22	2599.26	2338.53	1650.83
J-4	5567.91	5462.93	5320.47	4523.30	4257.15	4555.69	5586.94
J-4A	17188.57	16314.13	16676.44	16184.59	17356.40	17721.01	13587.35
J-5	12365.08	11656.03	12310.22	11747.92	9206.82	9680.12	8827.73
J-5A	8433.69	9265.66	7264.89	7917.81	8599.68	7845.91	10541.85
J-6	11703.33	12467.80	12599.12	12901.51	12553.21	12740.09	12671.51
J-6A	2001.68	7865.09	7666.45	7421.04	7350.24	7105.63	7106.23
J-7	5747.87	6477.29	6004.70	5592.10	4000.72	4035.82	7199.80
J-7A	2000.81	9558.61	9546.28	9755.05	4758.98	5238.84	8153.08
J-8	5470.37	4974.09	7181.65	3986.67	3675.28	8916.96	3005.03
J-8A	3359.63	2694.98	3536.52	4594.21	NA	4738.54	7066.21
J-9	5672.52	5861.67	3913.77	3969.32	7153.75	7710.42	9763.53
J-9A	9931.46	9432.26	7857.07	8168.34	6280.58	4089.58	4034.97
J-10	9892.67	9891.14	8933.09	9107.82	4743.96	4622.03	5207.35
J-10A	3674.48	2946.56	4191.72	NA	6740.04	5935.66	7165.46
J-11	8459.76	5919.02	7663.04	6893.34	6141.82	6860.89	5817.30
J-11A	6436.20	7722.78	7618.27	8267.06	7322.59	10028.07	6235.77
J-12	11746.97	11902.23	9598.21	6252.76	7765.33	8019.86	7805.12
J-12A	7754.87	8767.96	8529.02	6430.27	9090.48	9620.93	9423.88
J-13	7782.79	6191.80	5791.81	6739.21	3331.75	3792.72	4592.28
J-13A	3970.84	5297.17	6234.97	7644.11	NA	14860.06	8399.95
J-14	10600.00	8946.91	6201.89	8925.22	6860.95	8601.86	6952.50
J-14A	6859.19	NA	7403.59	7314.47	6912.85	7694.17	9232.75
J-15	8173.54	3071.19	4562.36	6816.93	4577.72	5874.61	5902.86
J-15A	8653.72	8456.59	8605.33	7491.75	9834.68	9933.13	11079.10
J-16	11786.66	7069.48	10968.49	12083.10	11719.67	10669.00	9665.92
J-16A	8549.11	9152.56	9330.08	9783.19	9525.92	9334.15	8555.23
J-17	3660.25	4334.00	5234.62	4029.61	5714.72	5261.35	4614.42

Note: NA = Not Available

Table 4.2: Location of Centroid of Conveyance using Burger et al. Approach, CCM.

Cross Section Number	Distance from the Left Bank in metres						
	Year						
	1976	1977	1978	1979	1980	1981	1983
J-1	4489.58	4417.63	4207.15	4382.88	4422.72	3957.24	5110.24
J-1A	4821.35	5197.90	4935.05	4431.33	4367.24	3989.62	5852.67
J-2	7528.52	7359.81	6674.90	7920.46	6104.34	6694.95	6463.27
J-2A	5168.31	4954.25	5682.28	5058.65	5980.90	6246.34	6501.65
J-3	4966.37	5574.69	5291.89	5737.23	6109.67	5308.03	5231.86
J-3A	2565.91	1602.26	2069.19	1117.85	2691.48	2471.11	1913.39
J-4	5036.49	4126.96	4728.76	NA	4000.75	4093.35	5568.09
J-4A	14749.69	16095.22	16173.82	17321.28	17667.29	18260.92	14363.88
J-5	NA	12096.30	12222.35	11873.72	9484.09	9771.79	9320.26
J-5A	8834.91	8769.63	7654.42	7780.27	8283.10	8040.67	9657.40
J-6	11381.30	11546.95	12112.54	12446.67	12169.30	12276.93	12501.30
J-6A	7520.48	7469.33	7515.65	7419.17	7529.18	7332.09	7114.92
J-7	7146.23	7936.24	6847.26	6617.17	7255.65	5698.32	8031.99
J-7A	7056.42	8616.36	7831.37	8226.75	6828.33	7136.02	7735.70
J-8	6199.50	6364.19	6552.94	5682.23	4609.61	5751.69	6054.65
J-8A	4154.98	4213.10	4401.51	4302.00	NA	4981.82	5289.17
J-9	5881.30	4932.24	3835.88	3650.55	5452.13	6368.52	6808.48
J-9A	9384.16	8784.37	8582.46	8371.89	5137.81	4915.69	5140.67
J-10	9781.06	10359.78	9752.60	9616.27	5378.96	5468.08	6801.51
J-10A	4346.24	4201.53	5453.56	5656.77	7320.16	7810.03	7658.84
J-11	7973.10	7022.66	7124.18	6651.36	6033.99	6577.24	5819.39
J-11A	1698.10	8457.64	7692.87	8035.08	7469.50	10528.62	7372.80
J-12	11635.86	11879.53	NA	6593.18	7937.70	8120.87	8091.29
J-12A	8423.80	8693.41	8997.00	8783.50	8757.30	8905.28	8550.87
J-13	6182.99	5082.36	5026.94	5464.08	4175.01	4444.23	3979.48
J-13A	4233.95	5096.75	5582.97	5204.75	NA	6860.19	7405.78
J-14	7663.80	7683.77	6995.25	8201.22	7856.56	8301.73	9316.92
J-14A	7304.16	7248.07	7350.11	7100.44	6763.32	7332.02	7658.26
J-15	4532.58	4800.09	6271.18	6121.45	5518.84	5857.62	5990.07
J-15A	8682.72	8395.17	8926.44	8448.96	8747.18	9451.07	10613.52
J-16	10050.67	10575.48	10345.09	10927.89	10979.26	10587.92	10444.19
J-16A	8640.26	8405.17	9110.73	9374.20	9816.57	9135.81	8762.26
J-17	4696.69	4568.89	5275.35	5269.48	6544.32	6155.93	5631.73

Note: NA = Not Available

Table 4.3: Location of Centroid of Area, ACM.

Cross Section Number	Distance from the Left Bank in metres						
	Year						
	1976	1977	1978	1979	1980	1981	1983
J-1	4636.87	4481.60	4175.54	4332.47	4516.07	4069.13	5232.99
J-1A	4706.88	4999.94	4957.67	4398.28	4411.58	4079.96	5806.57
J-2	7304.26	7318.51	6741.05	7202.12	5971.33	6706.30	6305.96
J-2A	4903.38	4675.75	5031.97	4750.15	5592.98	5667.88	5643.37
J-3	5184.74	5583.10	5336.67	5782.20	6334.44	5272.49	5050.09
J-3A	2707.62	1939.27	2197.16	1452.78	2971.76	2566.81	2187.35
J-4	4737.64	4243.58	4568.43	NA	3962.71	3939.76	5345.37
J-4A	14118.17	15460.68	15893.45	16418.71	16740.34	17425.38	14156.47
J-5	NA	11910.23	11995.50	11516.74	9950.52	10055.79	9661.56
J-5A	8663.71	8603.12	7619.42	7601.31	8529.63	8231.57	9412.83
J-6	11073.91	11007.55	11637.69	11850.04	11822.06	11935.35	11985.27
J-6A	7488.12	7352.74	7285.09	7488.34	7572.15	7301.03	7042.26
J-7	7018.92	7488.83	6307.88	6150.66	6665.00	5649.48	7143.96
J-7A	7637.60	8352.06	7839.04	8337.27	7443.29	7592.76	7922.11
J-8	6604.83	6471.75	6765.43	6037.08	5322.30	6401.10	6469.09
J-8A	4575.85	4496.13	4711.86	4606.06	NA	5323.10	5605.80
J-9	6033.13	5508.49	4636.02	4330.85	6054.55	6763.47	7198.12
J-9A	9986.21	9355.97	9127.85	9037.52	5805.95	5657.60	5659.05
J-10	9940.76	10579.72	10200.36	10034.09	5984.00	6034.54	7096.17
J-10A	4934.30	4476.42	5550.21	5734.06	7111.38	7201.15	7434.62
J-11	7815.65	7025.97	7028.46	6678.88	6180.21	6523.75	6035.37
J-11A	1765.59	8706.56	8096.44	8477.96	7721.21	9979.77	7750.12
J-12	11876.30	12042.96	NA	6948.72	7940.21	8067.85	8106.24
J-12A	8137.18	8551.70	8809.64	8488.07	8574.58	8647.82	8342.61
J-13	6224.49	5416.71	5258.27	5657.26	4696.78	4837.09	4544.81
J-13A	4398.28	5417.00	5927.81	5837.76	NA	6838.07	7876.39
J-14	7939.13	7735.46	7221.44	8395.51	8199.73	8682.25	9174.26
J-14A	7322.86	7151.23	7235.93	7040.60	6692.75	7155.86	7551.25
J-15	4625.88	4539.95	5634.47	5783.16	5221.96	5557.95	5887.36
J-15A	8892.47	8454.19	8877.99	8498.79	8632.08	9087.45	10374.54
J-16	9768.95	10072.29	9970.00	10470.83	10343.93	10177.92	10413.54
J-16A	8538.74	8220.87	8880.52	9051.24	9545.33	8910.62	8587.85
J-17	4591.79	4578.08	4962.09	4954.11	6124.29	6096.55	5844.60

Note: NA = Not Available

Table 4.4: Location of Thalweg Position.

Cross Section Number	Distance from the Left Bank in metres						
	Year						
	1976	1977	1978	1979	1980	1981	1983
J-1	6592.90	6845.00	4393.75	3506.76	4287.93	3395.21	4033.91
J-1A	5192.00	5192.00	5215.00	4063.54	3690.81	4375.45	4479.18
J-2	7703.24	2990.16	7344.31	9861.90	8673.46	8099.29	7856.91
J-2A	8251.17	5496.07	8474.45	8407.00	8334.64	8815.47	8795.20
J-3	7607.70	6615.04	5748.85	7906.56	7653.53	7650.65	8178.65
J-3A	667.65	1363.34	1694.42	583.52	2784.75	2634.35	669.46
J-4	1559.07	1175.32	4962.43	6135.26	3542.79	4670.03	6395.37
J-4A	16038.04	16536.86	17978.92	19073.22	19365.55	19429.24	19649.48
J-5	11111.56	11914.73	11111.44	10839.44	8334.65	8330.97	7310.21
J-5A	8327.57	7797.06	7335.63	6941.07	8703.09	7855.03	11237.28
J-6	12627.12	12355.45	13035.15	13334.38	12640.53	12112.63	13769.15
J-6A	8444.70	8200.41	7967.96	7886.75	8373.68	7155.00	7049.26
J-7	11725.89	11217.76	11818.28	5624.17	11620.70	11847.14	11821.11
J-7A	1807.73	3139.79	14637.14	2483.45	15005.72	2281.93	12201.66
J-8	11444.40	1997.95	2053.80	1822.48	4073.78	10140.83	9358.76
J-8A	3313.83	3591.73	1599.51	1111.31	NA	1387.91	969.61
J-9	3519.67	2312.70	2705.26	1722.46	2845.60	2227.01	3337.68
J-9A	7838.10	8250.07	8038.20	8110.38	3054.31	3075.00	3260.28
J-10	7839.28	7673.77	7886.55	7612.42	3477.92	3541.99	5376.59
J-10A	1880.12	5862.10	5781.23	6202.83	6559.29	5502.23	13497.23
J-11	9072.98	6172.27	7076.82	5072.32	4015.62	8238.68	7888.71
J-11A	7200.85	14598.79	14733.07	7017.97	6866.95	14590.06	6395.00
J-12	10619.62	6430.42	17107.85	5684.85	11094.37	6511.07	7698.51
J-12A	8401.78	8992.26	9678.22	9827.14	9240.04	9915.45	11311.26
J-13	8501.65	7856.88	9001.89	1698.19	1610.57	8008.59	1676.56
J-13A	1148.77	1369.66	1019.10	4862.54	NA	2570.94	5136.97
J-14	7238.86	4034.44	8809.53	3747.26	7180.24	3008.25	7379.45
J-14A	7495.96	7680.93	7670.93	7603.27	6580.19	8176.10	9514.81
J-15	7242.32	7467.39	8178.69	4028.20	6010.61	6044.39	6117.26
J-15A	9913.84	9900.75	10441.18	9607.92	9511.65	10353.49	11888.63
J-16	8810.53	12004.38	12627.33	13318.18	13541.06	10962.17	11091.18
J-16A	8775.28	9037.95	9557.11	9457.13	10083.40	9464.53	9759.80
J-17	5410.57	4260.67	3825.51	3794.60	4325.88	4123.34	3697.64

Note: NA = Not Available

4.1 General Comparison

An evaluation of the results of the location of centroid of flow conveyance using the finite element method is performed by comparison to the earlier approaches.

Plots of the results of CFEM versus CCM, ACM and thalweg are shown on Figures 4.3, 4.4, and 4.5, respectively. Figure 4.3 shows the plot of the result of CFEM in the x axis versus the result of CCM in the y axis. A line of prefect agreement (a line with the slope of 1:1) is also drawn in the same graph. This line indicates a one–to–one matching between the results of the two methods. Thus, if the results of CFEM and CCM match perfectly, all the plotted points would lie along this line. The more scatter in the plotted points, the worse the agreement between those variables.

In Figure 4.3, there is a relatively good agreement between the results of CFEM and CCM. Most of the plotted points are closely grouped around the line of prefect agreement, and the relatively high coefficient of correlation (r=0.915) shown in Table 4.5 reflects this condition. Very similar results for CFEM and CCM (with less than 10% different) are observed in cross sections characterized by the existence of one dominant sub-channel. In this situation, the influences of other small sub-channels are insignificant and the cross section will behave like a single channel. Therefore, the CFEM and CCM will be located in the dominant sub-channel with no significant difference. This situation is perhap due to the use of solely viscosity based equation in the analysis. It implies that only molecular viscosity governs the flow mechanism, while in natural channel this viscosity is usually neglectable and, if any, exist only in a very thin sub-layer. In the future, an effort should be directed to the inclusion of secondary flows, and turbulence in the model.

It should be noted, however, significant differences (more than 10 %) between the results of CFEM and CCM are observed in most cases. A closer look at at the results shows that these differences are found in cross sections characterized by the existence of at least two dominant sub-channels one at each bank. These discrepancies can be explained by the fact that in the application of the first moment to calculate the location of the centroid of flow conveyance, the flow conveyances are weighted by the horizontal distance (from a certain reference point). As the Brahmaputra River is a very wide river, even a slight difference in the calculated flow conveyance of any sub-channel between the Finite Element method and the Burger et al. approach will result in noticable difference in the location of the centroid of flow conveyance predicted by the two methods. As explained in Chapter 3, the Burger et al. (1988) approach uses an elemental approach in which the flow conveyance of each vertical strip is calculated separately, instead of as interconnected strips. The resulting elemental flow conveyance is therefore less accurate. In wider sub-channels, this inaccuracy becomes significant. As a result, the difference in the calculated flow conveyance of wide sub-channel using both methods will be apparent. Additionally, in these cross sections the results of CFEM are generally tend to shift to a wider and more dominant sub-channel compare to that of CCM.

It is therefore asserted that the result of CFEM would be a better indicator of lateral migration of a braided river as it is able to account for the location of the more dominant sub-channel. It is observed, however, that in some cross sections the location of CFEM does not indicate the bankline at risk of erosion, rather local erosion process seems to have more influence on the bankline erosion of these cross sections. It is an area of future research

Table 4.5: Correlation Matrix of CFEM, CCM, ACM, and Thalweg.

	CCM	CFEM	Thalweg	ACM
CCM	1.000	0.909	0.781	0.993
CFEM	-	1.000	0.686	0.905
Thalweg	-	-	1.000	0.753
ACM	-	-	-	1.000

to consider this local erosion process in the study of the river migration. This fact suggests that the inclusion of u and v, velocities component at x and y, respectively, is necessary.

Figure 4.4 shows the plot between the results of CFEM and ACM. This figure shows the same general pattern as Figure 4.3, with a correspondingly very high coefficient of correlation (r=0.905). A closer look in the results of CFEM and ACM reveals that they do not show any noticable differences in the same cases where the results of CFEM and CCM are comparable. In the case where a cross section comprises of two comparably dominant sub-channels at either bank, the result of CFEM again shows a significant difference from the results of ACM. The result of ACM therefore, seems to be less favourable compared to the result of CFEM as, by taking into account the flow area only, the result of ACM can not actually explain in which direction lateral migration (if any) is likely to take place. The CFEM more clearly indicates the location of a dominant sub-channel, defined in terms of actual flow capacity. The movement of this dominant sub-channel may, in turn, indicate in which direction is lateral migration likely to occur.

This similar behaviour of the results of CCM and ACM compared to the result of CFEM indicate that the results of CCM and ACM are apparently

similar. This similarity may also be partly due to an assumption in the two approaches (ACM and CCM) that the location of centroid of each strip lies mid-way across the width of each elemental strip rather than being displaced by the shape of the strip and the centroid of elemental conveyance, respectively. As a result, the plot of the results of CFEM either with the results of CCM or ACM will show the same pattern. The apparently close correspondence in the results of CCM and ACM (see Figure 4.6) also seem to indicate that neither method has any particular advantage over the other and that the CFEM would, simply due to its more realistic physical basis, be better than both methods.

While the result of CFEM does not show a significant difference from the results of CCM and ACM, in most cases it does show a wide scatter when it is plotted against the thalweg position (see Figure 4.5). The coefficient of correlation (r=0.686) for the CFEM values plotted against thalweg position is relatively low as well. These thalweg positions also show a wide scatter as well when plotted against the results of CCM and ACM as shown in Figure 4.7 and 4.8, respectively. These situations suggest that the thalweg position is not an appropriate measure to indicate lateral migration of a braided river migration.

The condition is physically reasonable in that a braided river consists of multiple channels where each sub-channel may become more dominant, but not necessarily the deepest, sub-channel, and then split into several sub-channels. These possibilities cause the thalweg position alone to be an inappropriate measure for capturing the general mechanism of migration of the braided river. For example, suppose that a cross section of the river experiences a splitting, a process which is indicated by the existence of at

least two sub-channels in the river. The location of the channel (or sub-channel) with the deepest point of the cross section does not necessarily indicate the more laterally erosive channel, and therefore does not indicate movement of the channel. Defining the thalweg does not necessarily indicate the tendency in the direction of lateral displacement of that cross section as a whole. Another sub-channel may impose more influence on the lateral migration of the river if its flow conveyance is much greater than the sub-channel with the deepest depth. In addition, the location of the deepest depth in a braided river may suffice only to indicate the location where vertical erosion is more prominent.

An additional example which further supports the inappropriateness of the use of the location of thalweg position in a braided river is as follows. Suppose that the above dominant sub-channels discussed in the previous paragraph are relatively comparable in their sizes and local conditions. These two sub-channels may 'compete' over the long term to become the one with the deepest depth. In face of this 'competition' the location of thalweg may change alternatively from one sub-channel on one side of the river to another sub-channel on the other side of the river. Even a slight change in the depth of a particular channel may cause the location of thalweg to change drastically from the left bank to the right without any significant change in the location of the centroid of conveyance. This situation may explain why the location of thalweg wanders around within the river belt of the Brahmaputra river from time to time as reported by Coleman (1969). An illustration of this circumstance is explained in Figure 4.9 which shows a time variation plot of the results of CFEM, CCM, ACM, and thalweg position of cross section J-7A. This time variation plot will be explained

further in the next section. This figure clearly shows that the location of thalweg position switches alternatively from one bank to another bank of the cross section, while the other measures (CFEM, CCM, and ACM) are relatively constant.

It is therefore asserted that the location of thalweg position is not an appropriate measure to indicate a lateral migration of a braided river. Furthermore, it appears that the results of CFEM are not particularly different from the results of CCM and ACM, especially in those cross sections with the existence of a single dominant sub-channel. However, in a cross section with the existence of at least two sub-channels, which is inherent in a braided river, the CFEM is preferable over the CCM and the ACM.

In the next section, a further evaluation to investigate the general trend of lateral displacement described by these measures as indicated by their variation over time is performed. A more in depth evaluation of the result of CFEM to determine the consistency of this measure by analysing the curve of relative conveyance is also performed .

4.2 Time Variation of the Results of CFEM, CCM, ACM, and Thalweg Position

A quantitative analysis on the trend of the results of these measures is not possible due to the limited length of the record. A qualitative analysis based on the results of CFEM, CCM, ACM, and THALWEG is therefore provided. A time variation plot of these measures at individual cross sections is used in this approach. An example of such a plot is shown in Figure 4.9. The time variation plots of these measures for the all cross sections are shown in the Appendix B.

In the previous section, it is explained that thalweg position is not an appropriate measure of lateral migration of a braided river. Therefore, this section only deals with the results of CFEM, CCM, and ACM. In Figure 4.9, it is clear that there is no significant diference in the results of CCM and ACM over the time period. The CCM and ACM values are relatively constant over the year 1976 to 1983, being located at about $8,000$ m from the left (east) bank. In the other hand, the result of CFEM shows significant change, but in an erratic pattern. In the year 1976, the location of CFEM is near the left bank, at $2,000$ m from the left bank. It then moves westward to a distant of about $10,000$ m from the left bank in the year 1977, and stays relatively constant in the year 1978 and 1979. In the next year, it moves eastwards to distant of about $5,000$ m from the left bank. In year 1981, it moves westward slightly, then further westward movement is observed in year 1983. This type of erratic movement is observed in most of the analysed cross sections. Out of the thirty three cross sections being analysed, there are only a few cross sections that show a general 'trend' of lateral migration during the period of study. These cross sections which show the general 'trend' to move westward are cross sections J-2A, J-6, J-8A, J-9, J-10A and J-16A. While the cross sections J-2, J-5, J-9A, J-10, and J-13 show an eastward 'trend', the remaining cross sections experience an erratic movement over the period of study and thus they do not show any general trend of movement.

4.3 Cumulative Relative Conveyance Curve

Relative conveyance at a point across a specified cross section is defined as the ratio of flow conveyance of cross section up to that point, to the total

flow conveyance of the complete cross section, stated in percent. The plot of the cumulative value of these relative conveyances will result in a cumulative of relative conveyance curve (CRCC). An example of of this curve is shown in Figure 4.10 showing a time variation of cumulative conveyance of cross section J-1. The CRCC curves for the each of the thirty three cross sections examined in this study are shown in Appendix C.

In a CRCC curve, a horizontal line indicates that, at this portion of the curve there is no additional flow conveyance, and therefore, there is no sub-channel. The height of a portion of this curve from one horizontal line to the next one indicates the contribution to the flow conveyance of that cross section. The higher vertical steps in the CRCC curve indicates that the sub-channels at those sections are more dominant, in terms of their flow conveyance, than the other sub-channels.

Other information contained in this CRCC curve is that the slope of a portion of this curve indicates the rate at which the corresponding sub-channel contributes to the overall channel conveyance. Thus, a steep portion of the curve indicates, for example, that the associated sub-channel is likely to have a deep bed. It should be noted that the CRCC curve can identify these characteristics, and that each CRCC curve is specific to the associated cross section. Thus the change in shape and/or pattern of this curve with space and time can show the overall differences in properties of different cross sections and the overall differences over time at a specific cross-section respectively. For example, should a cross section experience a lateral migration, movement of the vertical or near vertical lines would be observed in the CRCC curve indicating a shift in which one or more sub-channels are migrating consistently in one direction and thereby 'pushing'

the river belt in the direction of migration.

In Figure 4.10, the dominant sub-channel in year 1976, which is indicated by the highest portion of this curve at that cross section, is located at the right bank at 6,000 m to 8,000 m from the reference point (east bank). The sub-channel at the left bank is only a minor sub-channel at this time, contributing only about 15.0% of flow conveyance, while the right sub-channel contains about 65.0% flow conveyance. The amount of contribution of flow conveyance of a sub-channel can be obtained in the figure as the height of the portion of the curve contained in that sub-channel.

In the following year, 1977, the minor left bank sub-channel becomes more dominant with its contribution to the flow conveyance increasing to about 30.0%. The once dominant sub-channel becomes drastically less dominant and its contribution to the flow conveyance is reduced to about 20.0%. Another sub-channel, which contributes about 45.0% of the total flow conveyance, develops at a distance of 3,000 m to 5,000 m from the east bank. In the subsequent years up to 1981, the middle sub-channel seems to have coalesced with other sub channels and becomes the only channel. During these later years, the highest and the steepest portions remain stagnant, and thus the shapes of the curve do not shift significantly in an apparent pattern. This observation indicates that the river at that cross section does not experience apparent lateral movement.

In 1983, however, this cross section seems to experience 'splitting' where three sub-channels are formed, replacing the single sub-channel of the previous years. The first sub-channel is only minor, while the second, which is formed at 3,000 m to 5,000 m from the left bank, contains about 35.0% of flow conveyance. The last sub-channel, which is formed at about 6,000 m

to 10,000 m from the left bank, contributes about 60.0% of flow conveyance. This sub-channel seems to have 'pushed' the river out of its previous belt. There is no indication, however, whether this sub-channel will: further 'push' out the river belt; remain there; or even move back to east to join with another sub-channel. It seems that, although there was a significant eastward shift of the sub-channel from 1976 to 1977, the general tendency of the lateral migration of this cross section, within and out of the river belt, was not apparently observed during the years 1978 to 1981. In year 1983, the river shifted and pushed the river belt westward.

Examination of the CRCC curve of the thirty three cross sections reveals that during the period of the study, most of the analysed cross sections do not indicate lateral migration out of the river belt. It therefore, appears that the Brahmaputra river does not experience a specific trend of lateral migration out of the river belt over the period of study. The only conclusion that can be made is that, during the period of study, the river experiences an erratic sub-channel migration within the river belt. A similar pattern of migration was also reported by Coleman (1969).

Figure 4.3: Comparison of the results of CFEM and CCM

Figure 4.4: Comparison of the results of CFEM and ACM

Figure 4.5: Comparison of the results of CFEM and Thalweg

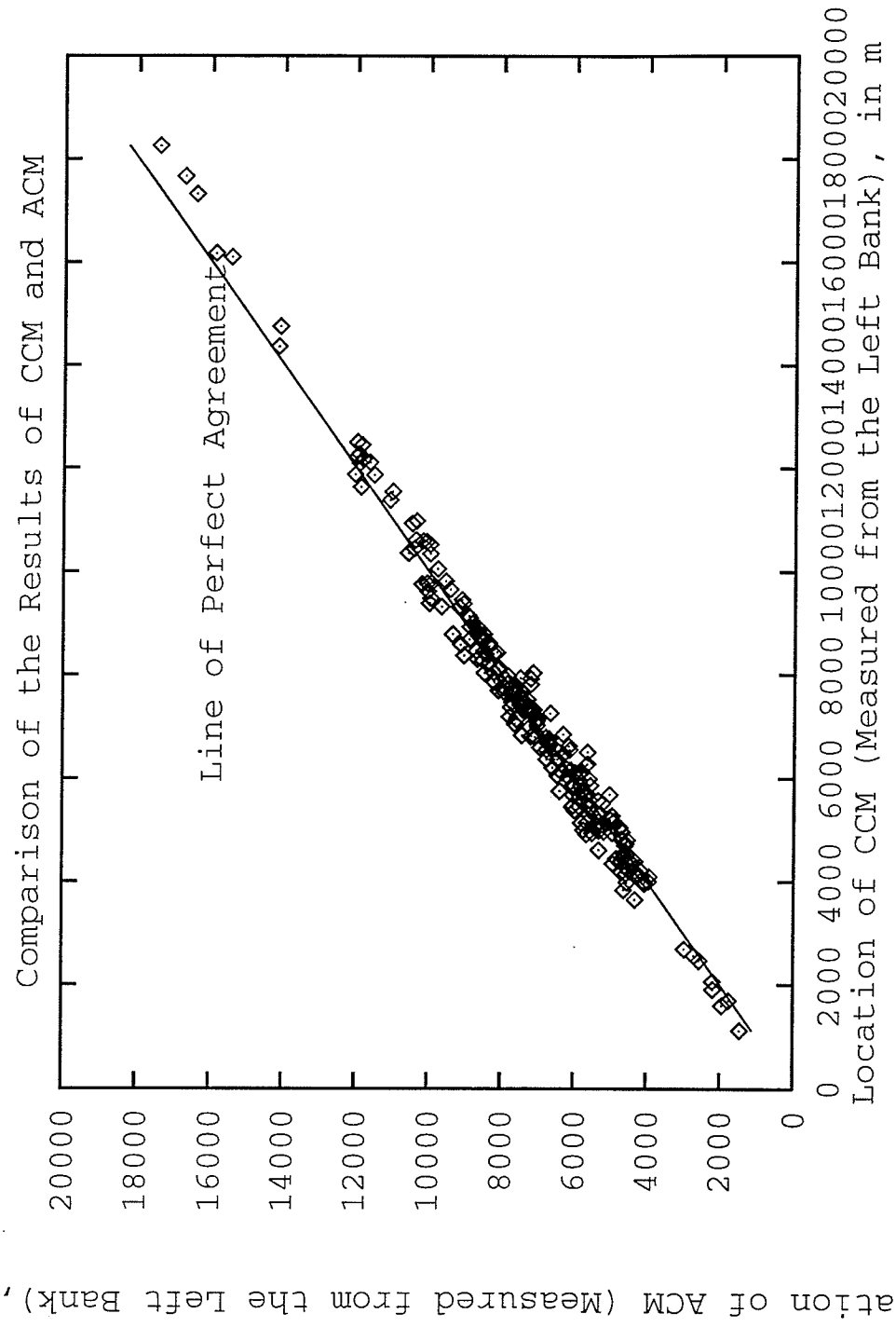

Figure 4.6: Comparison of the results of CCM and ACM

Figure 4.7: Comparison of the Results of CCM and Thalweg

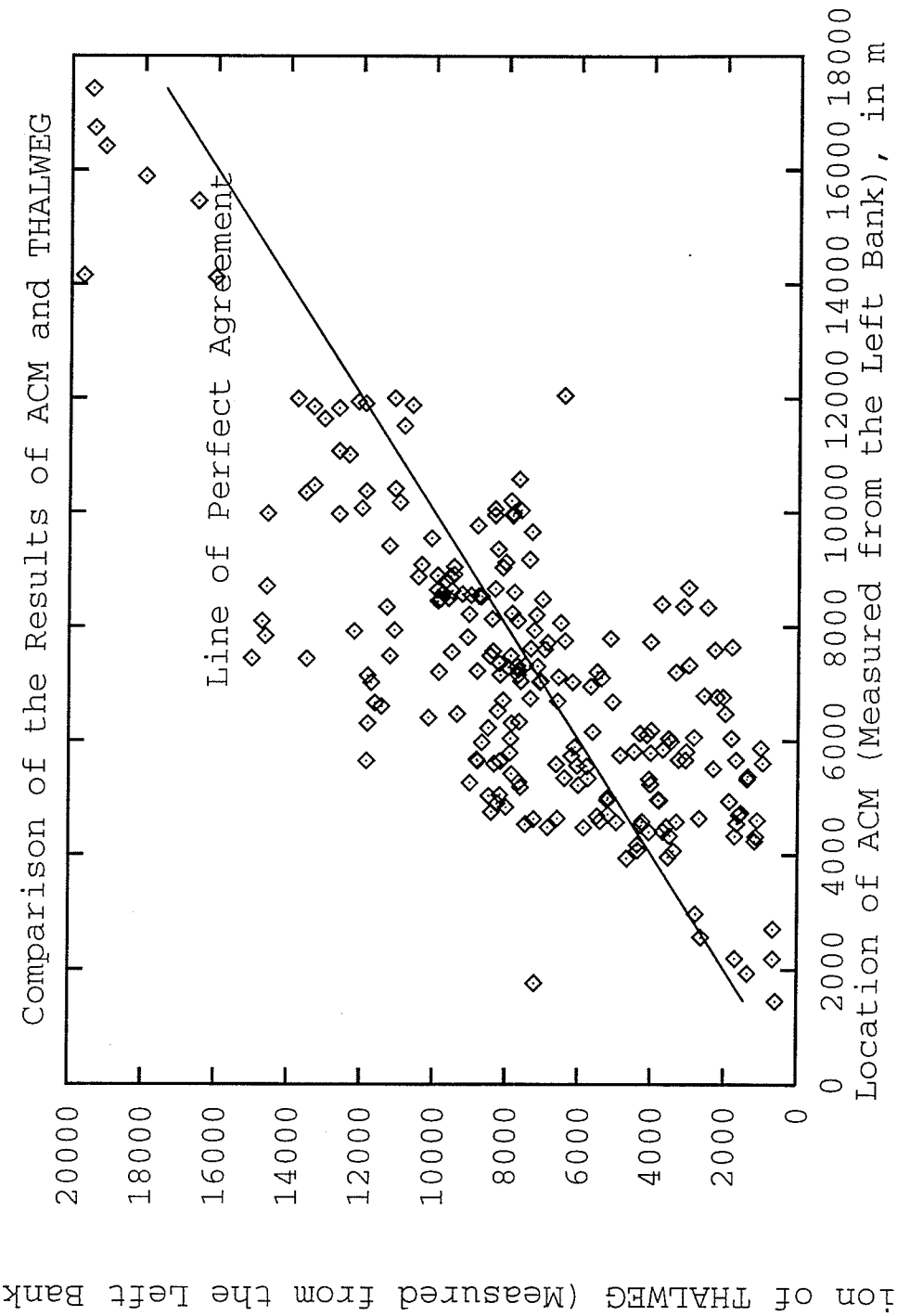

Figure 4.8: Comparison of the Results of ACM and Thalweg

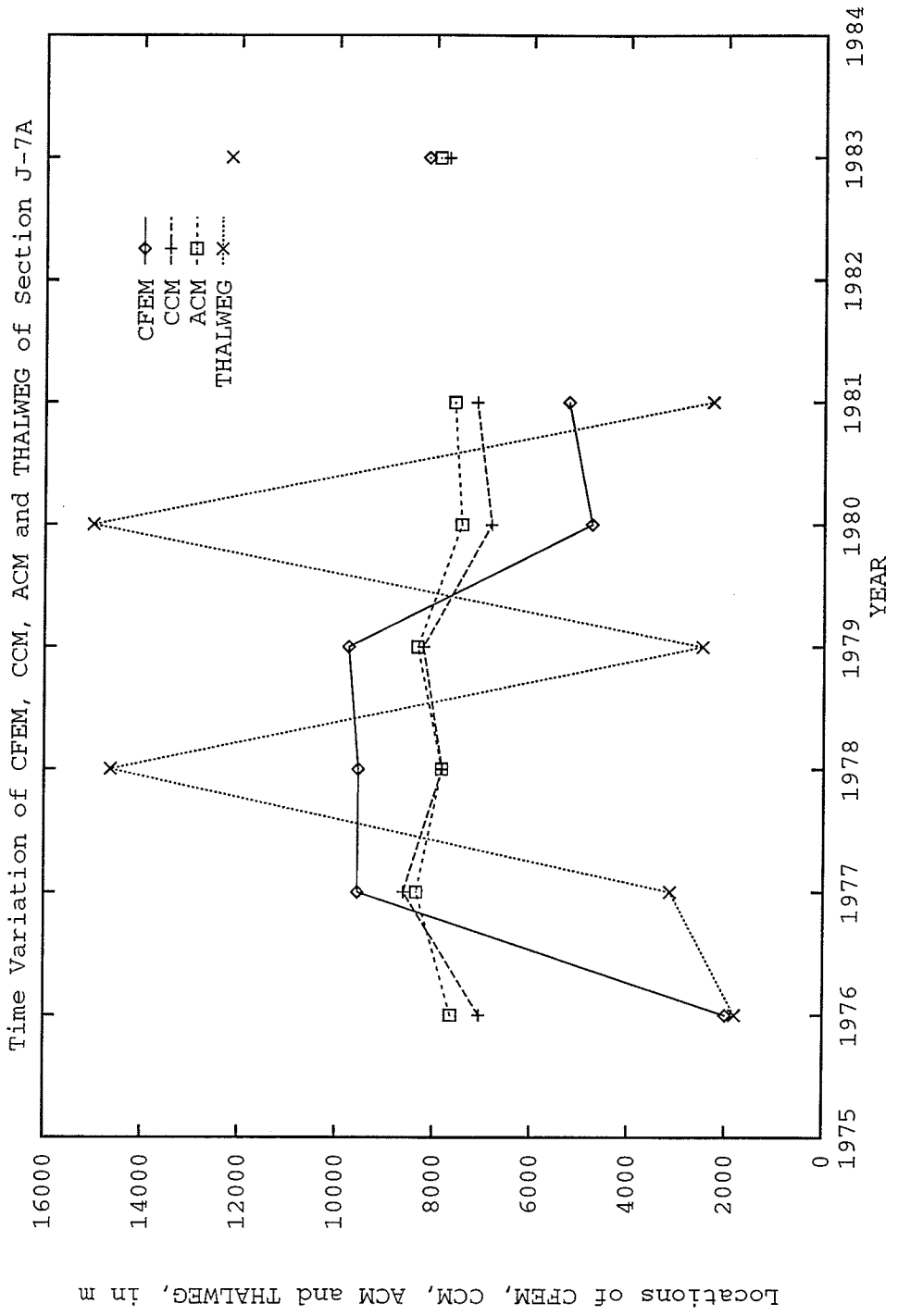

Figure 4.9: Time Variation of the Results of CFEM, CCM, ACM, and Thalweg of Cross Section J-7A

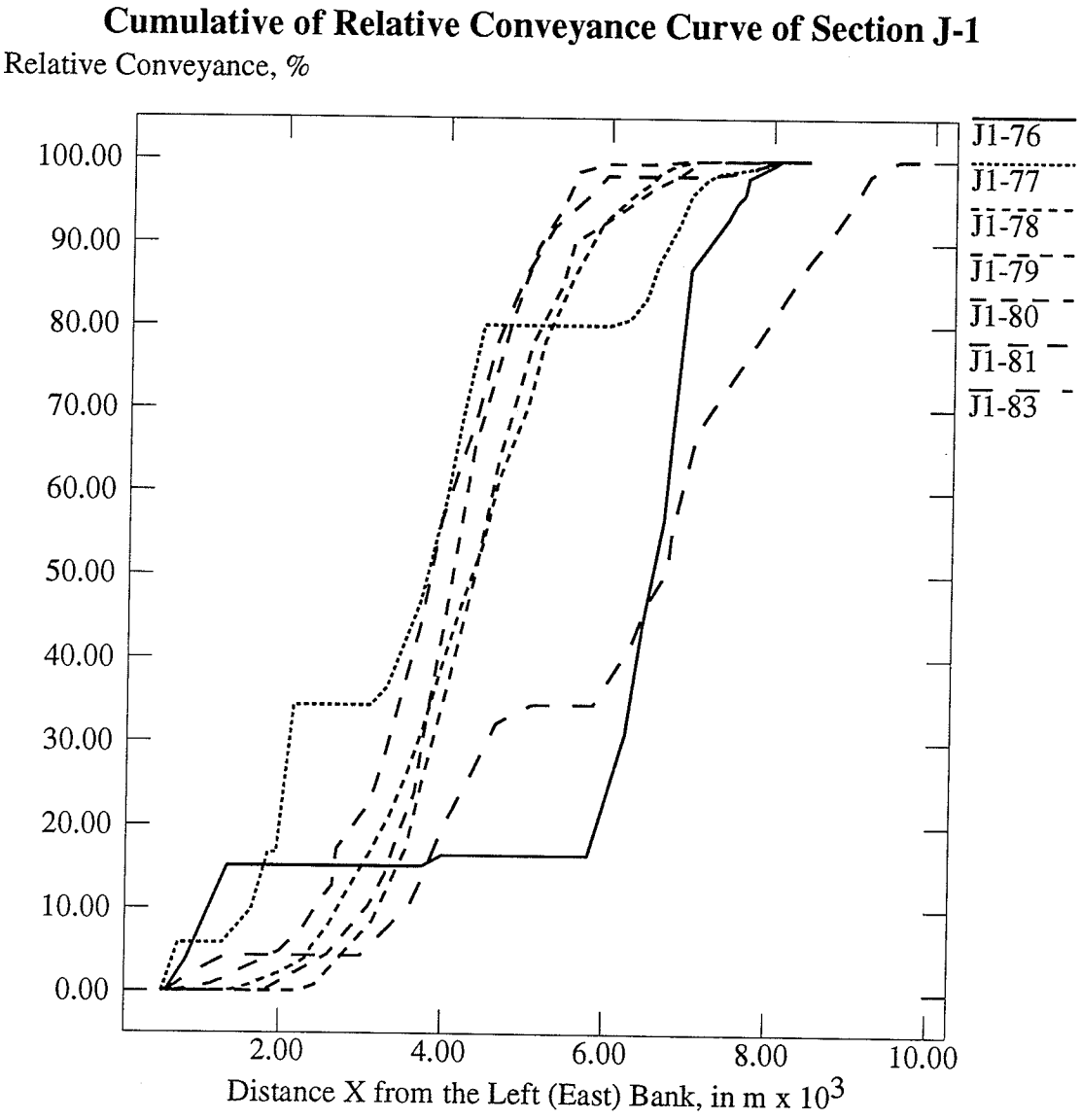

Figure 4.10: A Cumulative of Relative Conveyance Curve of J-1.

Chapter 5

CONCLUSIONS AND RECOMMENDATIONS

The advantage of this approach is that it overcomes the problem of negative flow conveyance encountered in an approach proposed by the Burger et al. (1988). Because a negative flow conveyance is physically impossible, this method should provide a more realistic results. The approach proposed in this study can also detect more realistically the location of the more dominant sub-channels. The value of the approach is demonstrated by its application to the Brahmaputra River in Bangladesh. The results of this study lead to the following conclusions.

5.1 Conclusions

1. The location of the centroid of flow conveyance calculated using the finite element method does not show a significant difference with that of the earlier methods for cases where a single dominant sub-channel exists in the cross section. This is partly because of using only a viscosity based equation in the analysis. This constant viscosity, in fact, would not be able to explain the flow interaction between elements. Therefore, the consideration of secondary flows and mechanism of turbulence should be included in future work.

2. In the case where a cross section is truly composed of multiple channels, a condition typical of braided rivers, the result of CFEM would seem to be superior to other methods as it explicitly considers the 'true' measure of flow capacity in a river, namely, flow conveyance and calculates that flow conveyance in a consistent fashion recognising the relationship between adjacent elemental strips of the cross section. Additionally, the CFEM is able to indicate the location of a more dominant sub-channel, which is assumed as an indicator of an overall cross section lateral migration. However, it is observed that in some cross sections the location of CFEM does not show the bank lines which is likely to experience erosion, rather, local erosion seems to influence this rivier migration. Again, the inclusion of secondary flows and the turbulence mechanism in the model would be usefull in modelling this local processes.

3. The use of a cumulative relative conveyance curve can facilitate the understanding of the channelization process of a braided river. This curve is specific to a cross section, so that any change in the shape and conveyance of that cross section with time or change in conditions with distance along the river can be monitored.

4. The Brahmaputra river did not experience a noticable migration out of the river belt during the period of study. The time variation of the result of CFEM for every cross section indicates that most of the analysed cross sections do not show any specific pattern of lateral migration. However, the results of CFEM do indicate the existence of an erratic lateral movement within the river belt in most analysed cross sections. As a whole, the Brahmaputra river, therefore, does not

experience an overall lateral migration over the period of study.

5. The location of thalweg may not be an appropriate measure in identifying the migration of the braided Brahmaputra river. The use of thalweg can assist in understanding of local process of erosion.

5.2 Recommendations

1. In order to evaluate the results of the locations of centroid of flow conveyance quantitatively, a longer period of data acquisition is necessary. In addition, data acquisition at additional sites is necessary. It should be emphasized on having an equally spaced cross section measurements to allow a formal statistical analysis on the trend of the migration, if any, over time and space.

2. Expansion of the approach into three dimensional analysis, with the inclusion of secondary flows and turbulence mechanism, would provide a better understanding the processes of lateral migration of the Brahmaputra river.

3. In order to support an unsteady three dimensional analysis, it is necessary to have more frequent time variation of the cross section data and flow discharge during flood period. A much closer cross section measurements which able to fairly depict the configuration of the channel would be necessary.

Bibliography

[1] ANDREWS, E. D., 1982. "Bank Stability and Channel Width Adjustment, East Fork River, Wyoming". Water Resources Research, 18(4):1184-1192.

[2] BWDB (Bangladesh Water Development Board), 1978. Morphological Features of Major Rivers of Bangladesh, Part I - Report. Dacca: Directorate of River Morphology, Research and Training.

[3] BREBBIA, C. A., and A. FERRANTE, 1983. Computational Hydraulics. Butterwoths & Co. (Publisher) Ltd, London. 289 p.

[4] BRISTOW, S., 1987. "Brahmaputra River: Channel Migration and Deposition". in : Recent Developments in Fluvial Sedimentology, Frank G. Ethridge, et. al. , (ed.), Society of Economic Paleontologist and Mineralogist, Special Publication no. 39:43-74.

[5] BURGER, J. W., G. J. KLAASSEN, and A. PRINS, 1988. "Bank Erosion and Channel Processes in the Jamuna River, Bangladesh". Paper Presented at the International Symposium on the Impact of River Bank Erosion, Flood Hazard, and the Problem of Population Displacement, Dhaka, Bangladesh.

[6] CHANG, H. H., 1977. "Minimum Stream Power for Rivers and Deltas". Journal of Hydraulics Division, ASCE, 103(HY12):1375-1389.

[7] CHANG, H. H., 1979. "Minimum Stream Power and River Channel Patterns". Journal of Hydrology, 41:303-327.

[8] CHANG, H. H., 1982. "Mathematical Model for Erodible Channels". Journal of Hydraulics Division, ASCE, 108(HY5):678-689.

[9] CHOWDHURY, E. H., 1988. Impacts of River Bank Erosion Hazard in the Brahmaputra-Jamuna Floodplain: A Study of Population Displacement and Response Strategies. PhD. thesis, Department of Geography, University of Manitoba, Winnipeg, Canada. 434 p.

[10] COLEMAN, J., 1969. "Brahmaputra River: Channel Processes and Sedimentation". Sedimentary Geology, Elsevier Pub. Co., Amsterdam, Netherlands, 3:129-139.

[11] FINLAYSON, B. A. and SCRIVEN, L. E., 1967. "The Method of Weighted Residuals–A Review". Applied Mechanics Reviews, 19(9):735-748.

[12] GARG, S. P., 1976. FORTRAN IV and Engineering Applications, Nem Chand & Bros, Roorkee, India, p. 552.

[13] GOSWAMI, D., 1985. "Brahmaputra River, Assam, India: Physiography, Basin Denudation, and Channel Aggradation". Water Resources Research, 21(7): 959-978.

[14] GOULTER, I., and DUBOIS, D., 1988. "Methods for Presenting Trends in Channel Capacity Movement as an Indicator of River Bank Erosion Risk in the Jamuna River". Paper Presented at the International Symposium on the Impact of River Bank Erosion, Flood Hazard, and the Problem of Population Displacement, Dhaka, Bangladesh.

[15] GRAF, W. L., 1984. "A Probabilistic Approach to the Spatial Assesment of River Channel Instability". Water Resources Research, 20(7):953-962.

[16] HARVEY, A. M., 1969. "Channel Capacity and the Adjustment of Streams to Hydrologic Regime". Journal of Hydrology, 8:82-98.

[17] KHAN, Md., A. O. A., 1988. Statistical Analysis of Bank Erosion of the Brahmaputra River in Bangladesh. MSc. Thesis, Department of Civil Engineering, University of Manitoba, Winnipeg, Canada, 149 p.

[18] KOUTITAS, C. G., 1983. Elements of Computational Hydraulics. Pentech Press, London:Plymouth, 137 p.

[19] LATIF, A., 1969. "Investigation of the Brahmaputra River". Journal of the Hydraulics Division, ASCE, 95(HY5):1687-1698.

[20] MOSLEY, M. P., 1982. "Analysis of the Effect of Changing Discharge on Channel Morphology and Instrem Uses in a Braided River, Ohau River, New Zealand". Water Resources Research, 18(4):800-812.

[21] PETROBANGLA, 1983. Techno Economics Study for Gas Supply to Western Zone: Appendices, Dhaka.

[22] PICKUP, G., and R. F. WARNER, 1976. "Effect of Hydrologic Regime on Magnitude and Frequency of Dominant Discharge". Journal of Hydrology, 29:51-75.

[23] RILEY, S. J., 1972. "A Comparison of Morphometrics Measures of Bankfull Discharge". Journal of Hydrology, 17:23-31.

[24] STENE, L. P., 1988. "Brahmaputra-Jamuna Channel Behaviour, Bangladesh: 1976-1983". Presented at the International Symposium on the Impact of River Bank Erosion, Flood Hazard, and the Problem of Population Displacement, Dhaka, Bangladesh.

[25] WILLIAMS, G. P., 1978. "Bankfull Discharge of Rivers". Water Resources Research, 14(6):1141-1154.

[26] YEN, C. L., 1970. "Bed Topography Effect on Flow in A Meander". Journal of the Hydraulics Division, ASCE, 96(HY1):57-73.

[27] YANG, C. T., 1976. "Minimum Unit Stream Power and Fluvial Hydraulics", Journal of Hydraulics Division, ASCE, 102(HY7):919-934.

Appendix A

THE GALERKIN METHOD (Brebbia and Ferrante, 1983)

In this section the formulation of the solution of a Poisson's equation with a problem domain as shown in Figure A.1 is demonstrated.

A.1 The Finite Element Formulation

The problem domain is discretized into m triangular elements, interconnected at n nodes. The next step is to choose a field function, which in this case, is the simplest field function as shown by Equation (A.1).

$$\phi = \alpha_1 + \alpha_2 x + \alpha_3 y \tag{A.1}$$

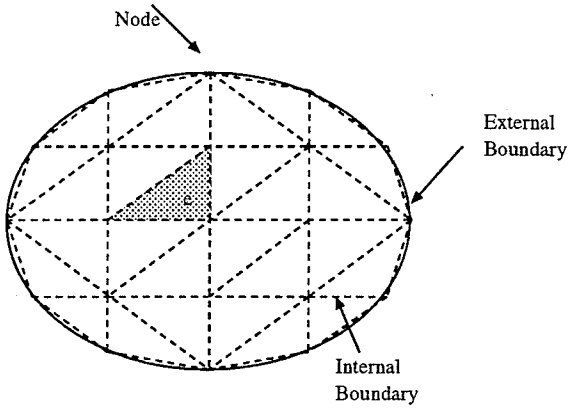

Figure A.1: Discretization of the problem domain.

Application of the Equation (A.1) to each node of an element e will result in:

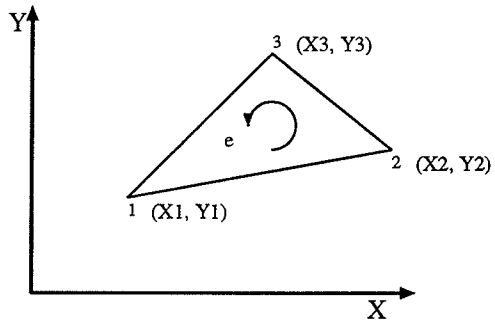

Figure A.2: Triangular Element.

$$\phi_1 = \alpha_1 + \alpha_2 x_1 + \alpha_3 y_1 \tag{A.2}$$

$$\phi_2 = \alpha_1 + \alpha_2 x_2 + \alpha_3 y_2 \tag{A.3}$$

$$\phi_3 = \alpha_1 + \alpha_2 x_3 + \alpha_3 y_3 \tag{A.4}$$

which can be written in the matrix form as:

$$\begin{Bmatrix} \phi_1 \\ \phi_2 \\ \phi_3 \end{Bmatrix} = \begin{bmatrix} 1 & x_1 & y_1 \\ 1 & x_2 & y_2 \\ 1 & x_3 & y_3 \end{bmatrix} \begin{Bmatrix} \alpha_1 \\ \alpha_2 \\ \alpha_3 \end{Bmatrix} \tag{A.5}$$

Taking the inverse of the Equation (A.5) will gives:

$$\begin{Bmatrix} \alpha_1 \\ \alpha_2 \\ \alpha_3 \end{Bmatrix} = \begin{bmatrix} C_{11} & C_{12} & C_{13} \\ C_{21} & C_{22} & C_{23} \\ C_{31} & C_{32} & C_{33} \end{bmatrix} \begin{Bmatrix} \phi_1 \\ \phi_2 \\ \phi_3 \end{Bmatrix} \tag{A.6}$$

where:

$$
\begin{aligned}
C_{11} &= (x_2y_3 - x_3y_2)/A_e \\
C_{12} &= (x_3y_1 - x_1y_3)/A_e \\
C_{13} &= (x_1y_2 - x_2y_1)/A_e \\
C_{21} &= (y_2 - y_3)/A_e \\
C_{22} &= (y_3 - y_1)/A_e \\
C_{23} &= (y_1 - y_2)/A_e \\
C_{31} &= (x_3 - x_2)/A_e \\
C_{32} &= (x_1 - x_3)/A_e \\
C_{33} &= (x_2 - x_1)/A_e
\end{aligned}
\tag{A.7}
$$

and A_e is the area of the element e. Equation (A.6) can then be written as:

$$
\begin{aligned}
\alpha_1 &= C_{11}\phi_1 + C_{12}\phi_2 + C_{13}\phi_3 \\
\alpha_2 &= C_{21}\phi_1 + C_{22}\phi_2 + C_{23}\phi_3 \\
\alpha_3 &= C_{31}\phi_1 + C_{32}\phi_2 + C_{33}\phi_3
\end{aligned}
\tag{A.8}
$$

Subtitution of the Equation (A.8) to The Equation (A.1) will give:

$$
\phi = \phi_1\psi_1 + \phi_2\psi_2 + \phi_3\psi_3 \tag{A.9}
$$

where:

$$
\begin{aligned}
\psi_1 &= C_{11} + C_{21}x + C_{31}y \\
\psi_2 &= C_{12} + C_{22}x + C_{32}y \\
\psi_3 &= C_{13} + C_{23}x + C_{33}y
\end{aligned}
\tag{A.10}
$$

By using these ψ_i,s as the weighting function, the error minimization function of the Poisson's equation using the Galerkin method will be:

$$
\int_{\Omega^e}\left(\frac{\partial^2\phi}{\partial x^2} + \frac{\partial^2\phi}{\partial y^2} - c\right)\psi_i d\Omega + \int_{\Gamma_2^e}\left(\bar{q} - n_x\frac{\partial\phi}{\partial x} - n_y\frac{\partial\phi}{\partial y}\right)\psi_i d\Gamma = 0 \tag{A.11}
$$

Reduction of the order of the first term of the above differential equation by integration by parts will result in:

$$\int_{\Omega^e}(\frac{\partial^2\phi}{\partial x^2}+\frac{\partial^2\phi}{\partial y^2}-c)\psi_i d\Omega = -\int_{\Omega_e}(\frac{\partial\phi}{\partial x}\frac{\partial\psi_i}{\partial x}+\frac{\partial\phi}{\partial y}\frac{\partial\psi_i}{\partial y})d\Omega-\int_{\Omega_e}c\psi_i d\Omega + \int_{\Gamma_2^e}(n_x\frac{\partial\phi}{\partial x}+n_y\frac{\partial\phi}{\partial y})\psi_i d\Gamma \quad \text{(A.12)}$$

The Equation (A.11) can then be written as:

$$\int_{\Omega_e}(\frac{\partial\phi}{\partial x}\frac{\partial\psi_i}{\partial x}+\frac{\partial\phi}{\partial y}\frac{\partial\psi_i}{\partial y}-c\psi_i)d\Omega-\int_{\Gamma_2^e}\bar{q}\psi_i d\Gamma=0 \quad \text{(A.13)}$$

Substitution of Equations (A.9) and (A.10) into Equation (A.13) gives:

$$\begin{aligned}
&\int_{\Omega^e}[(\phi_1C_{21} + \phi_2C_{22}+\phi_3C_{23})C_{21}+(\phi_1C_{31}+\phi_2C_{32}+\phi_3C_{33})C_{31}]d\Omega \quad \text{(A.14)}\\
&\quad - c(C_{11}+C_{21}x+C_{31}y)-\int_{\Gamma_2^e}\bar{q}(C_{11}+C_{21}x+C_31y)d\Gamma=0\\
&\int_{\Omega^e}[(\phi_1C_{21} + \phi_2C_{22}+\phi_3C_{23})C_{22}+(\phi_1C_{31}+\phi_2C_{32}+\phi_3C_{33})C_{32}]d\Omega\\
&\quad - c(C_{12}+C_{22}x+C_{32}y)-\int_{\Gamma_2^e}\bar{q}(C_{12}+C_{22}x+C_32y)d\Gamma=0\\
&\int_{\Omega^e}[(\phi_1C_{21} + \phi_2C_{22}+\phi_3C_{23})C_{23}+(\phi_1C_{31}+\phi_2C_{32}+\phi_3C_{33})C_{33}]d\Omega\\
&\quad - c(C_{13}+C_{23}x+C_{33}y)-\int_{\Gamma_2^e}\bar{q}(C_{13}+C_{23}x+C_33y)d\Gamma=0
\end{aligned}$$

In the matrix form, Equation (A.14) is:

$$\int_{\Omega^e}\begin{bmatrix} C_{21}^2+C_{31}^2 & C_{22}C_{21}+C_{32}C_{31} & C_{23}C_{21}+C_{33}C_{31}\\ C_{21}C_{22}+C_{31}C_{32} & C_{22}^2+C_{32}^2 & C_{23}C_{22}+C_{33}C_{32}\\ C_{21}C_{23}+C_{31}C_{33} & C_{22}C_{23}+C_{32}C_{33} & C_{23}^2+C_{33}^2 \end{bmatrix}\begin{Bmatrix}\phi_1\\ \phi_2\\ \phi_3\end{Bmatrix}d\Omega$$

$$=\int_{\Gamma_2^e}\bar{q}\begin{Bmatrix}C_{11}+C_{21}x+C_{31}y\\ C_{12}+C_{22}x+C_{32}y\\ C_{13}+C_{23}x+C_{33}y\end{Bmatrix}d\Gamma+c\begin{bmatrix}C_{11} & C_{12}x & C_{13}y\\ C_{21} & C_{22}x & C_{23}y\\ C_{31} & C_{32}x & C_{33}y\end{bmatrix} \quad \text{(A.15)}$$

In a more compact form, the above equation becomes:

$$\mathbf{K^e}\phi^{\mathbf{e}}-\mathbf{P^e}=\mathbf{0} \quad \text{(A.16)}$$

Since all coefficients in the first term of Equations (A.15) are constant, the $\mathbf{K}^e$ matrix is:

$$\mathbf{K}^e = \mathbf{\Omega}^e \begin{bmatrix} C_{21}^2 + C_{31}^2 & C_{22}C_{21} + C_{32}C_{31} & C_{23}C_{21} + C_{33}C_{31} \\ C_{21}C_{22} + C_{31}C_{32} & C_{22}^2 + C_{32}^2 & C_{23}C_{22} + C_{33}C_{32} \\ C_{21}C_{23} + C_{31}C_{33} & C_{22}C_{23} + C_{32}C_{33} & C_{23}^2 + C_{33}^2 \end{bmatrix} \tag{A.17}$$

with vector ϕ^e is:

$$\phi^e = \begin{Bmatrix} \phi_1 \\ \phi_2 \\ \phi_3 \end{Bmatrix} \tag{A.18}$$

The second term of Equation (A.15) will be considered only if there is at least one side of an element coincident with the external boundary Γ_2.

The general formulation of the Galerkin method for a triangular element will be:

$$\begin{bmatrix} k_{11}^e & k_{12}^e & k_{13}^e \\ k_{21}^e & k_{22}^e & k_{23}^e \\ k_{31}^e & k_{32}^e & k_{33}^e \end{bmatrix} \begin{Bmatrix} \phi_1 \\ \phi_2 \\ \phi_3 \end{Bmatrix} - \begin{Bmatrix} P_1^e \\ P_2^e \\ P_3^e \end{Bmatrix} = \begin{Bmatrix} 0 \\ 0 \\ 0 \end{Bmatrix} \tag{A.19}$$

A.2 Assembling The Total Matrix

Equation (A.19) is a manifestation of an application of the Galerkin method to one generic element e out of m elements on the problem domain. The expression of the whole system can be obtained by summing the contributions from all elements and all sides on Γ_2. Mathemathically, this method will lead to:

$$\sum_{e=1}^{m} \int_{\Omega^e} \left(\frac{\partial \psi}{\partial x} \frac{\partial \psi_i}{\partial x} + \frac{\partial \psi}{\partial y} \frac{\partial \psi_i}{\partial y} \right) d\Omega - \sum_{e=1}^{m} \int_{\Omega^e} c\psi_i d\Omega - \sum_{e=1}^{s} \int_{\Gamma_2^e} q\psi_i d\Gamma = 0 \tag{A.20}$$

In a more compact form:

$$\mathbf{K}\phi - \mathbf{P} = \mathbf{0} \tag{A.21}$$

or

$$\begin{bmatrix} k_{11} & k_{12} & \cdots & k_{1n} \\ k_{21} & k_{22} & \cdots & k_{2n} \\ k_{31} & k_{32} & \cdots & k_{3n} \\ \vdots & \vdots & \ddots & \vdots \\ k_{n1} & k_{n2} & \cdots & k_{nn} \end{bmatrix} \begin{Bmatrix} \phi_1 \\ \phi_2 \\ \phi_3 \\ \vdots \\ \phi_n \end{Bmatrix} - \begin{Bmatrix} P_1 \\ P_2 \\ P_3 \\ \vdots \\ P_n \end{Bmatrix} = \begin{Bmatrix} 0 \\ 0 \\ 0 \\ \vdots \\ 0 \end{Bmatrix} \tag{A.22}$$

where n is the number of nodes of the discretized problem domain. In Equation (A.22), matrix K and P are known. The solution of the above equation will result in the nodal values of ϕ_i.

A.3 Introduction of the Boundary Conditions

The boundary conditions in the domain Γ_1 can be introduced to the system equation by subtituting prescribed nodal values into the corresponding unknown nodal variable. In a simple way, this step can be performed by first eliminating the rows corresponding to these prescribed unknowns, and then adding the contributions of those prescribed unknowns to the right hand side of Equation (A.22). Suppose, in the system Equation (A.22), the values of the unknown variables at nodes 1 and 2 are known (i.e. $\phi_1 = \bar{\phi}_1$ and $\phi_2 = \bar{\phi}_2$), the system equation becomes:

$$\begin{bmatrix} k_{33} & k_{34} & \cdots & k_{3n} \\ k_{43} & k_{44} & \cdots & k_{4n} \\ \vdots & \vdots & \ddots & \vdots \\ k_{n3} & k_{n4} & \cdots & k_{nn} \end{bmatrix} \begin{Bmatrix} \phi_3 \\ \phi_4 \\ \vdots \\ \phi_n \end{Bmatrix} = \begin{Bmatrix} P_3 - k_{31}\bar{\phi}_1 - k_{32}\bar{\phi}_2 \\ P_4 - k_{41}\bar{\phi}_1 - k_{42}\bar{\phi}_2 \\ \vdots \\ P_n - k_{n1}\bar{\phi}_1 - k_{n2}\bar{\phi}_2 \end{Bmatrix} \tag{A.23}$$

A.4 Solution of the System of Equations

The system equation of Equation (A.23) is a set of simultaneous linear equations with $n-b+1$ expressions and unknowns, where b is the number of the prescribed nodal unknowns. The solution of this equation is quite straightforward by several existing methods such as Gauss-Jordan's method, Gauss elimination technique, and Cholesky's method. In this study, this system equation is solved by using Gauss elimination technique.

Appendix B

TIME VARIATION OF CFEM, CCM, ACM, AND THALWEG

Note that these curves are given in an increasing numerical order of cross-section with the cross-section number specified at the top of the graph.

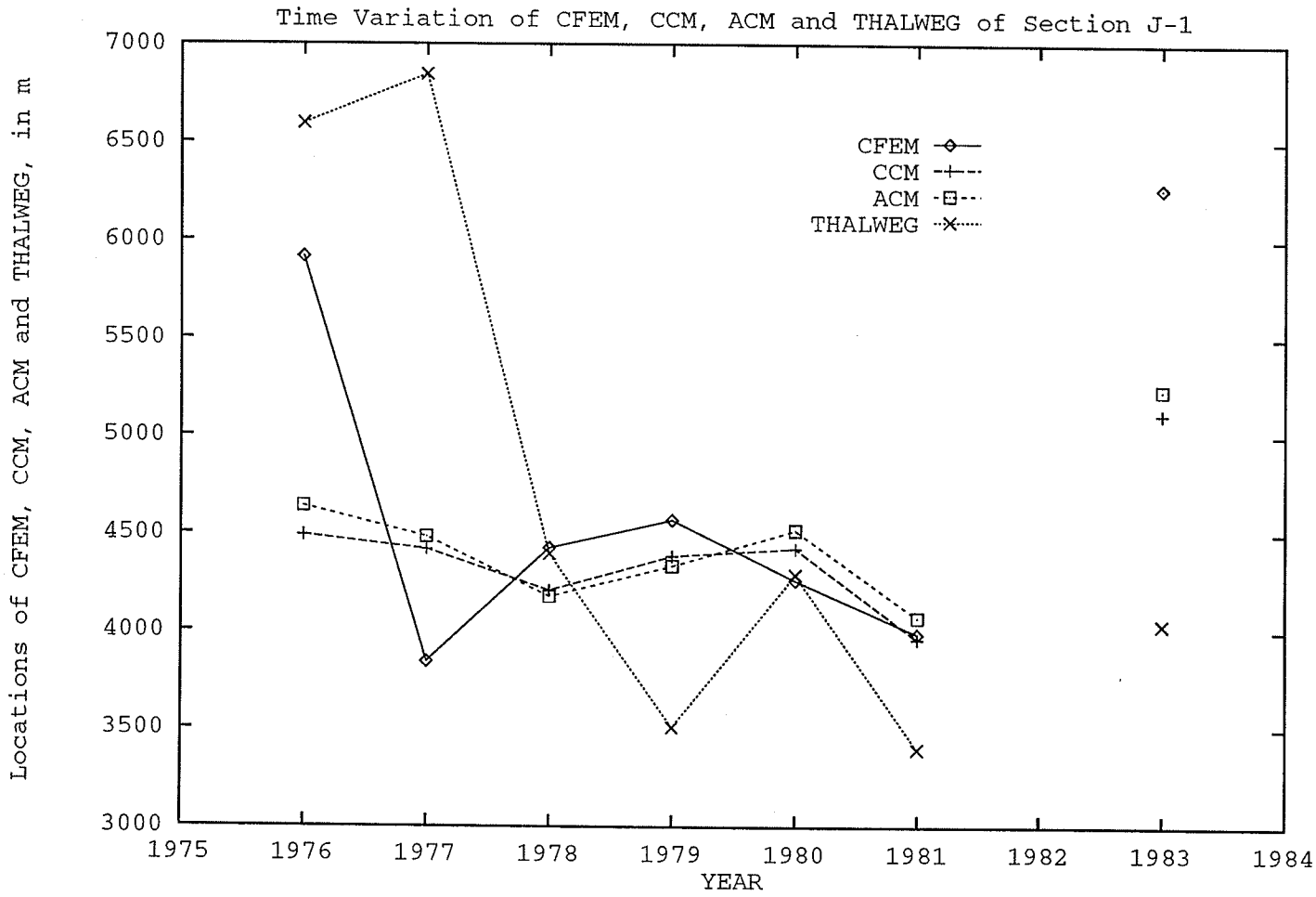
Time Variation of CFEM, CCM, ACM and THALWEG of Section J-1
Locations of CFEM, CCM, ACM and THALWEG, in m
YEAR
CFEM
CCM
ACM
THALWEG
7000
6500
6000
5500
5000
4500
4000
3500
3000
1975
1976
1977
1978
1979
1980
1981
1982
1983
1984

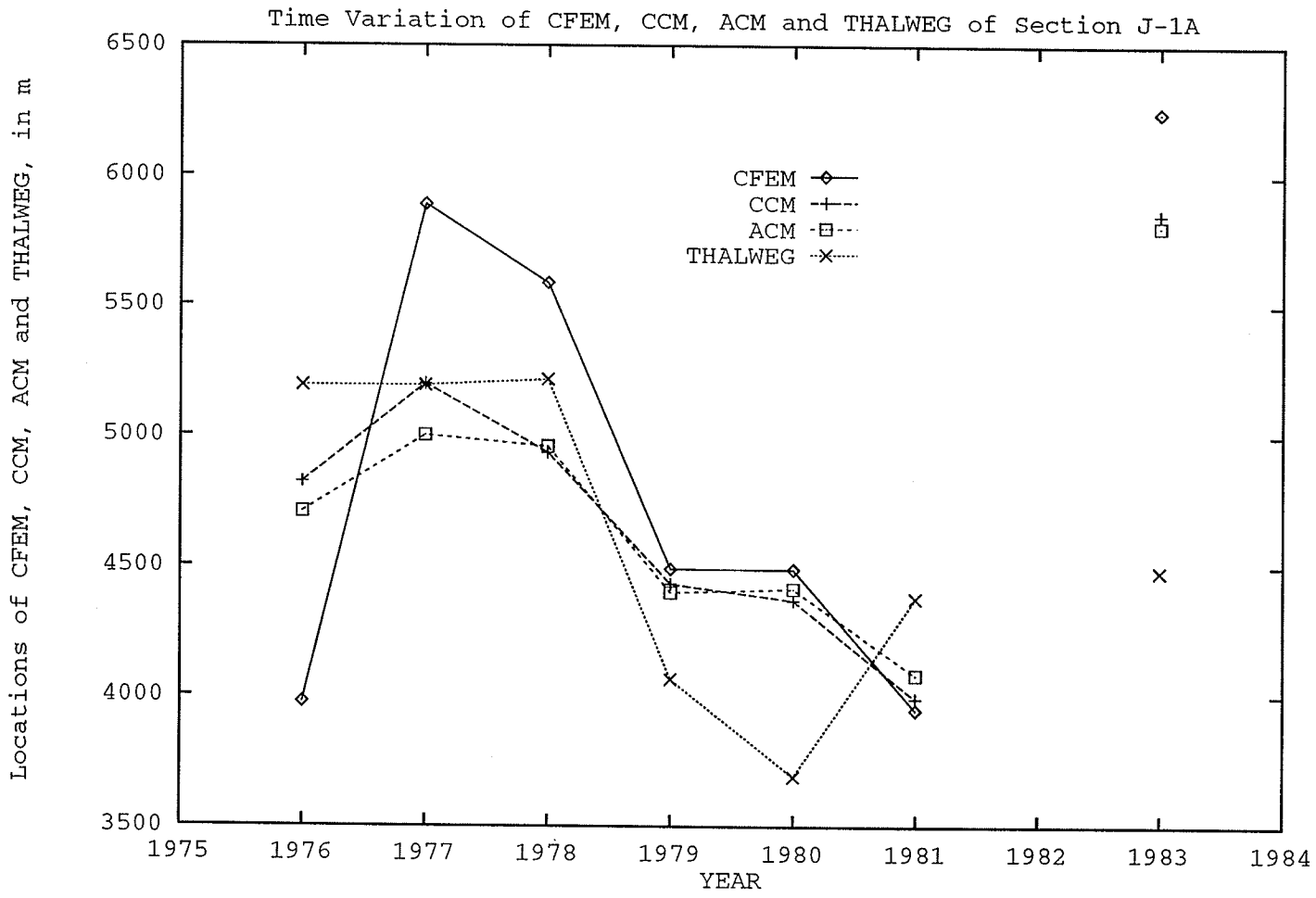
Time Variation of CFEM, CCM, ACM and THALWEG of Section J-1A
Locations of CFEM, CCM, ACM and THALWEG, in m
YEAR
CFEM
CCM
ACM
THALWEG
6500
6000
5500
5000
4500
4000
3500
1975
1976
1977
1978
1979
1980
1981
1982
1983
1984

Comparison of the Results of CFEM, CCM, ACM and THALWEG of Section J-2
Locations of CFEM, CCM, ACM and THALWEG, in m
10000
9000
8000
7000
6000
5000
4000
3000
2000
1975
1976
1977
1978
1979
1980
1981
1982
1983
1984
YEAR
CFEM
CCM
ACM
THALWEG

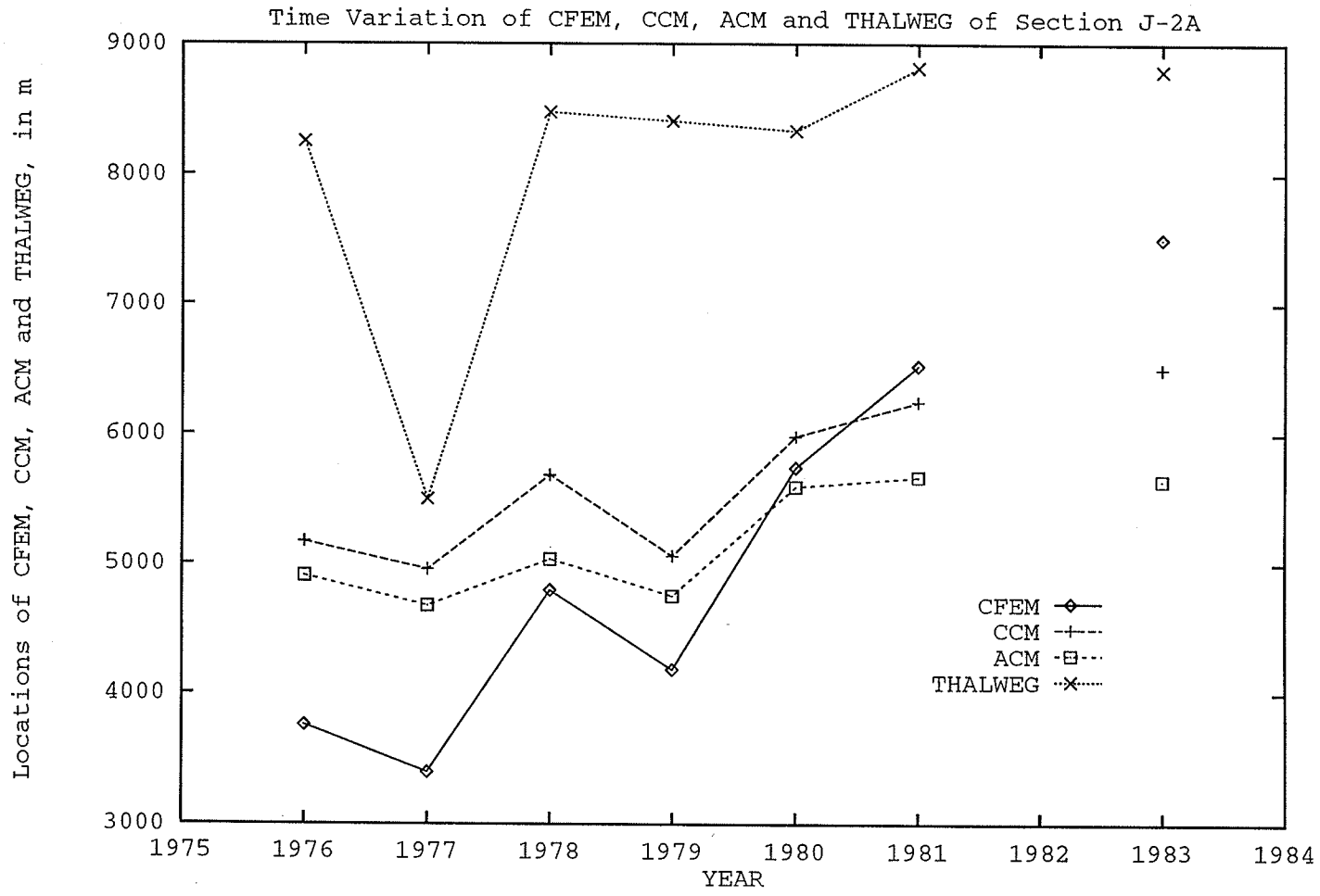
Time Variation of CFEM, CCM, ACM and THALWEG of Section J-2A
Locations of CFEM, CCM, ACM and THALWEG, in m
YEAR
9000
8000
7000
6000
5000
4000
3000
1975
1976
1977
1978
1979
1980
1981
1982
1983
1984
CFEM
CCM
ACM
THALWEG

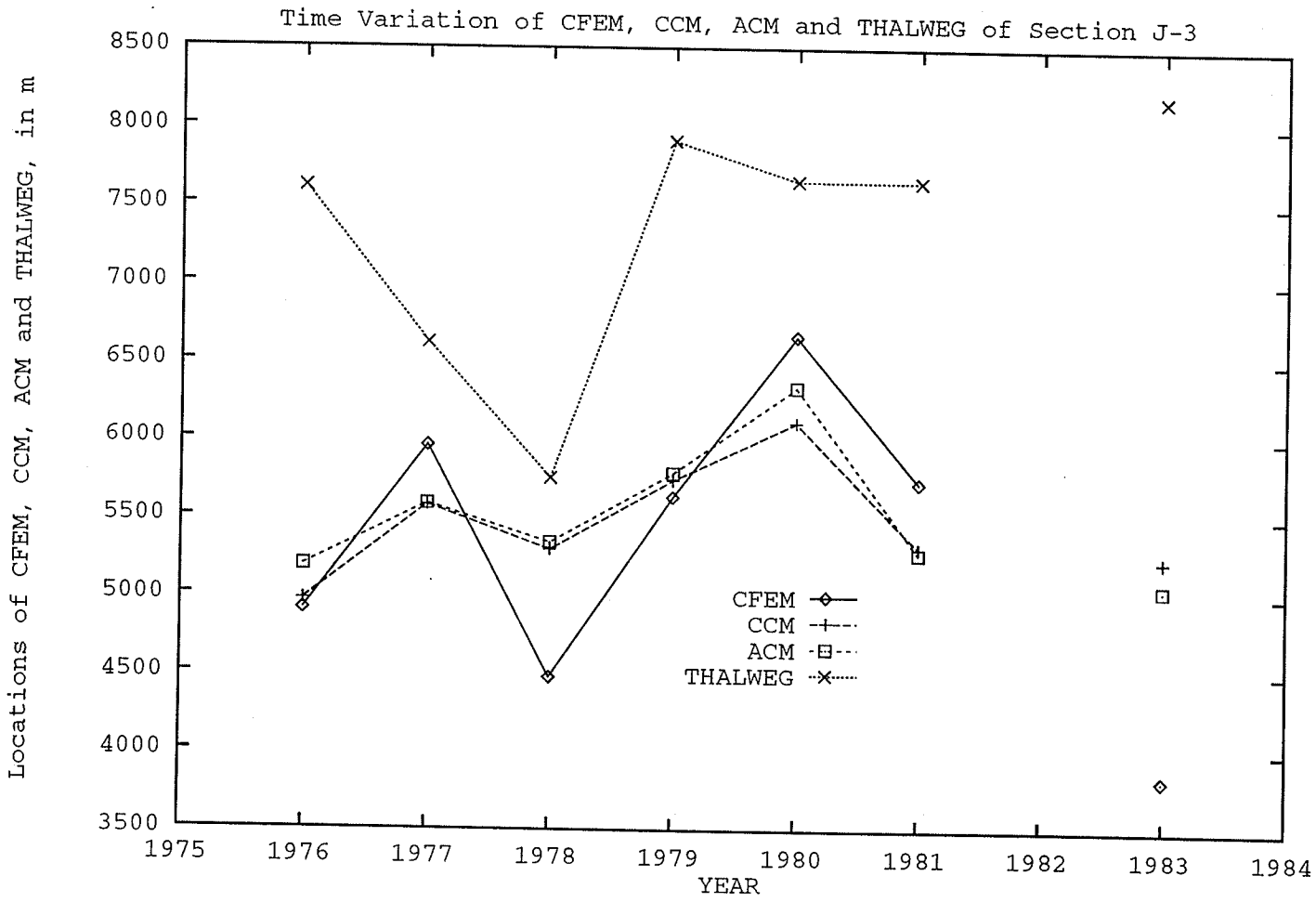
Time Variation of CFEM, CCM, ACM and THALWEG of Section J-3
Locations of CFEM, CCM, ACM and THALWEG, in m
YEAR
8500
8000
7500
7000
6500
6000
5500
5000
4500
4000
3500
1975
1976
1977
1978
1979
1980
1981
1982
1983
1984
CFEM
CCM
ACM
THALWEG

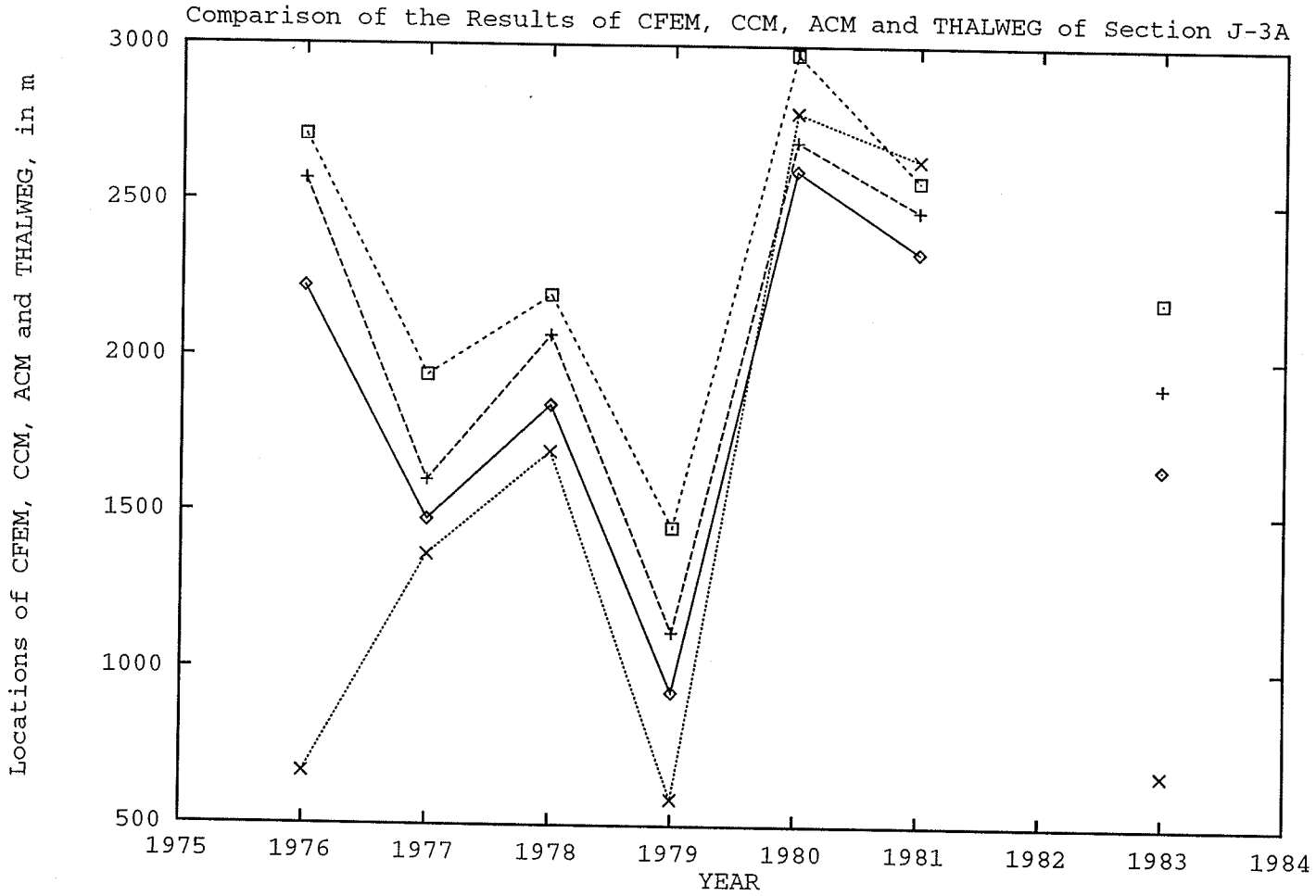
Comparison of the Results of CFEM, CCM, ACM and THALWEG of Section J-3A
Locations of CFEM, CCM, ACM and THALWEG, in m
3000
2500
2000
1500
1000
500
1975
1976
1977
1978
1979
1980
1981
1982
1983
1984
YEAR

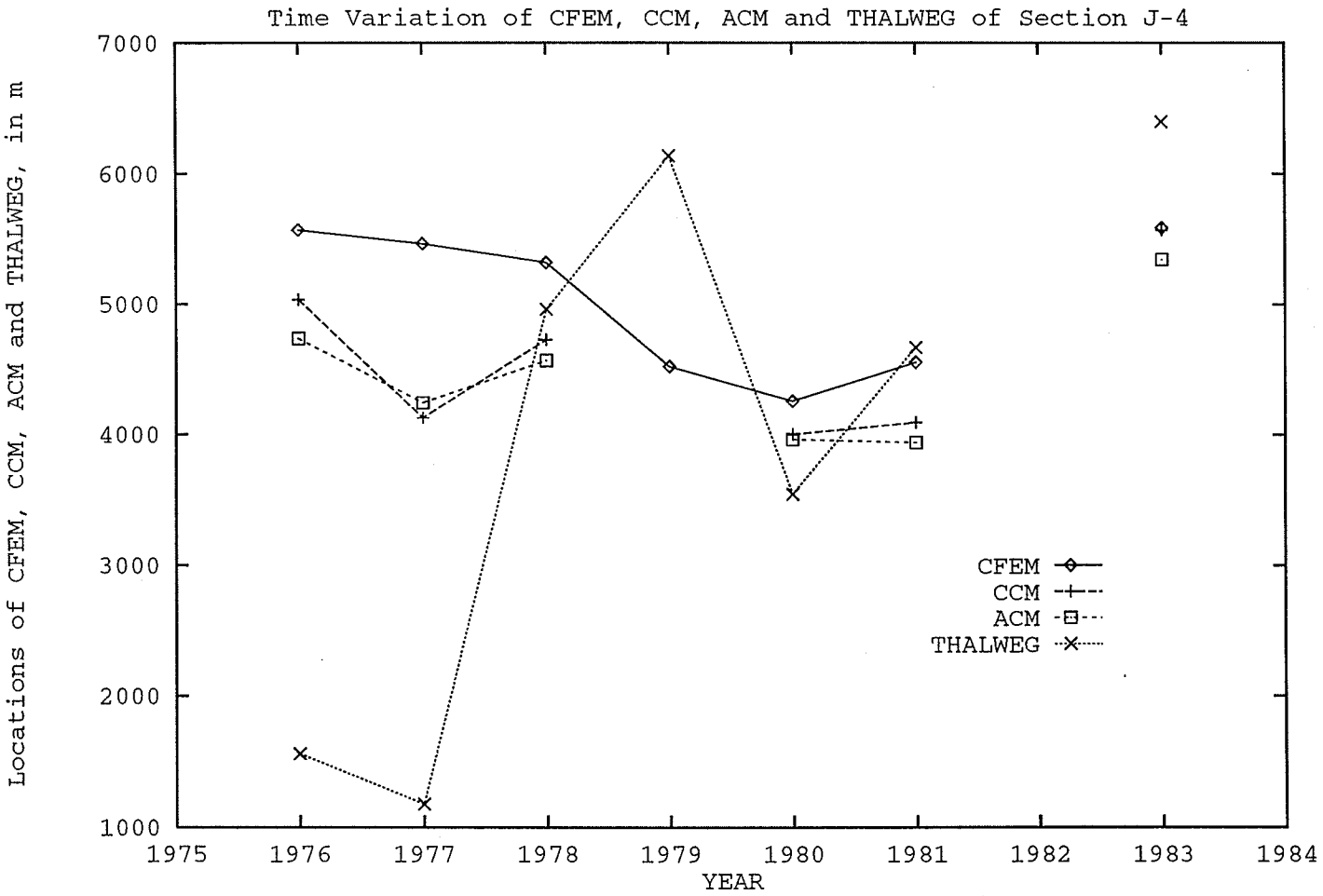
Time Variation of CFEM, CCM, ACM and THALWEG of Section J-4
Locations of CFEM, CCM, ACM and THALWEG, in m
YEAR
7000
6000
5000
4000
3000
2000
1000
1975
1976
1977
1978
1979
1980
1981
1982
1983
1984
CFEM
CCM
ACM
THALWEG

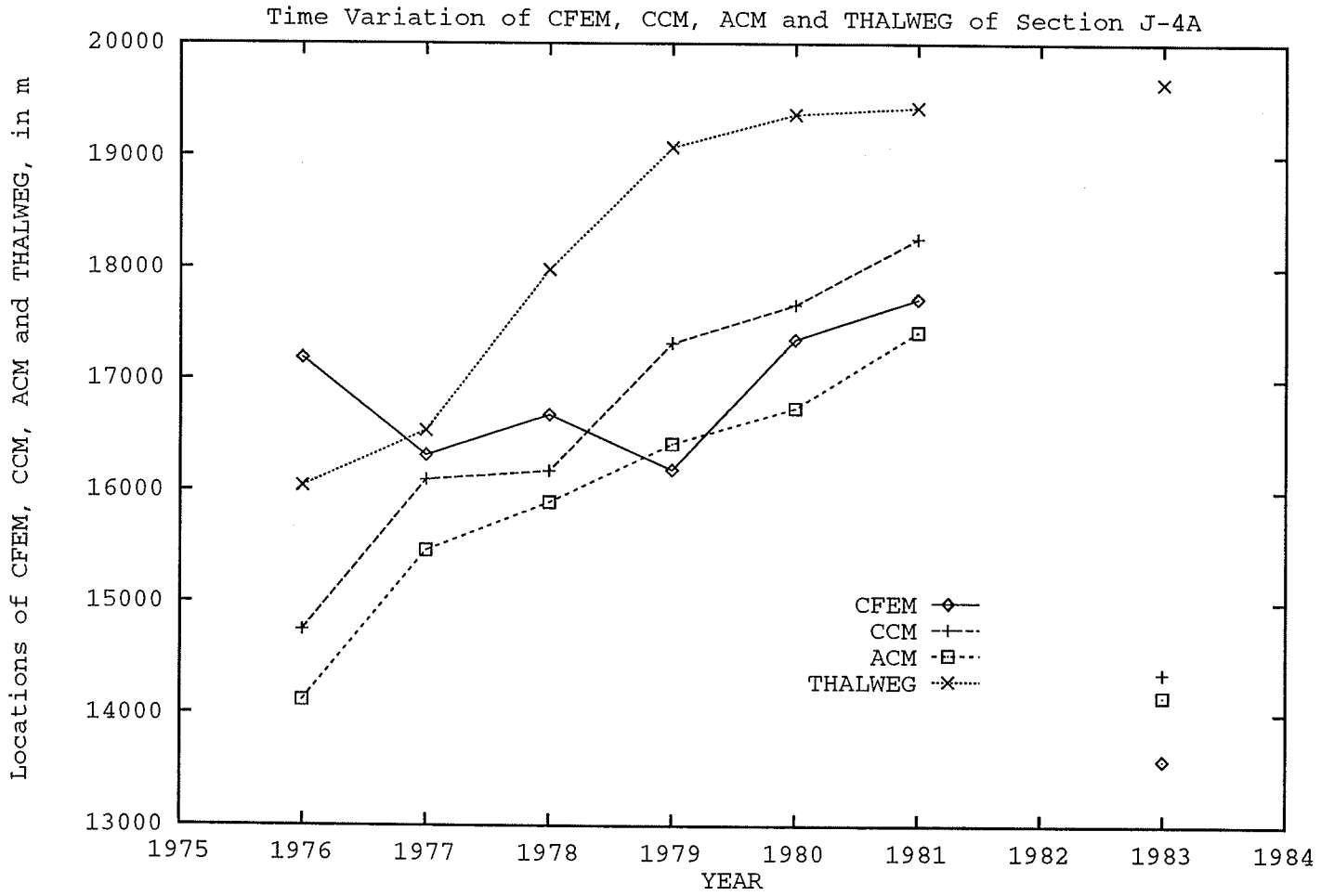
Time Variation of CFEM, CCM, ACM and THALWEG of Section J-4A
Locations of CFEM, CCM, ACM and THALWEG, in m
YEAR
20000
19000
18000
17000
16000
15000
14000
13000
1975
1976
1977
1978
1979
1980
1981
1982
1983
1984
CFEM
CCM
ACM
THALWEG

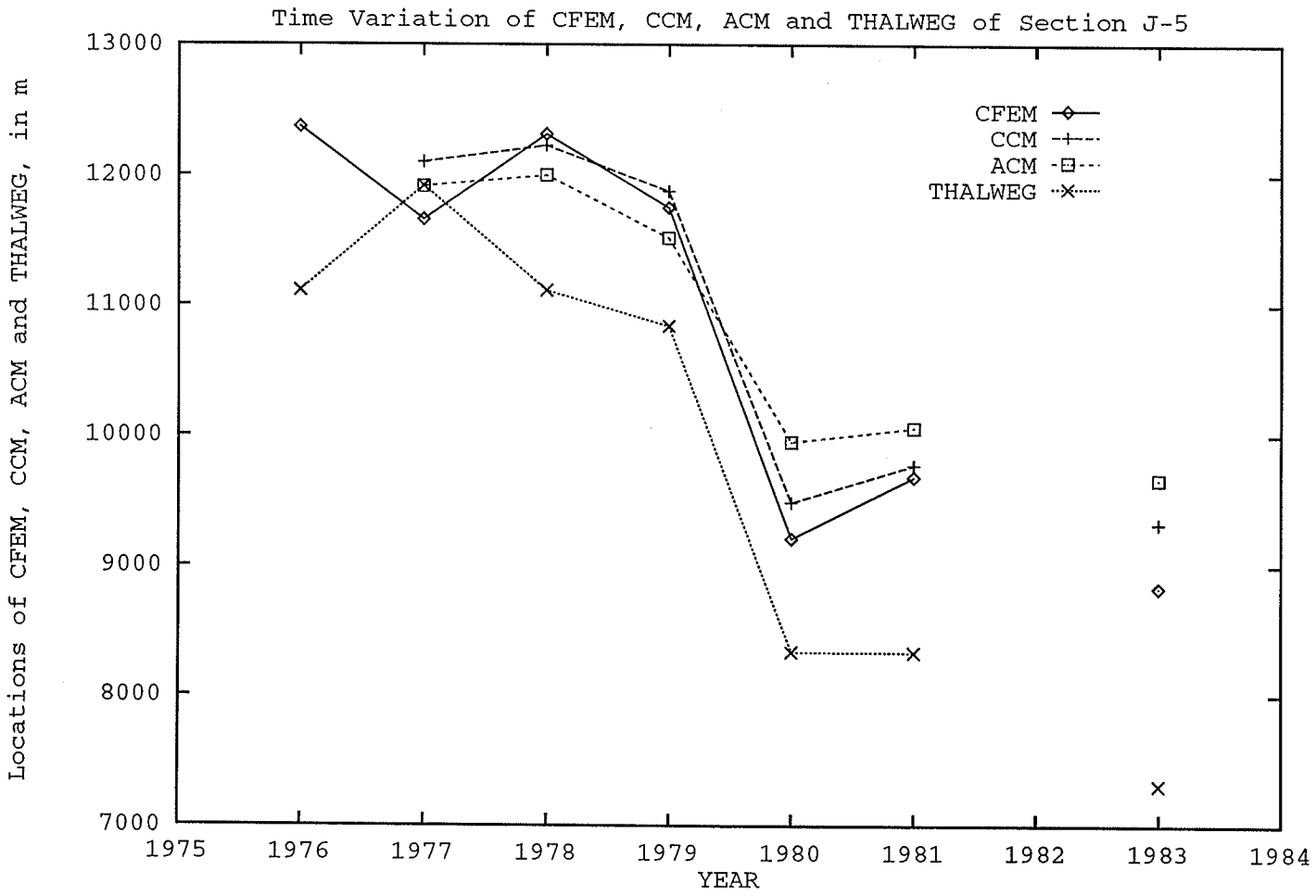
Time Variation of CFEM, CCM, ACM and THALWEG of Section J-5
Locations of CFEM, CCM, ACM and THALWEG, in m
YEAR
CFEM
CCM
ACM
THALWEG
13000
12000
11000
10000
9000
8000
7000
1975
1976
1977
1978
1979
1980
1981
1982
1983
1984

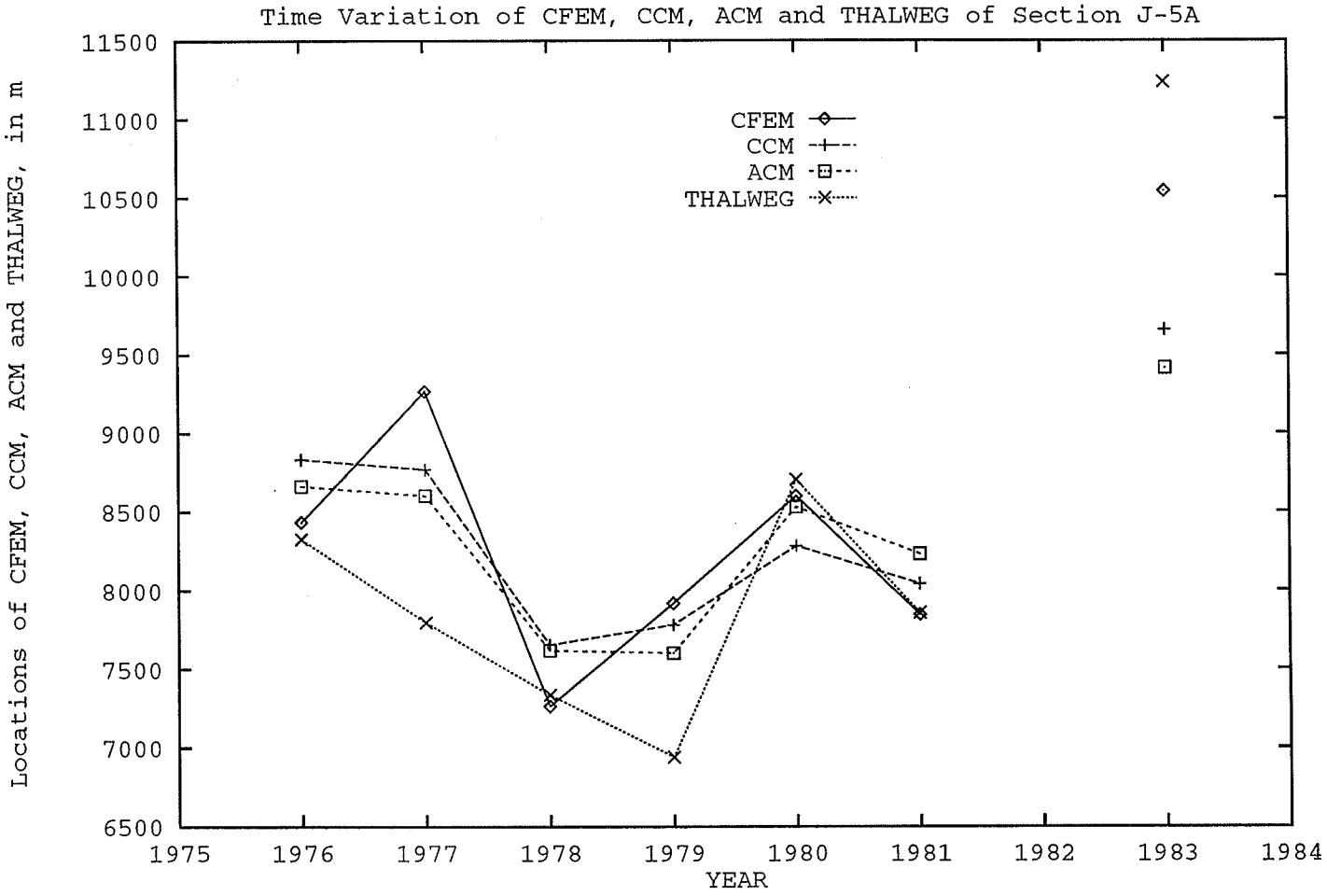
Time Variation of CFEM, CCM, ACM and THALWEG of Section J-5A
Locations of CFEM, CCM, ACM and THALWEG, in m
YEAR
CFEM
CCM
ACM
THALWEG
11500
11000
10500
10000
9500
9000
8500
8000
7500
7000
6500
1975
1976
1977
1978
1979
1980
1981
1982
1983
1984

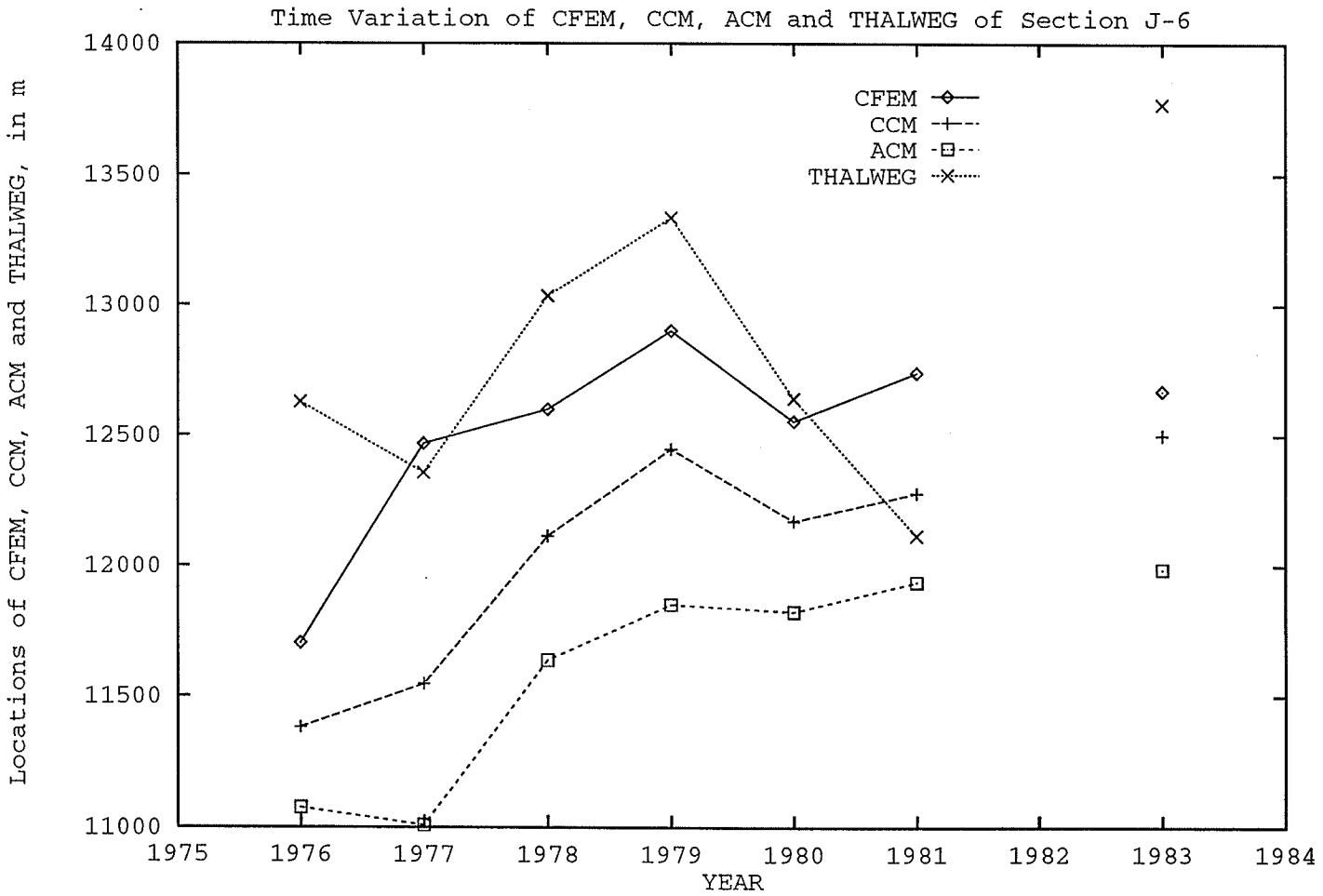
Time Variation of CFEM, CCM, ACM and THALWEG of Section J-6
Locations of CFEM, CCM, ACM and THALWEG, in m
YEAR
CFEM
CCM
ACM
THALWEG
14000
13500
13000
12500
12000
11500
11000
1975
1976
1977
1978
1979
1980
1981
1982
1983
1984

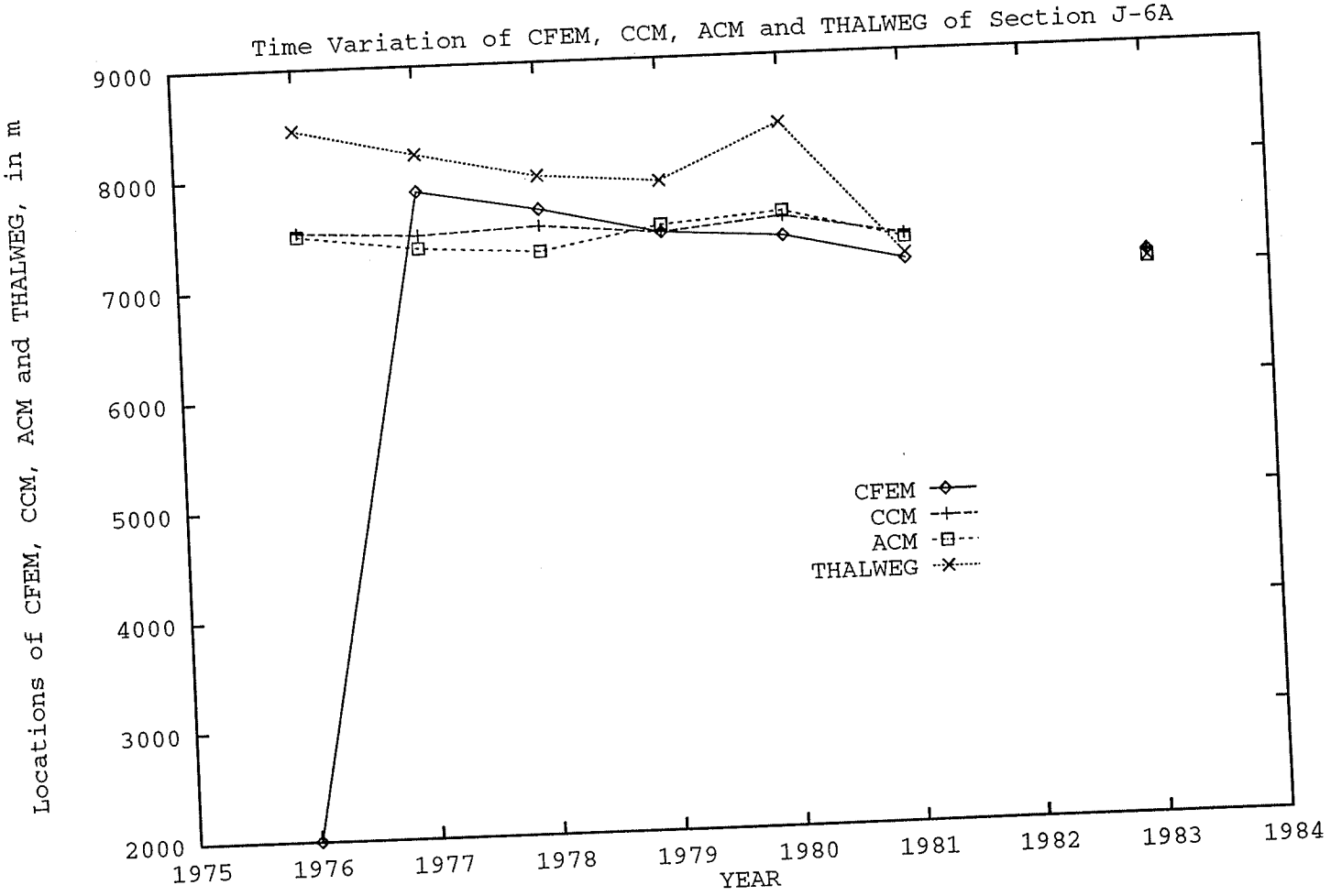
Time Variation of CFEM, CCM, ACM and THALWEG of Section J-6A
Locations of CFEM, CCM, ACM and THALWEG, in m
9000
8000
7000
6000
5000
4000
3000
2000
1975
1976
1977
1978
1979
1980
1981
1982
1983
1984
YEAR
CFEM
CCM
ACM
THALWEG

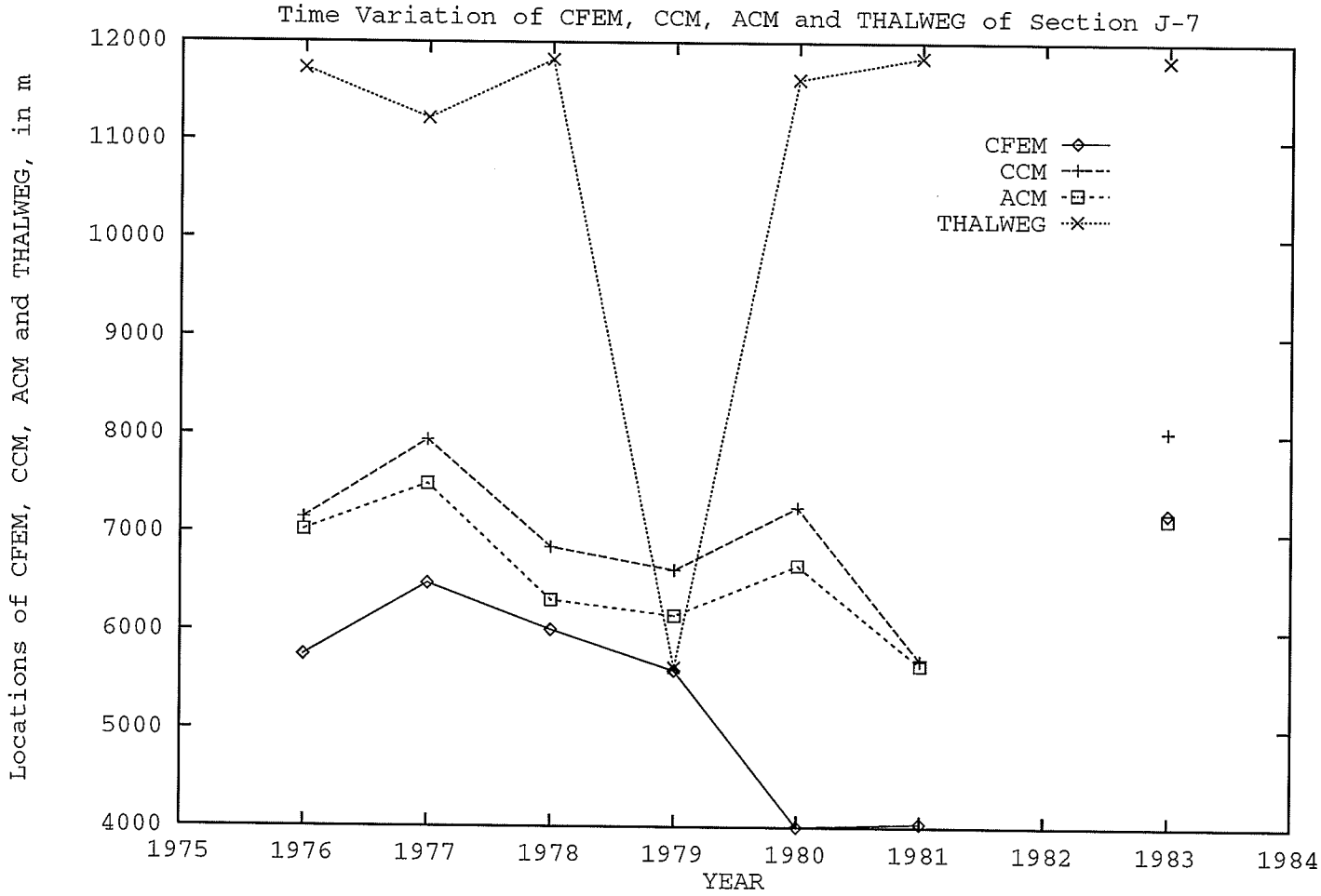
Time Variation of CFEM, CCM, ACM and THALWEG of Section J-7
Locations of CFEM, CCM, ACM and THALWEG, in m
YEAR
CFEM
CCM
ACM
THALWEG
12000
11000
10000
9000
8000
7000
6000
5000
4000
1975
1976
1977
1978
1979
1980
1981
1982
1983
1984

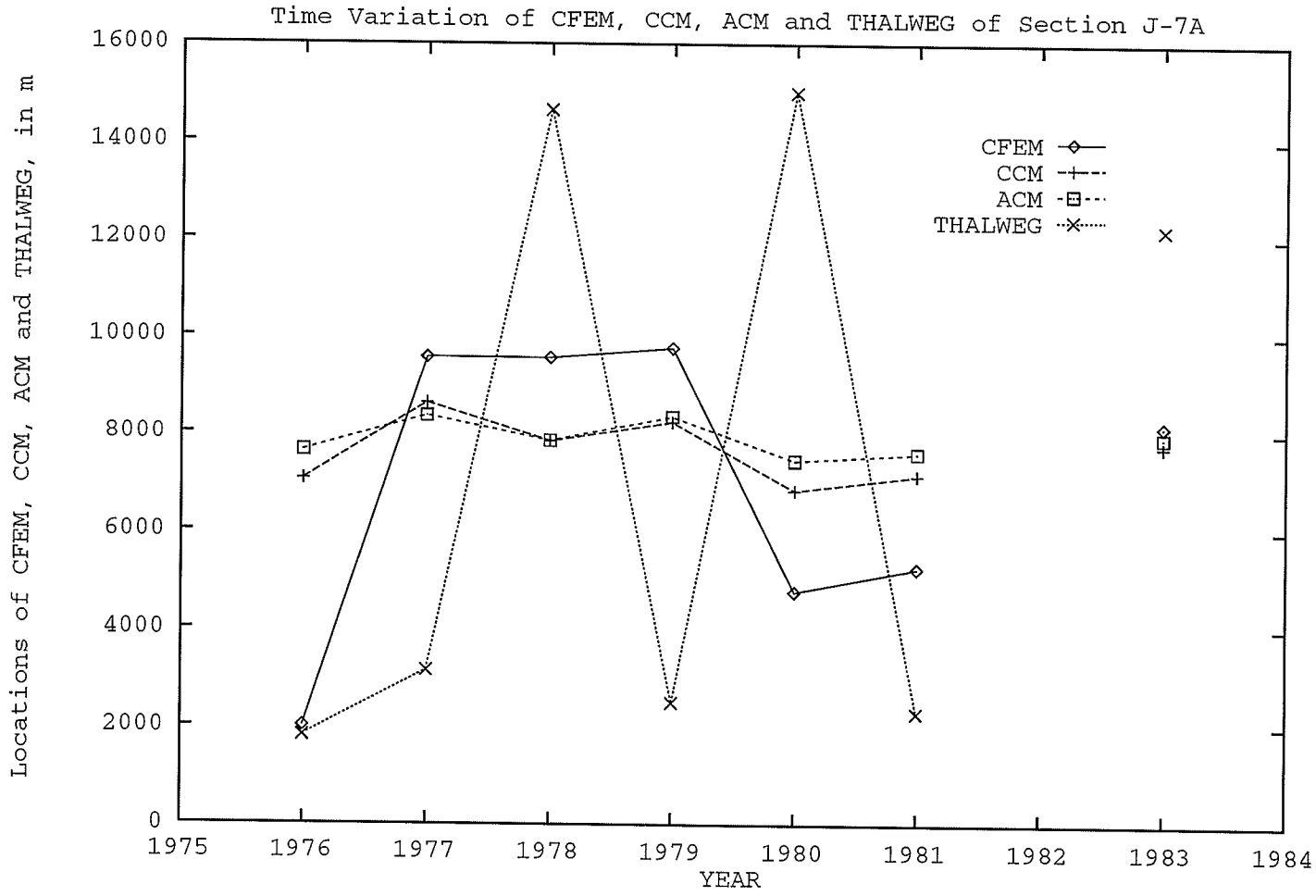
Time Variation of CFEM, CCM, ACM and THALWEG of Section J-7A
Locations of CFEM, CCM, ACM and THALWEG, in m
YEAR
CFEM
CCM
ACM
THALWEG
16000
14000
12000
10000
8000
6000
4000
2000
0
1975
1976
1977
1978
1979
1980
1981
1982
1983
1984

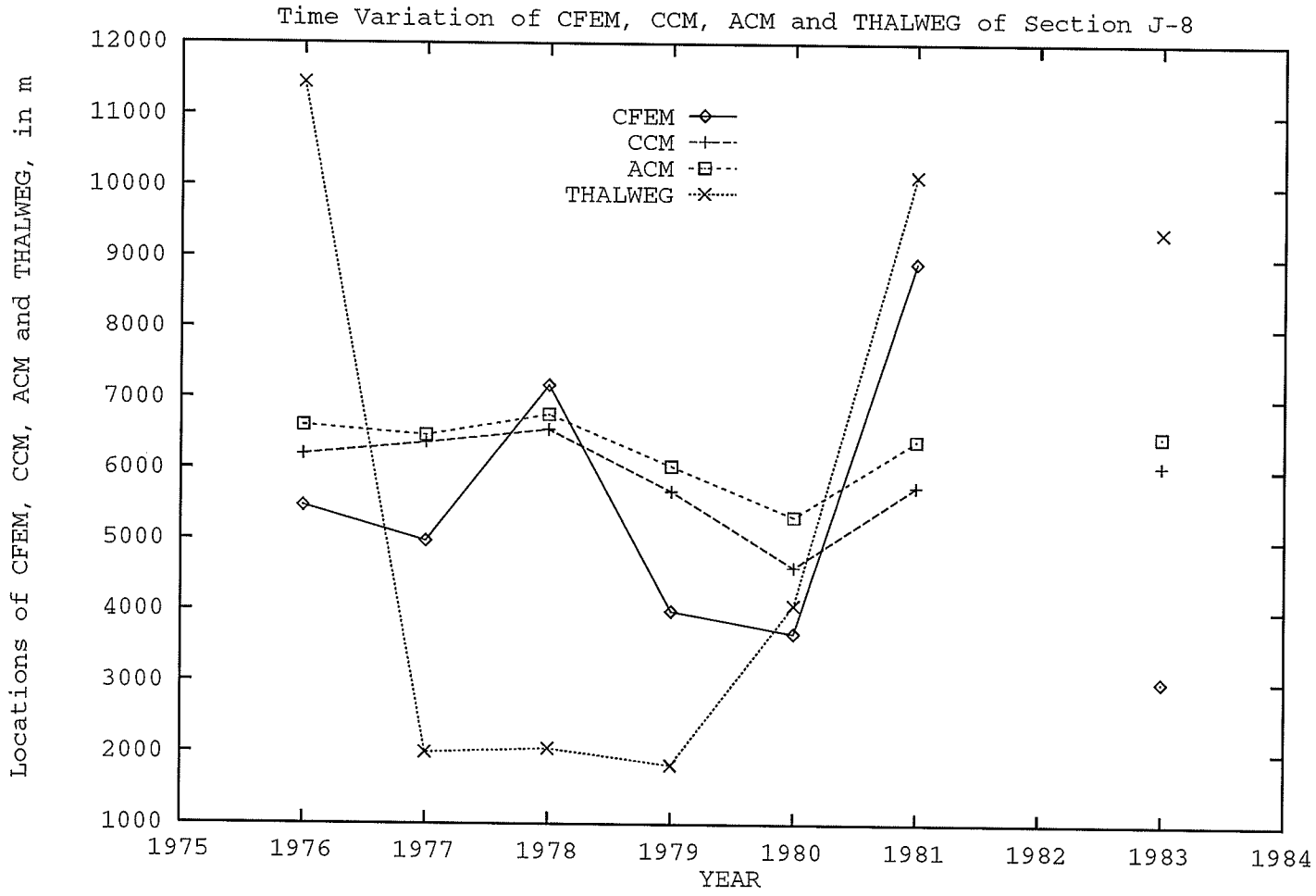
Time Variation of CFEM, CCM, ACM and THALWEG of Section J-8
Locations of CFEM, CCM, ACM and THALWEG, in m
YEAR
CFEM
CCM
ACM
THALWEG
12000
11000
10000
9000
8000
7000
6000
5000
4000
3000
2000
1000
1975
1976
1977
1978
1979
1980
1981
1982
1983
1984

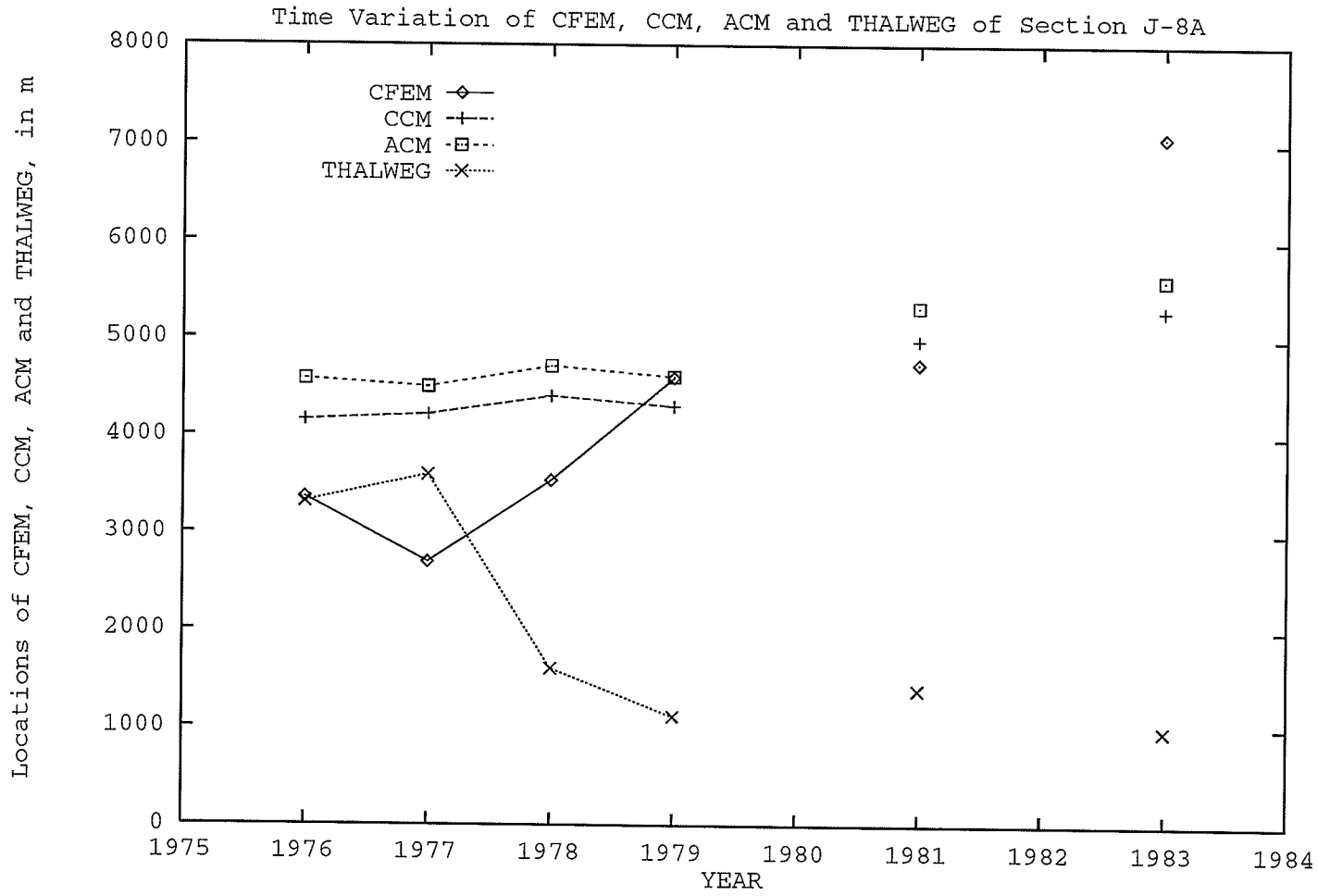
Time Variation of CFEM, CCM, ACM and THALWEG of Section J-8A
Locations of CFEM, CCM, ACM and THALWEG, in m
YEAR
CFEM
CCM
ACM
THALWEG
8000
7000
6000
5000
4000
3000
2000
1000
0
1975
1976
1977
1978
1979
1980
1981
1982
1983
1984

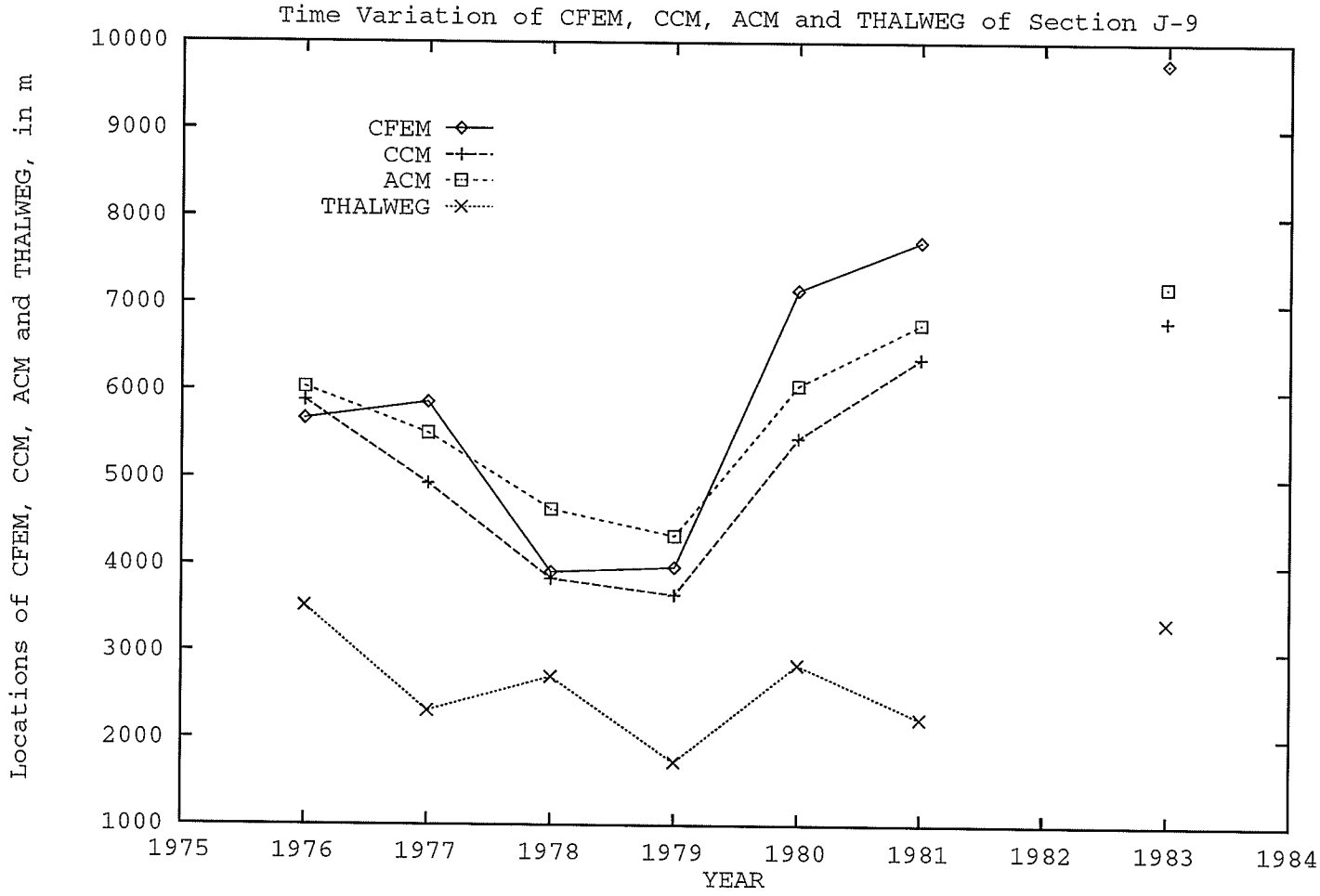
Time Variation of CFEM, CCM, ACM and THALWEG of Section J-9
Locations of CFEM, CCM, ACM and THALWEG, in m
YEAR
CFEM
CCM
ACM
THALWEG
10000
9000
8000
7000
6000
5000
4000
3000
2000
1000
1975
1976
1977
1978
1979
1980
1981
1982
1983
1984

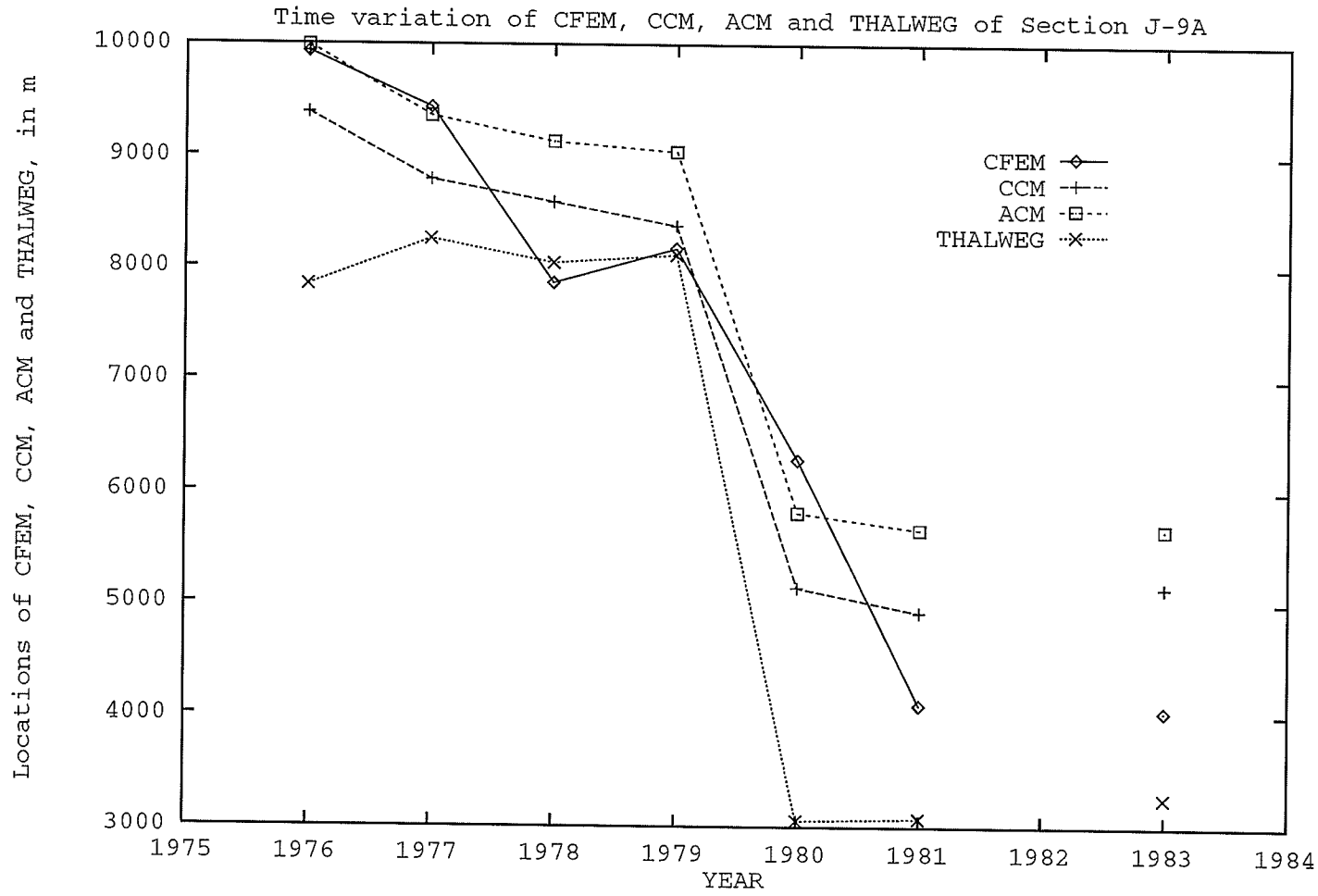
Time variation of CFEM, CCM, ACM and THALWEG of Section J-9A
Locations of CFEM, CCM, ACM and THALWEG, in m
YEAR
CFEM
CCM
ACM
THALWEG
10000
9000
8000
7000
6000
5000
4000
3000
1975
1976
1977
1978
1979
1980
1981
1982
1983
1984

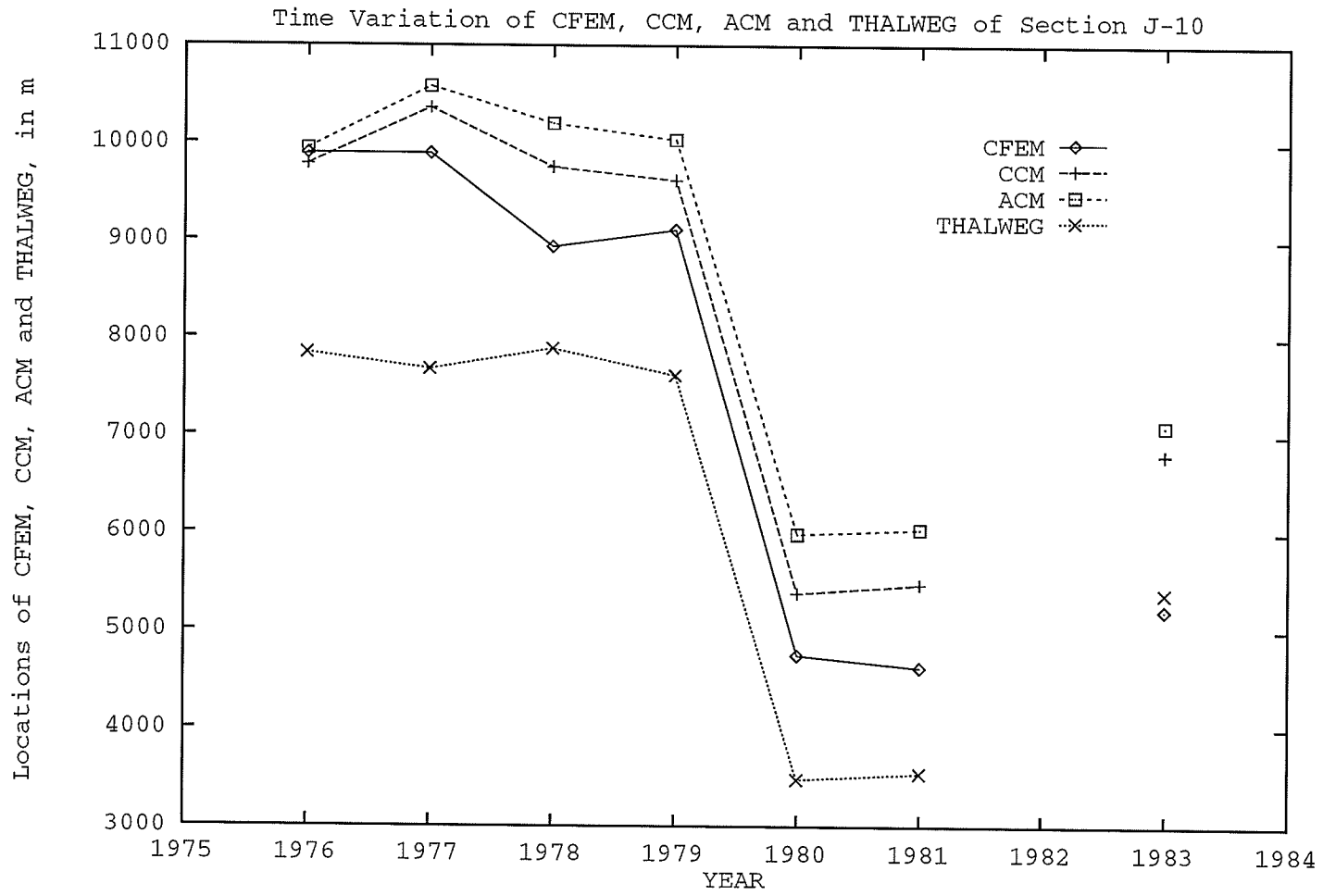
Time Variation of CFEM, CCM, ACM and THALWEG of Section J-10
Locations of CFEM, CCM, ACM and THALWEG, in m
YEAR
CFEM
CCM
ACM
THALWEG
11000
10000
9000
8000
7000
6000
5000
4000
3000
1975
1976
1977
1978
1979
1980
1981
1982
1983
1984

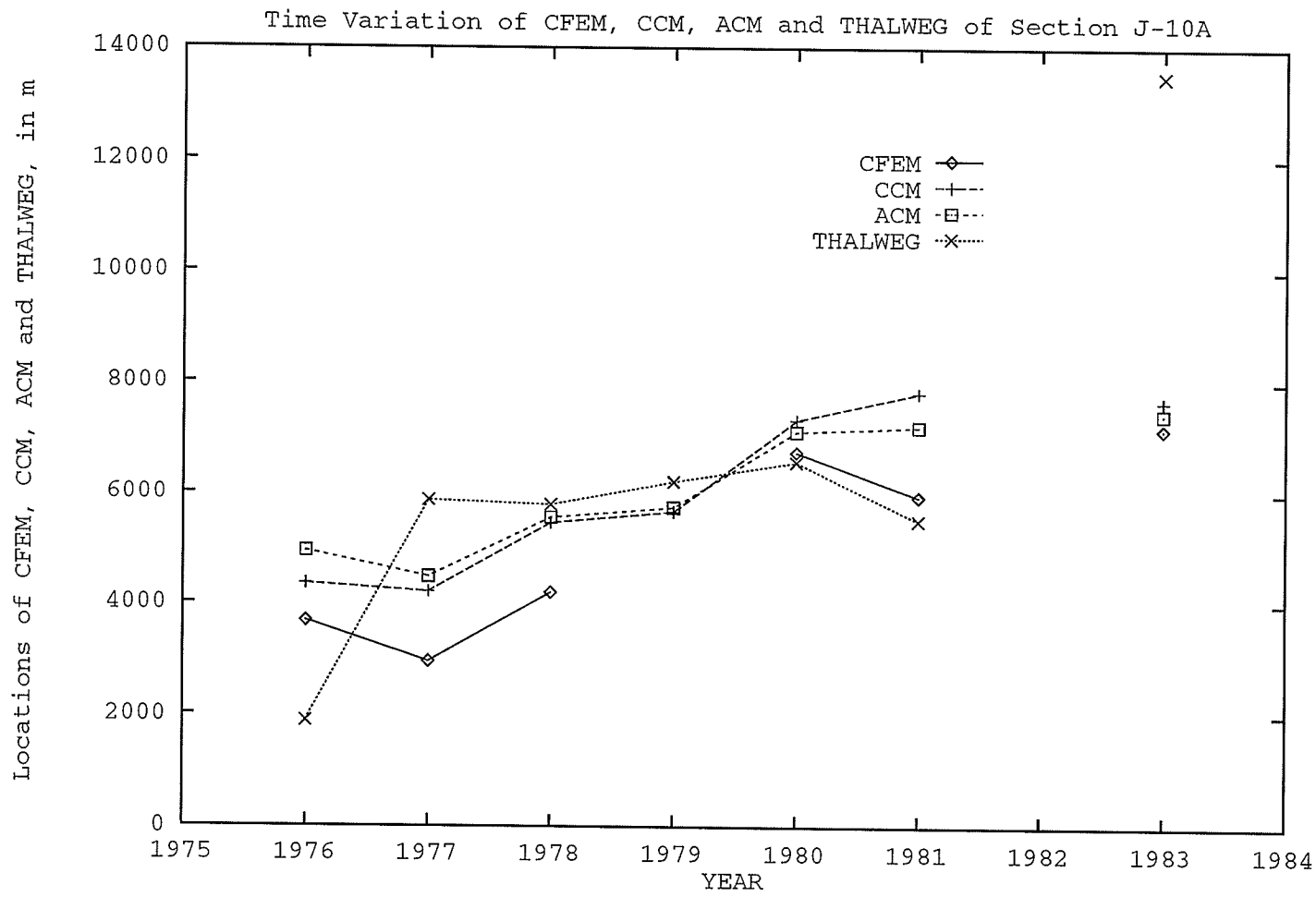
Time Variation of CFEM, CCM, ACM and THALWEG of Section J-10A
Locations of CFEM, CCM, ACM and THALWEG, in m
YEAR
CFEM
CCM
ACM
THALWEG
0
2000
4000
6000
8000
10000
12000
14000
1975
1976
1977
1978
1979
1980
1981
1982
1983
1984

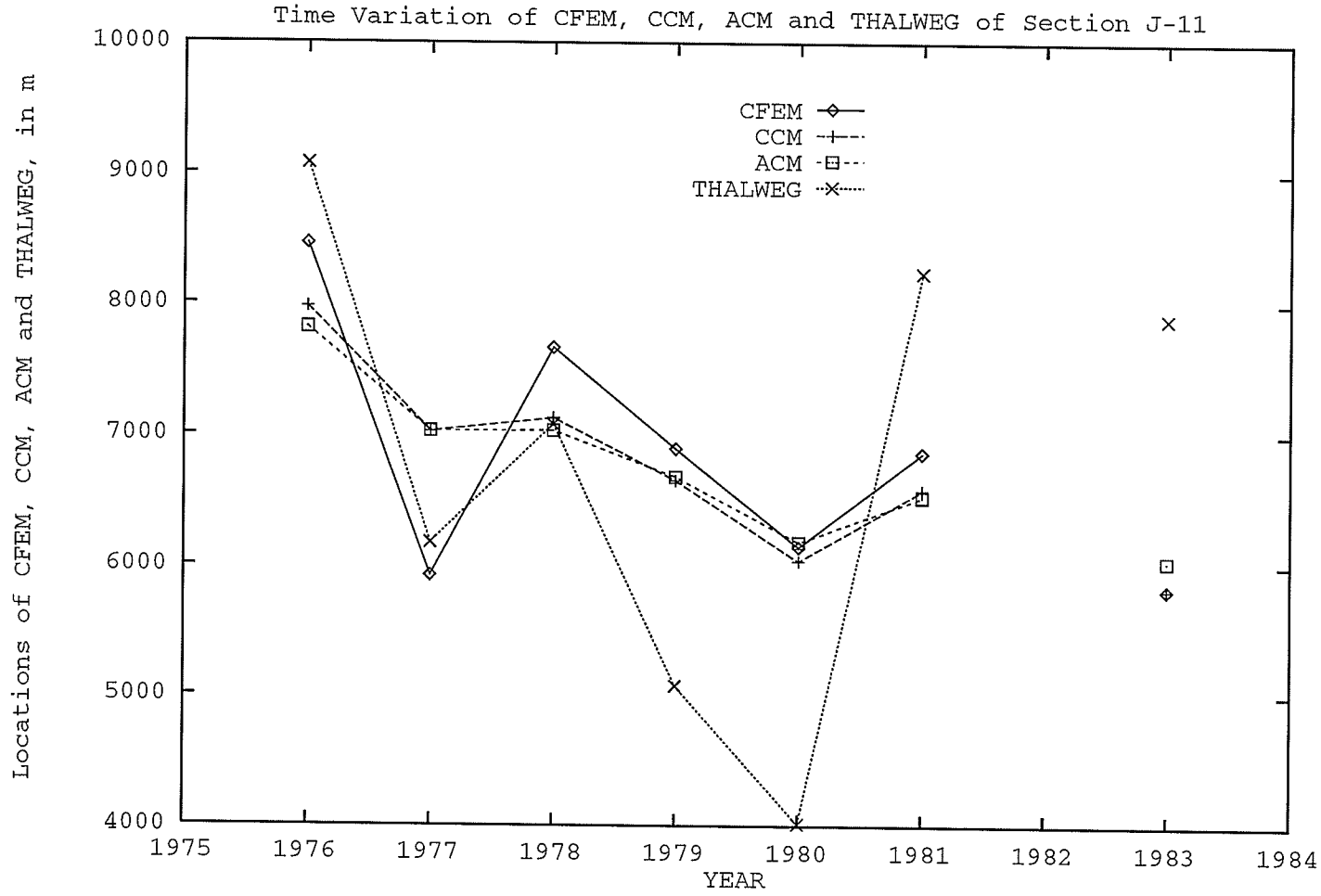
Time Variation of CFEM, CCM, ACM and THALWEG of Section J-11
Locations of CFEM, CCM, ACM and THALWEG, in m
YEAR
CFEM
CCM
ACM
THALWEG
10000
9000
8000
7000
6000
5000
4000
1975
1976
1977
1978
1979
1980
1981
1982
1983
1984

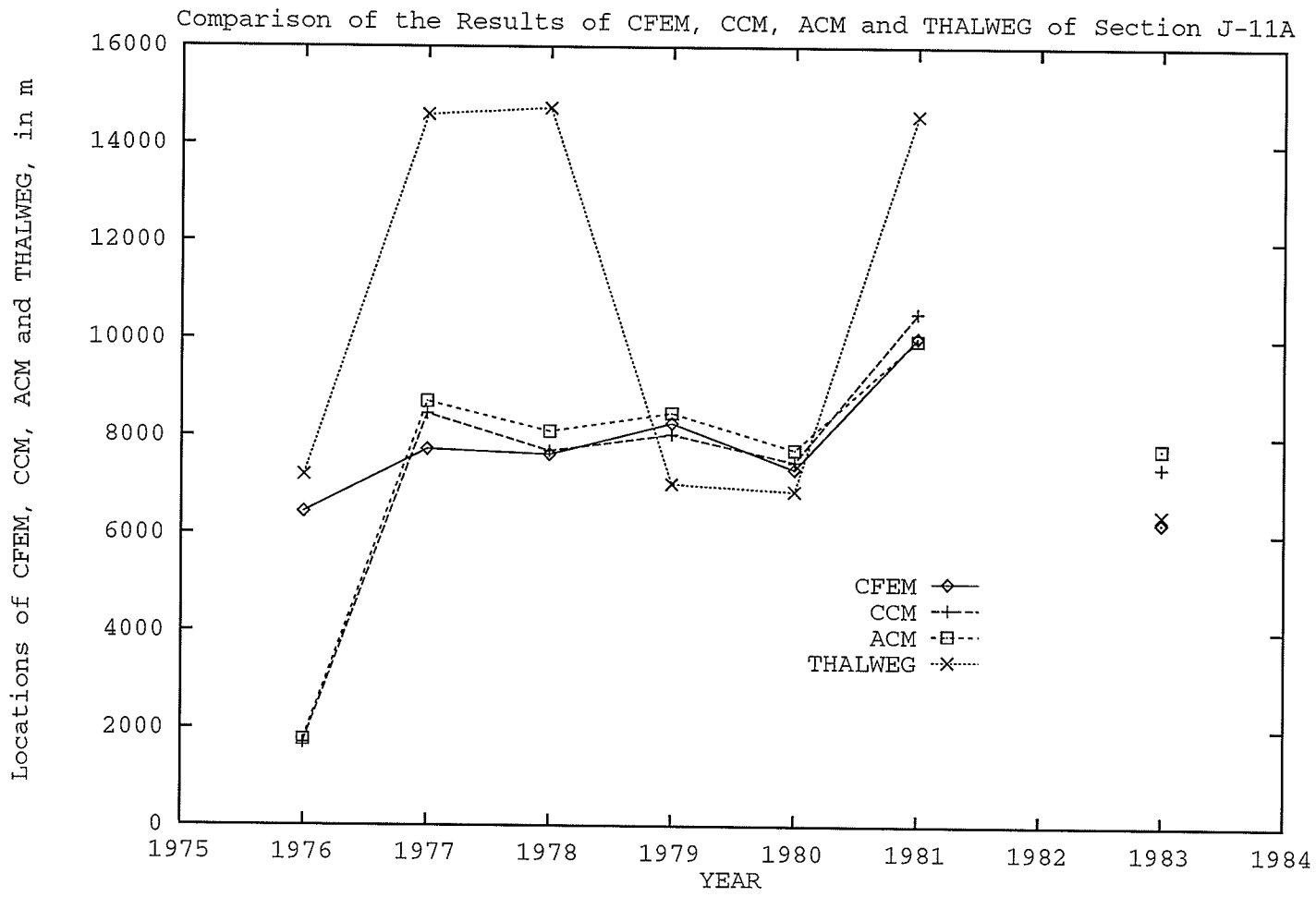
Comparison of the Results of CFEM, CCM, ACM and THALWEG of Section J-11A
Locations of CFEM, CCM, ACM and THALWEG, in m
YEAR
16000
14000
12000
10000
8000
6000
4000
2000
0
1975
1976
1977
1978
1979
1980
1981
1982
1983
1984
CFEM
CCM
ACM
THALWEG

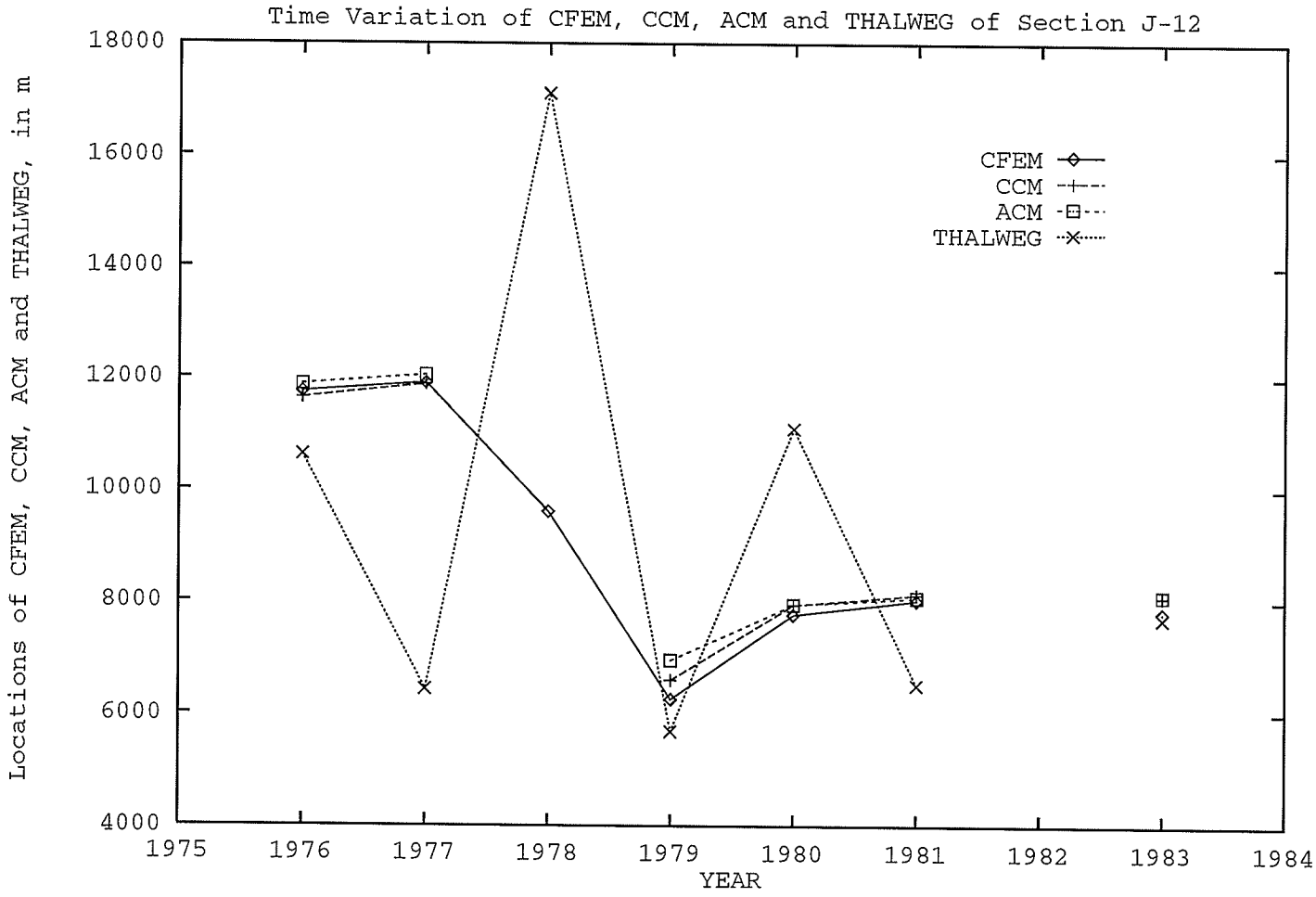
Time Variation of CFEM, CCM, ACM and THALWEG of Section J-12
Locations of CFEM, CCM, ACM and THALWEG, in m
YEAR
CFEM
CCM
ACM
THALWEG
18000
16000
14000
12000
10000
8000
6000
4000
1975
1976
1977
1978
1979
1980
1981
1982
1983
1984

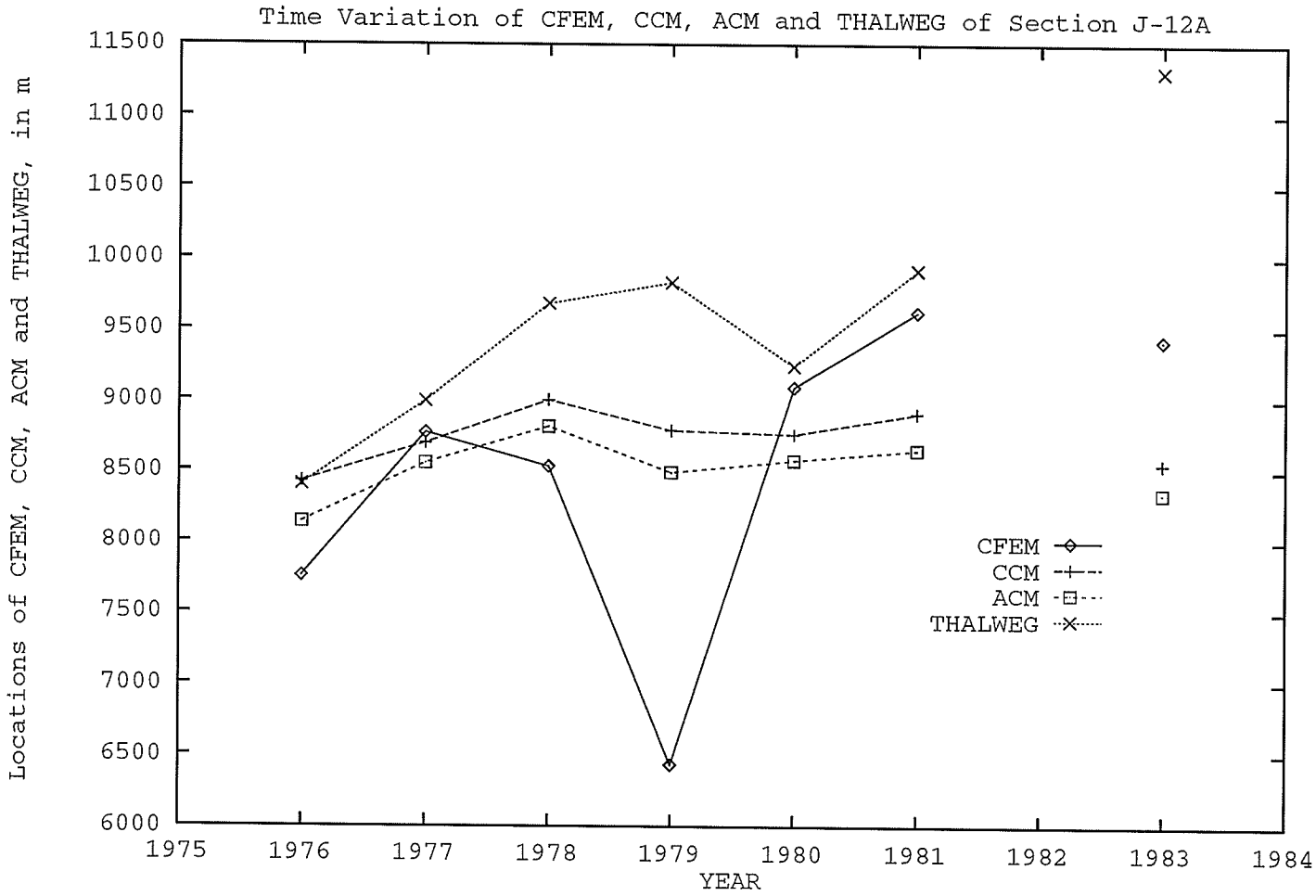
Time Variation of CFEM, CCM, ACM and THALWEG of Section J-12A
Locations of CFEM, CCM, ACM and THALWEG, in m
YEAR
11500
11000
10500
10000
9500
9000
8500
8000
7500
7000
6500
6000
1975
1976
1977
1978
1979
1980
1981
1982
1983
1984
CFEM
CCM
ACM
THALWEG

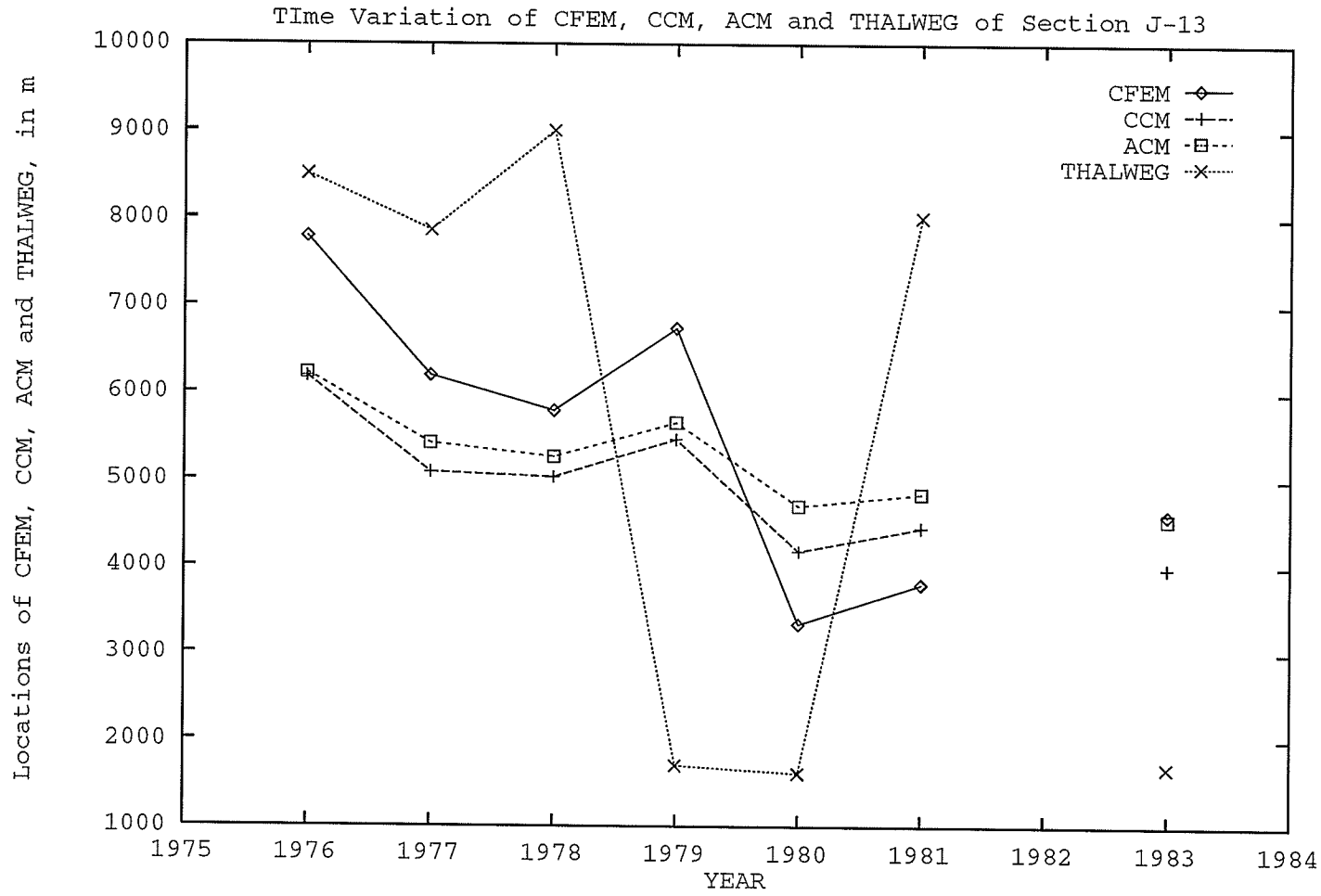
TIme Variation of CFEM, CCM, ACM and THALWEG of Section J-13
Locations of CFEM, CCM, ACM and THALWEG, in m
YEAR
CFEM
CCM
ACM
THALWEG
10000
9000
8000
7000
6000
5000
4000
3000
2000
1000
1975
1976
1977
1978
1979
1980
1981
1982
1983
1984

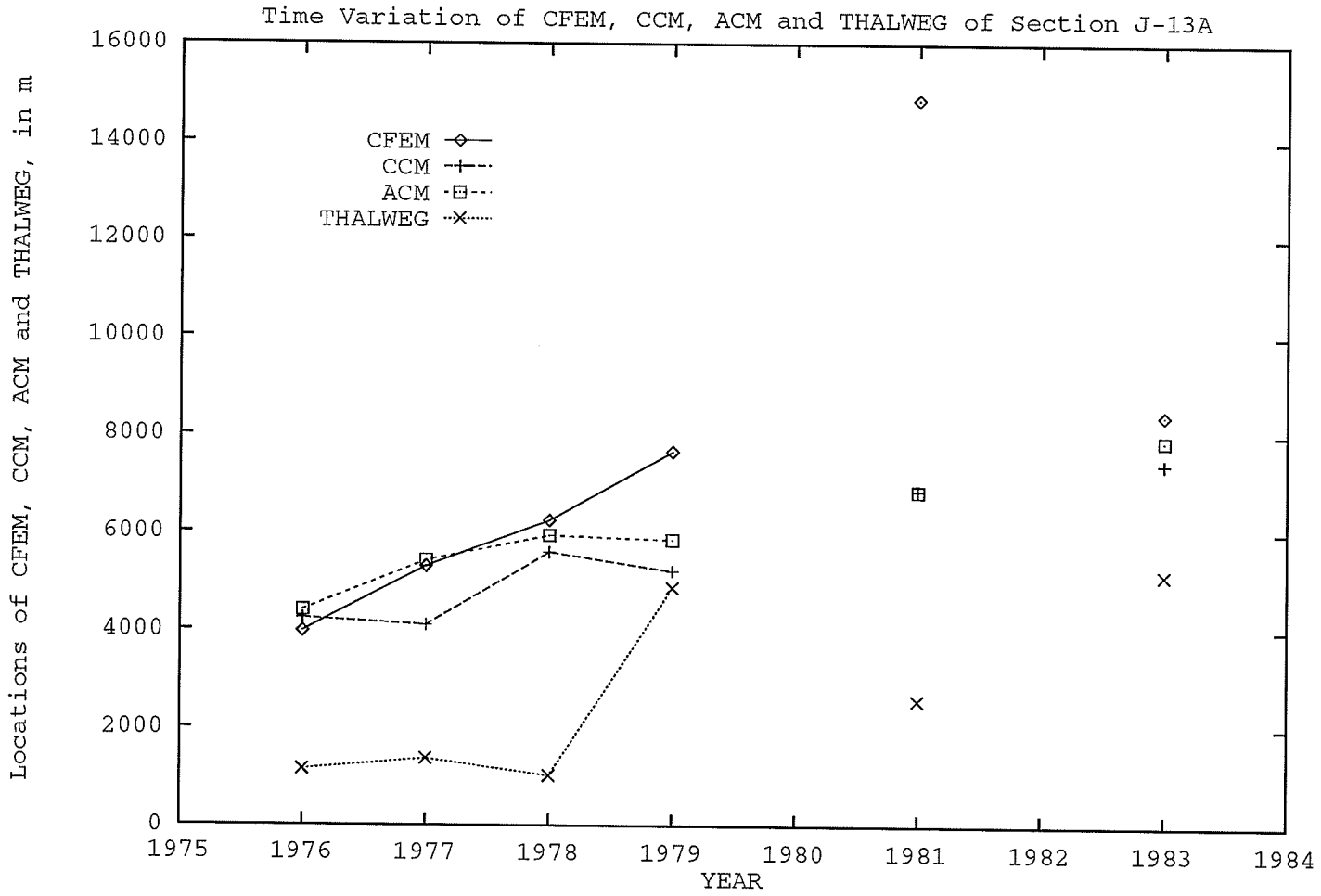
Time Variation of CFEM, CCM, ACM and THALWEG of Section J-13A
Locations of CFEM, CCM, ACM and THALWEG, in m
YEAR
CFEM
CCM
ACM
THALWEG
16000
14000
12000
10000
8000
6000
4000
2000
0
1975
1976
1977
1978
1979
1980
1981
1982
1983
1984

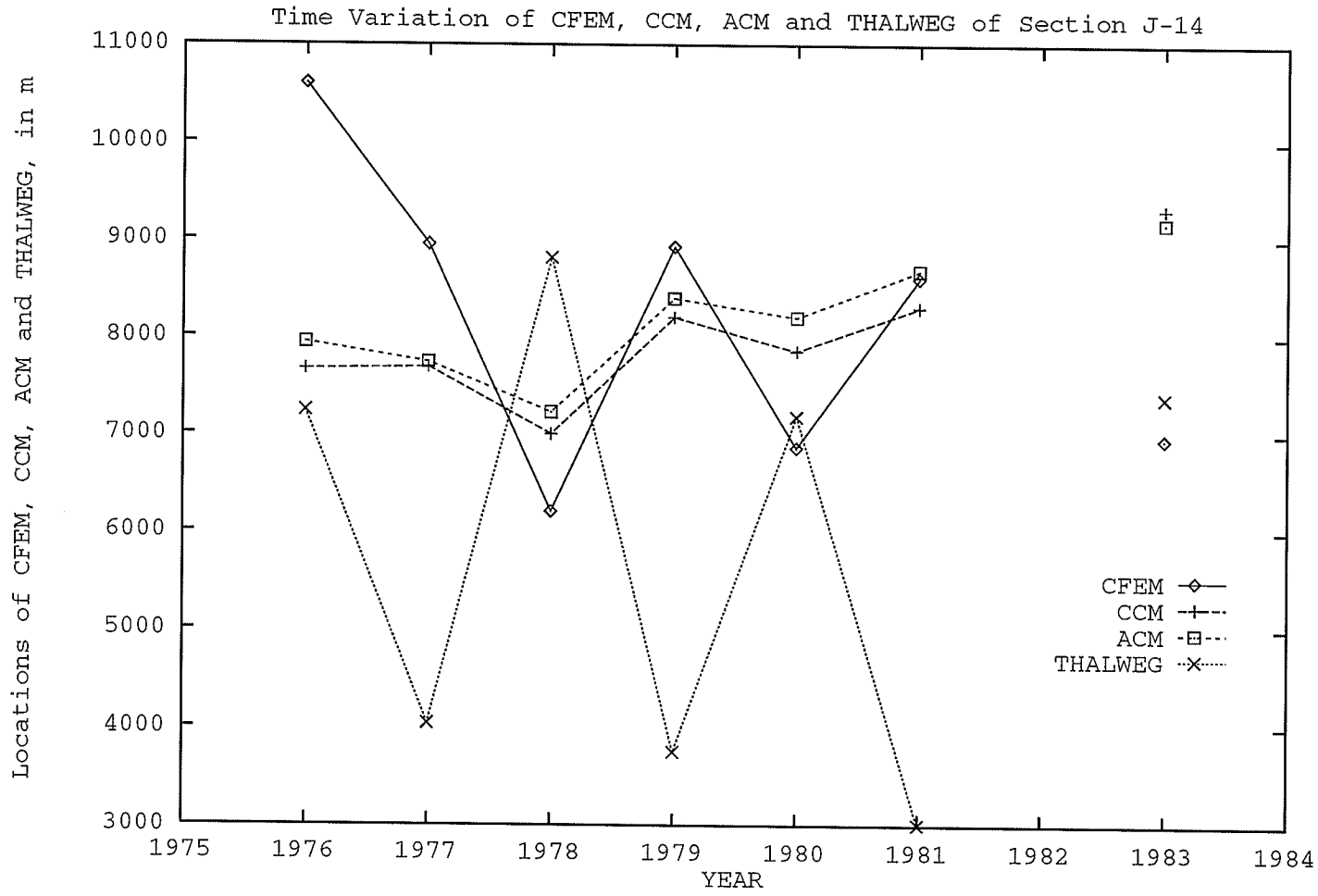
Time Variation of CFEM, CCM, ACM and THALWEG of Section J-14
Locations of CFEM, CCM, ACM and THALWEG, in m
YEAR
11000
10000
9000
8000
7000
6000
5000
4000
3000
1975
1976
1977
1978
1979
1980
1981
1982
1983
1984
CFEM
CCM
ACM
THALWEG

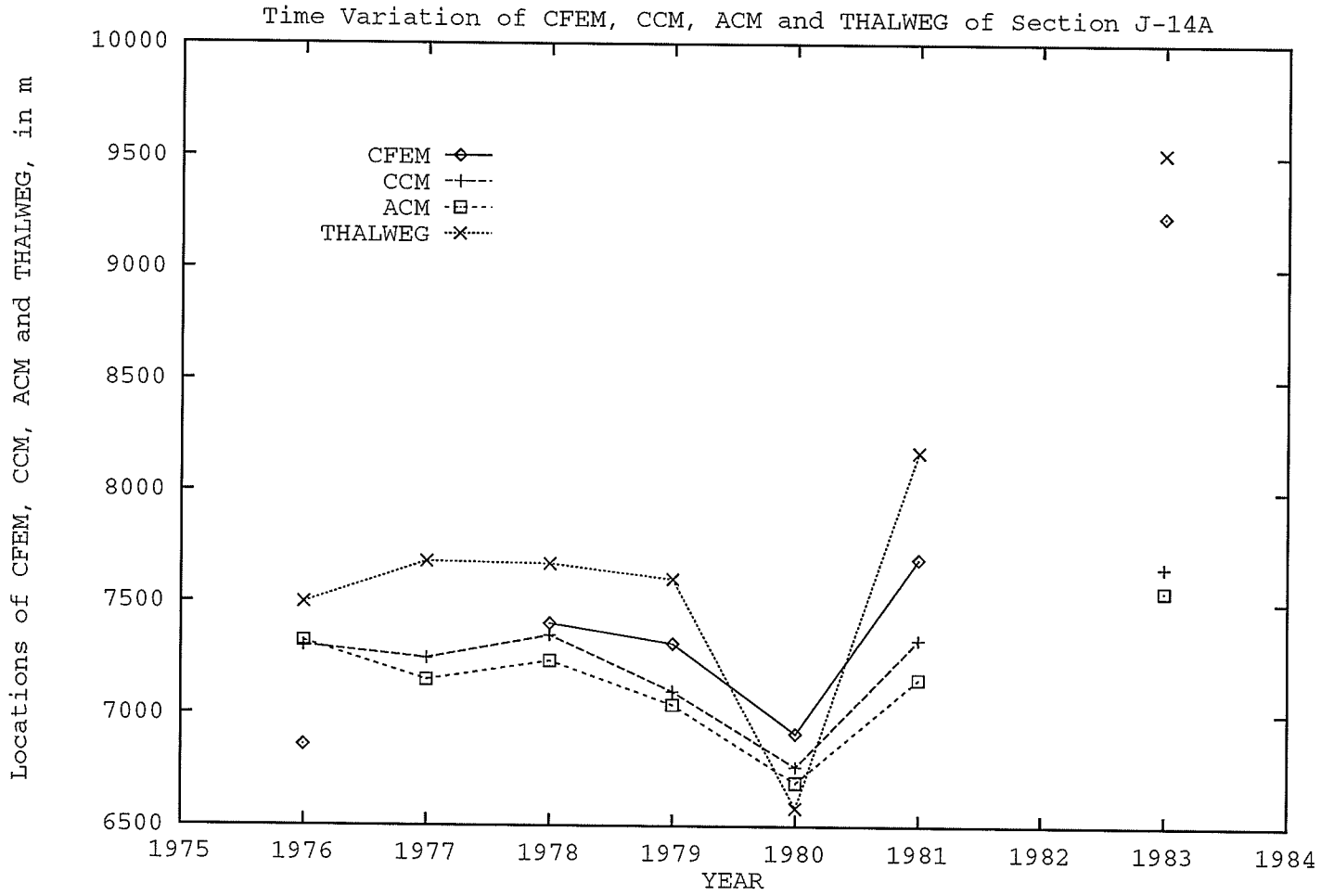
Time Variation of CFEM, CCM, ACM and THALWEG of Section J-14A
Locations of CFEM, CCM, ACM and THALWEG, in m
YEAR
CFEM
CCM
ACM
THALWEG
10000
9500
9000
8500
8000
7500
7000
6500
1975
1976
1977
1978
1979
1980
1981
1982
1983
1984

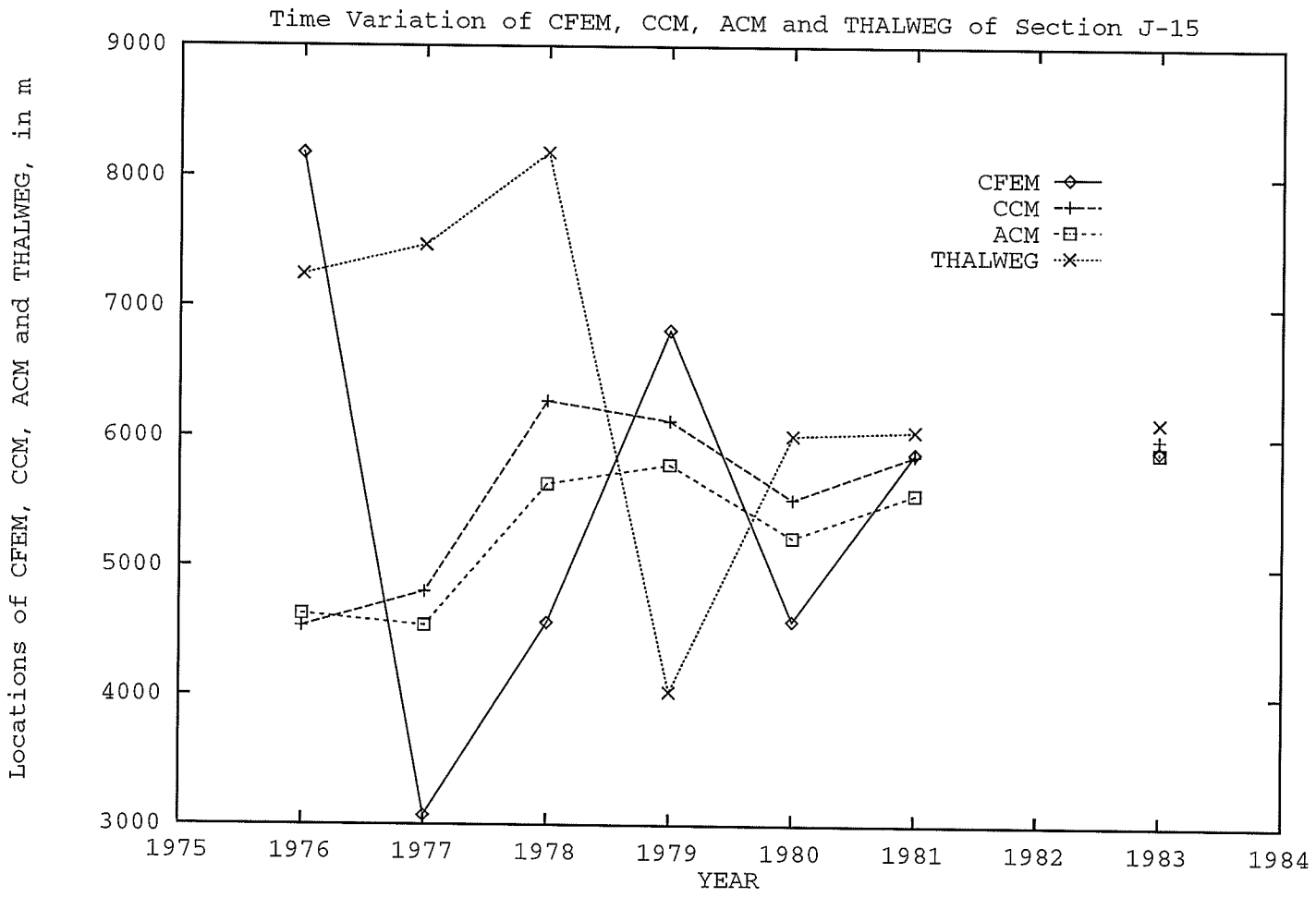
Time Variation of CFEM, CCM, ACM and THALWEG of Section J-15
Locations of CFEM, CCM, ACM and THALWEG, in m
YEAR
CFEM
CCM
ACM
THALWEG
9000
8000
7000
6000
5000
4000
3000
1975
1976
1977
1978
1979
1980
1981
1982
1983
1984

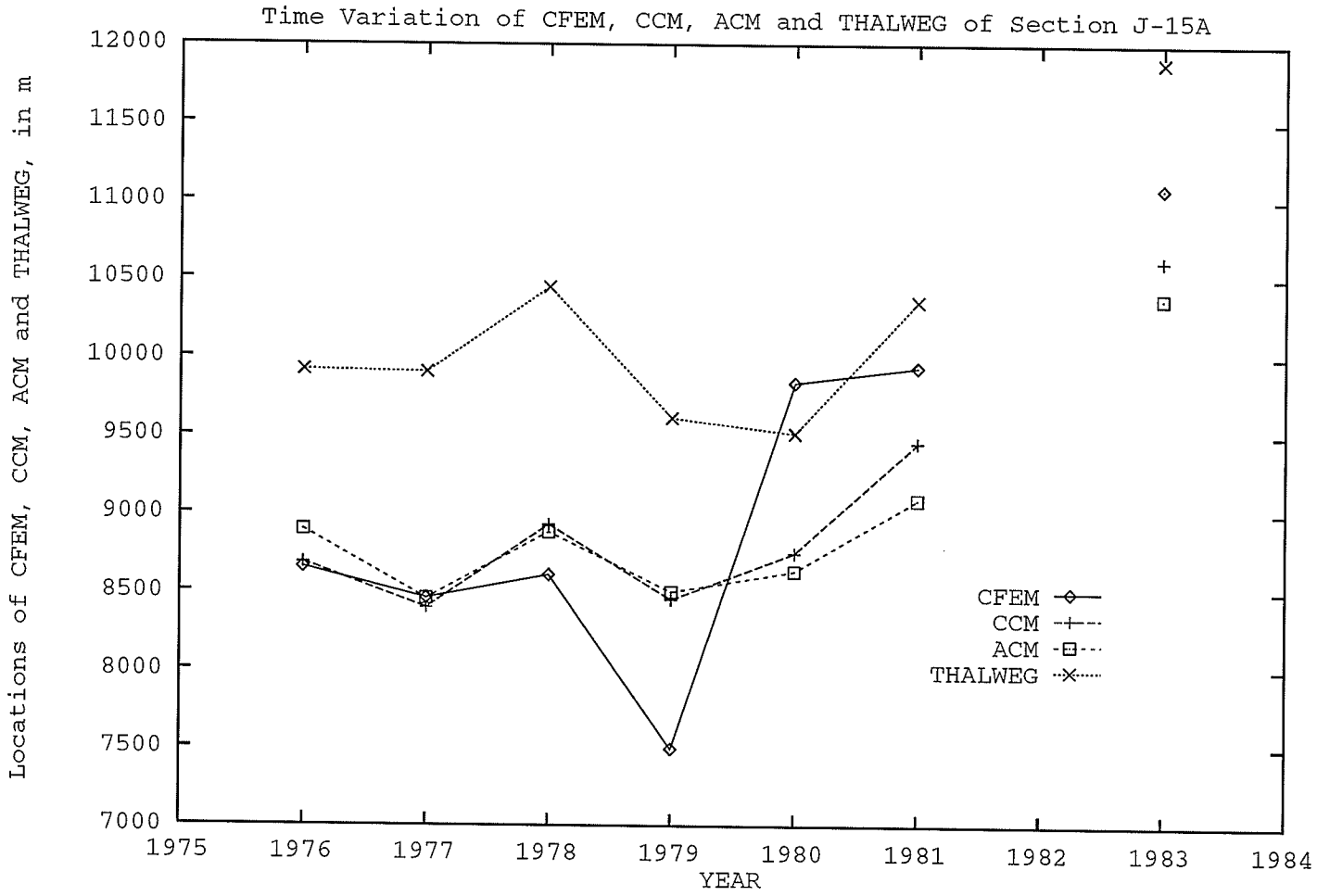
Time Variation of CFEM, CCM, ACM and THALWEG of Section J-15A
Locations of CFEM, CCM, ACM and THALWEG, in m
YEAR
12000
11500
11000
10500
10000
9500
9000
8500
8000
7500
7000
1975
1976
1977
1978
1979
1980
1981
1982
1983
1984
CFEM
CCM
ACM
THALWEG

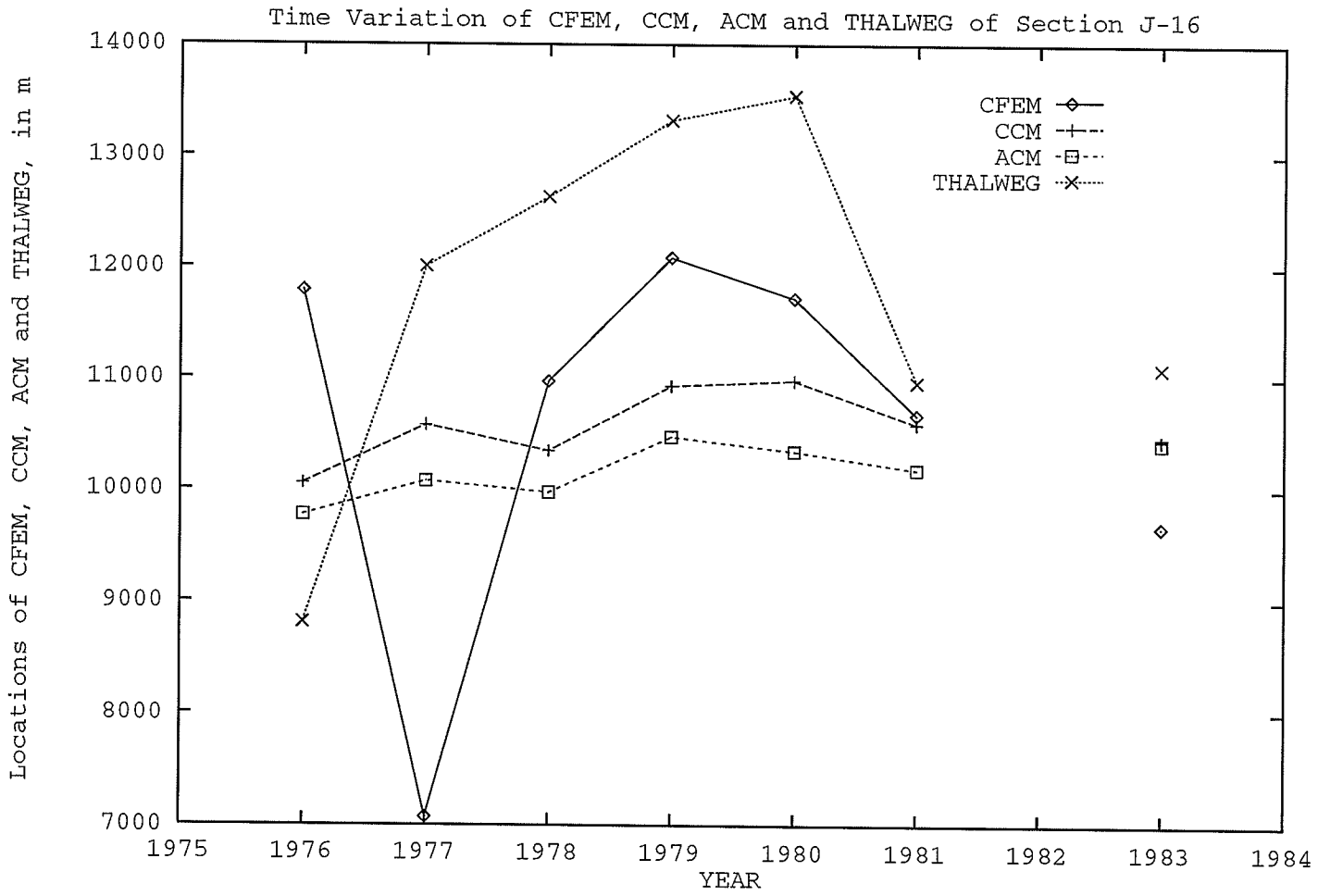
Time Variation of CFEM, CCM, ACM and THALWEG of Section J-16
Locations of CFEM, CCM, ACM and THALWEG, in m
YEAR
CFEM
CCM
ACM
THALWEG
14000
13000
12000
11000
10000
9000
8000
7000
1975
1976
1977
1978
1979
1980
1981
1982
1983
1984

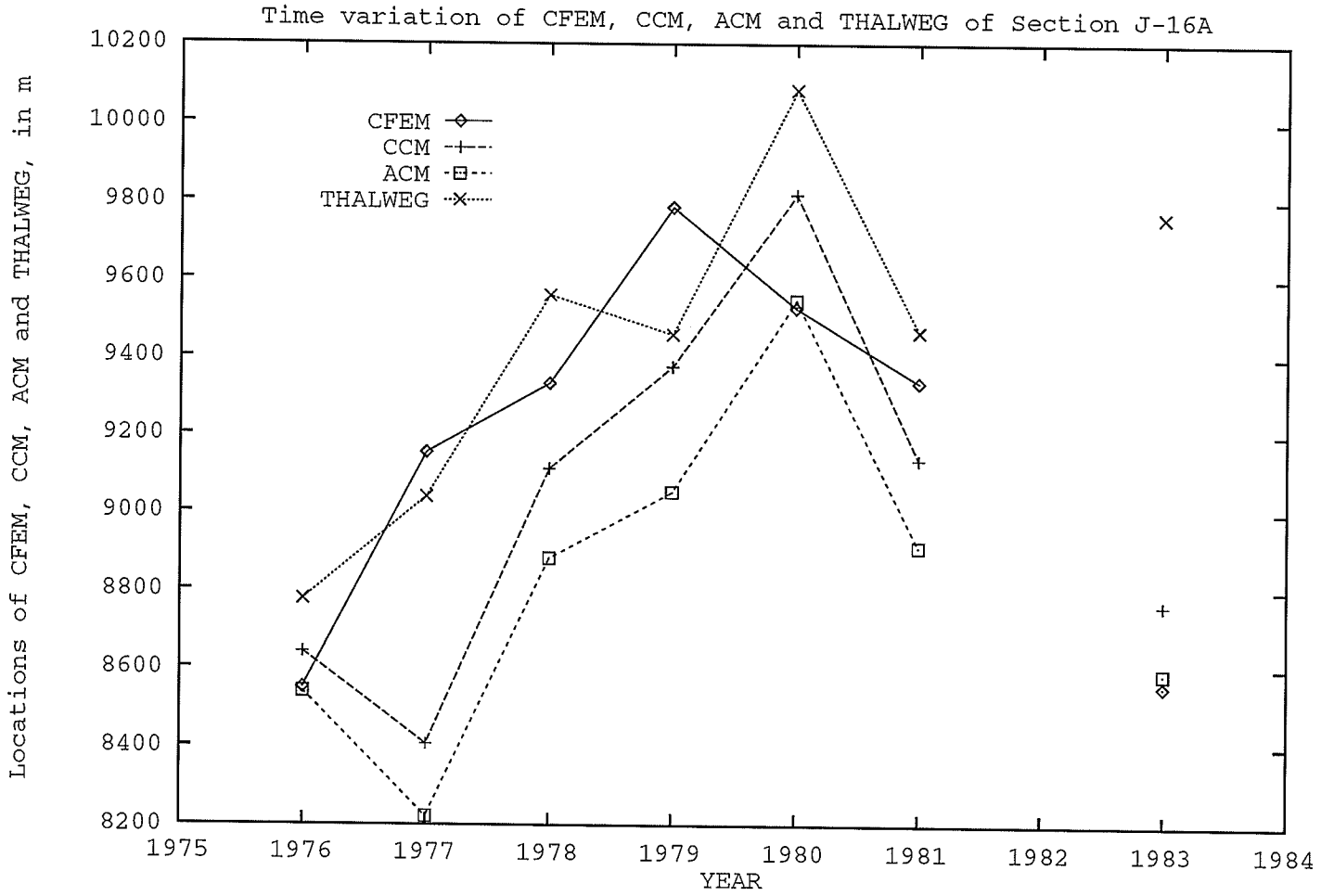
Time variation of CFEM, CCM, ACM and THALWEG of Section J-16A
Locations of CFEM, CCM, ACM and THALWEG, in m
YEAR
CFEM
CCM
ACM
THALWEG
10200
10000
9800
9600
9400
9200
9000
8800
8600
8400
8200
1975
1976
1977
1978
1979
1980
1981
1982
1983
1984

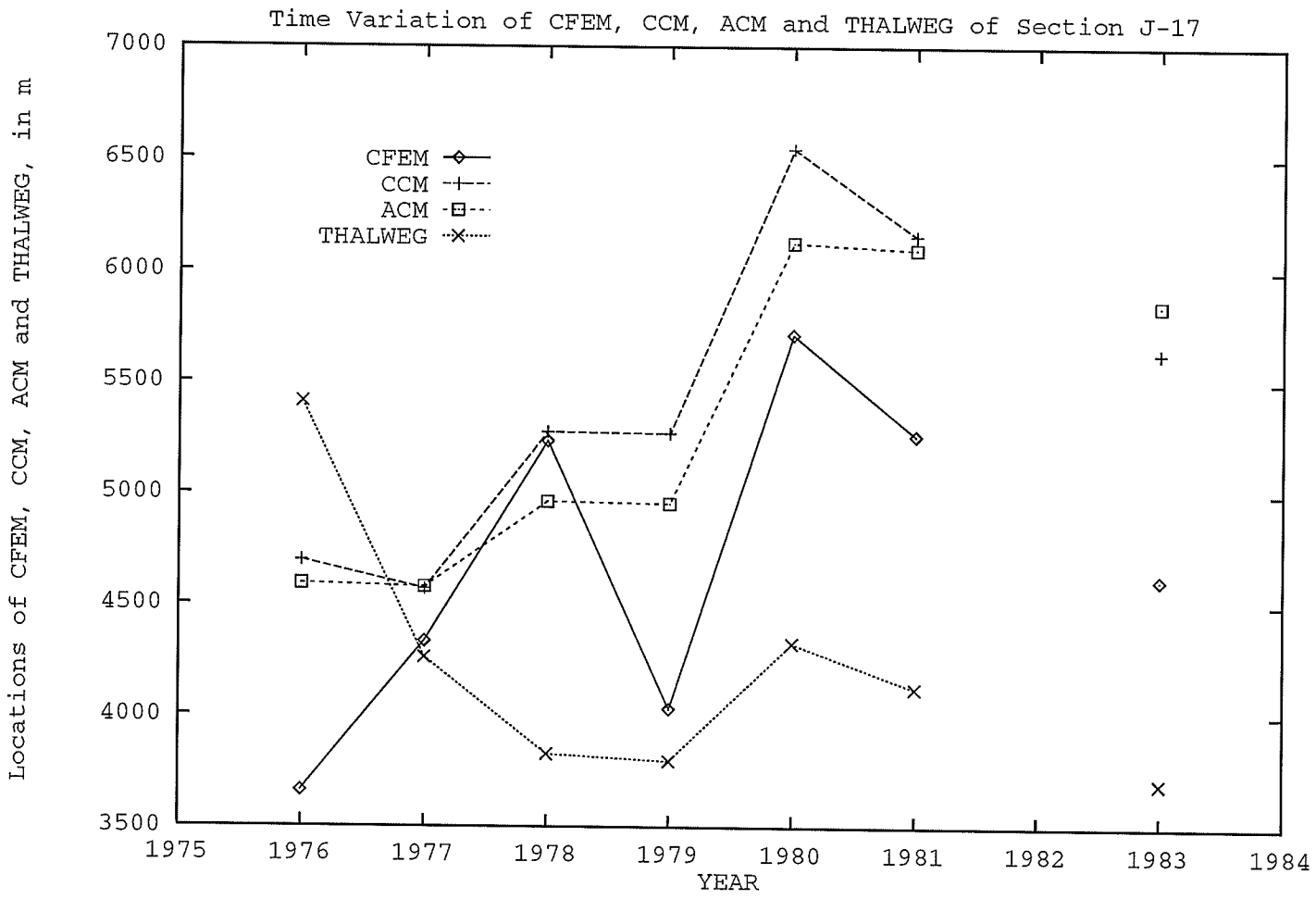
Time Variation of CFEM, CCM, ACM and THALWEG of Section J-17
Locations of CFEM, CCM, ACM and THALWEG, in m
YEAR
CFEM
CCM
ACM
THALWEG
7000
6500
6000
5500
5000
4500
4000
3500
1975
1976
1977
1978
1979
1980
1981
1982
1983
1984

Appendix C

CURVES OF CUMULATIVE OF RELATIVE CONVEYANCE

Note that these curves are given in an increasing numerical order of cross-section with the cross-section number specified at the top of the graph.

Cumulative of Relative Conveyance Curve of Section J-1

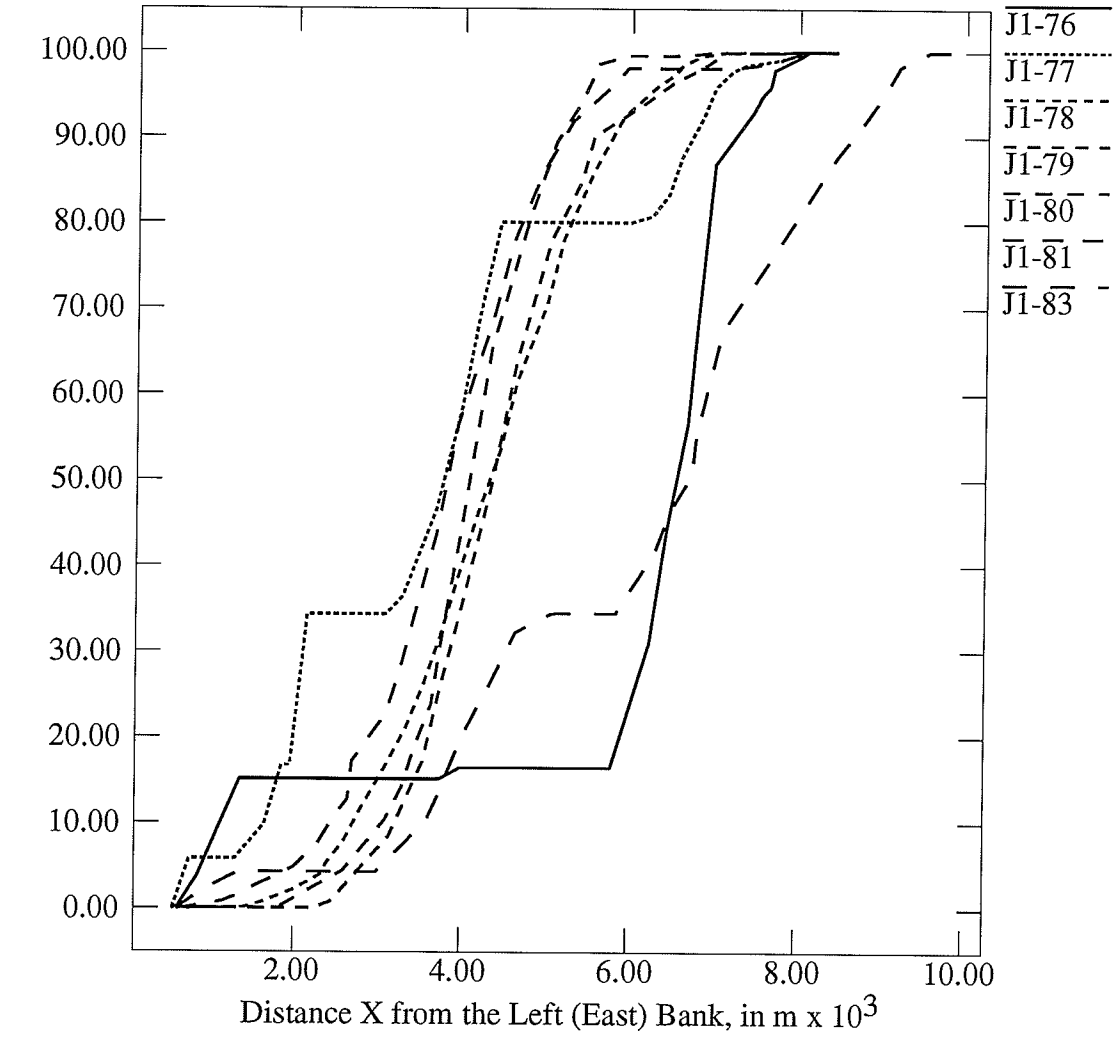

Cumulative of Relative Conveyance Curve of Section J-1A

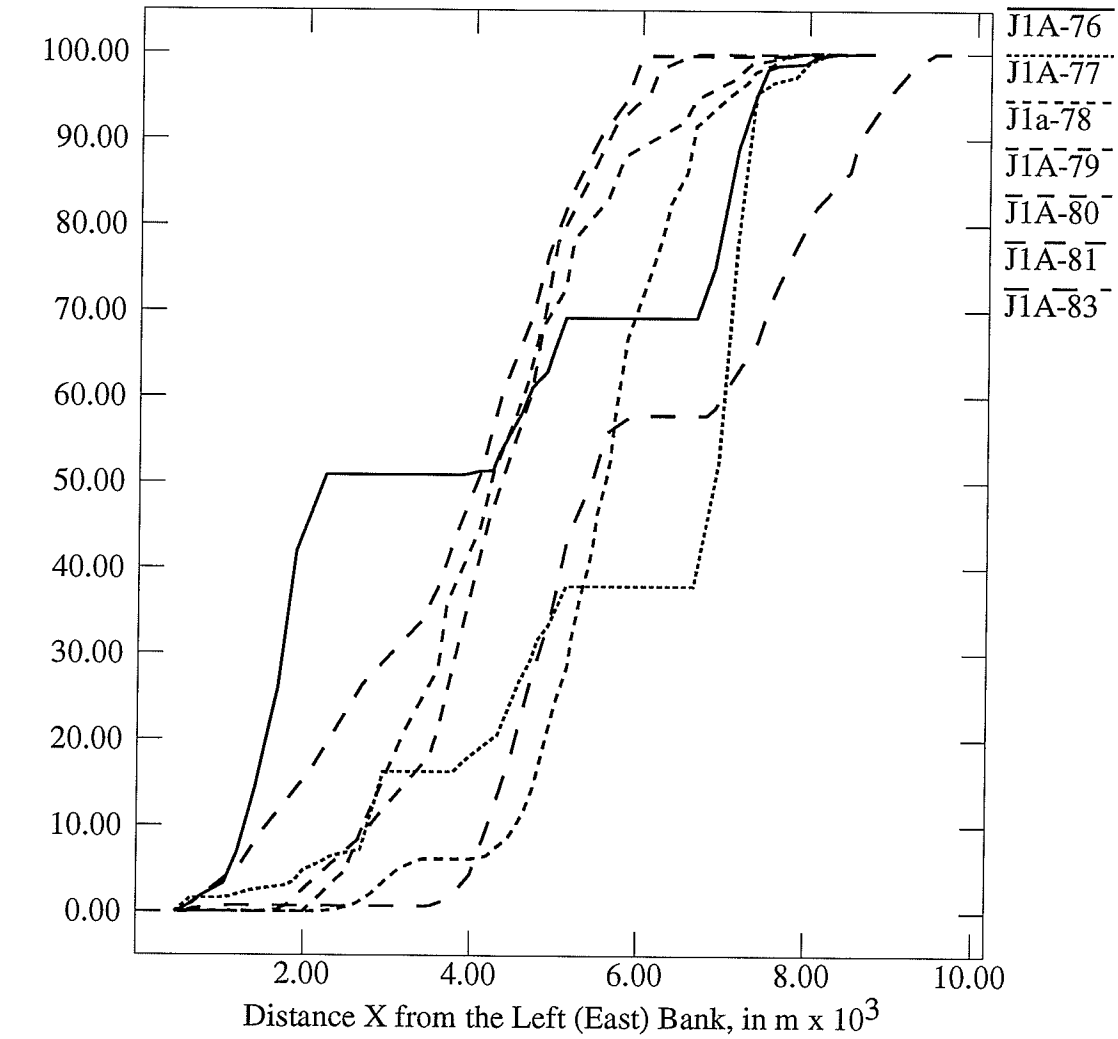

Cumulative of Relative Conveyance Curve of Section J-2

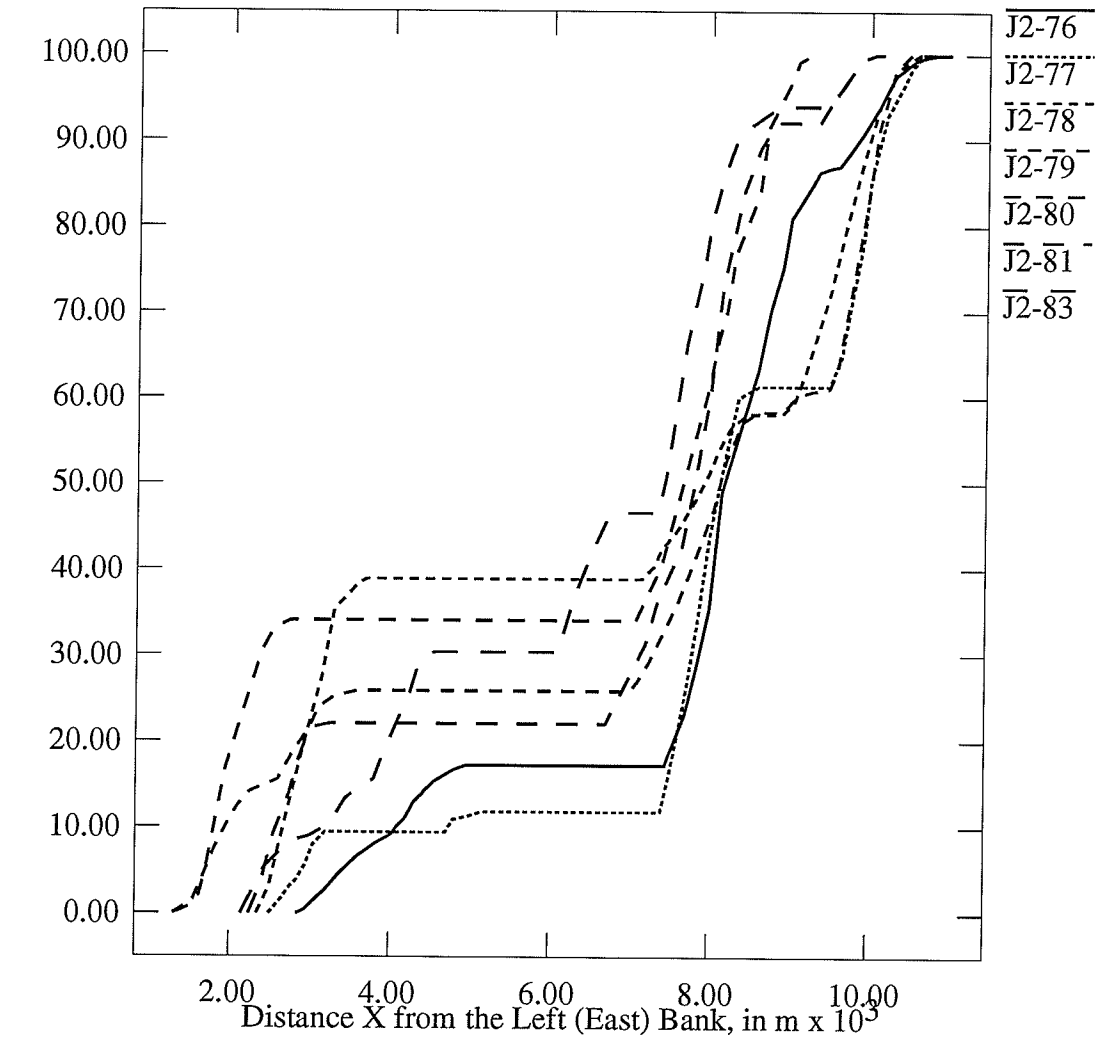

Cumulative of Relative Conveyance Curve of Section J-2A

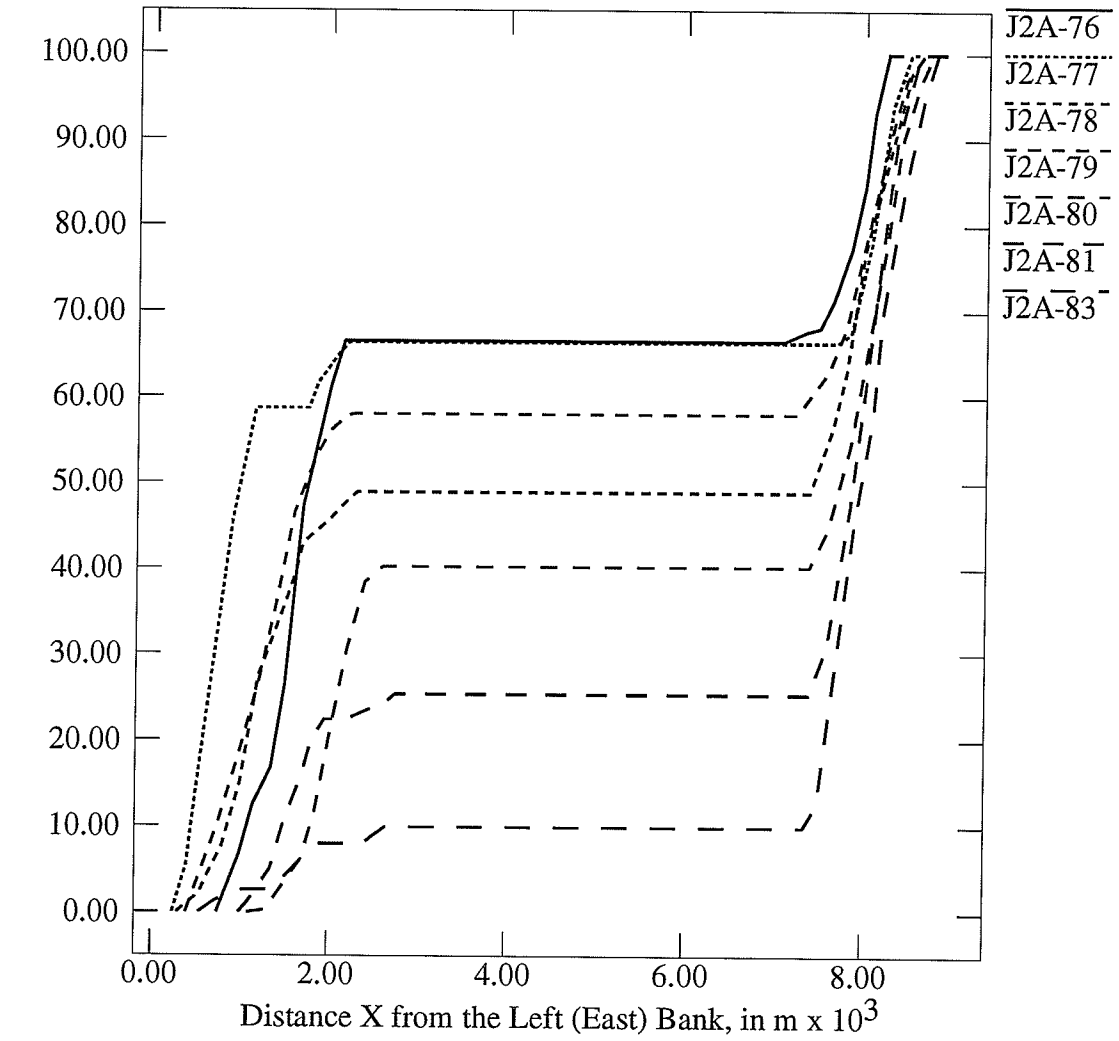

Cumulative of Relative Conveyance Curve of Section J-3

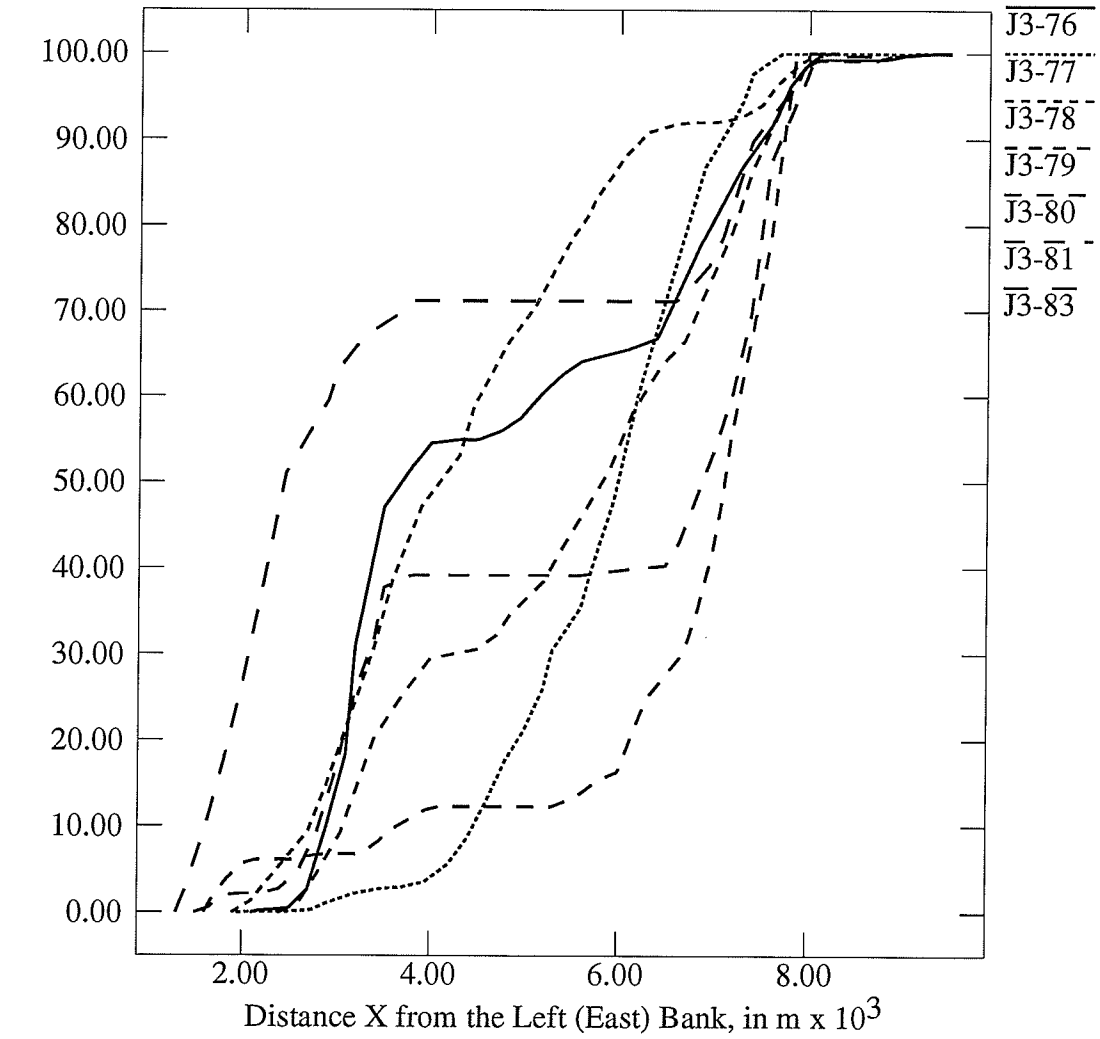

Cumulative of Relative Conveyance Curve of Section J-3A

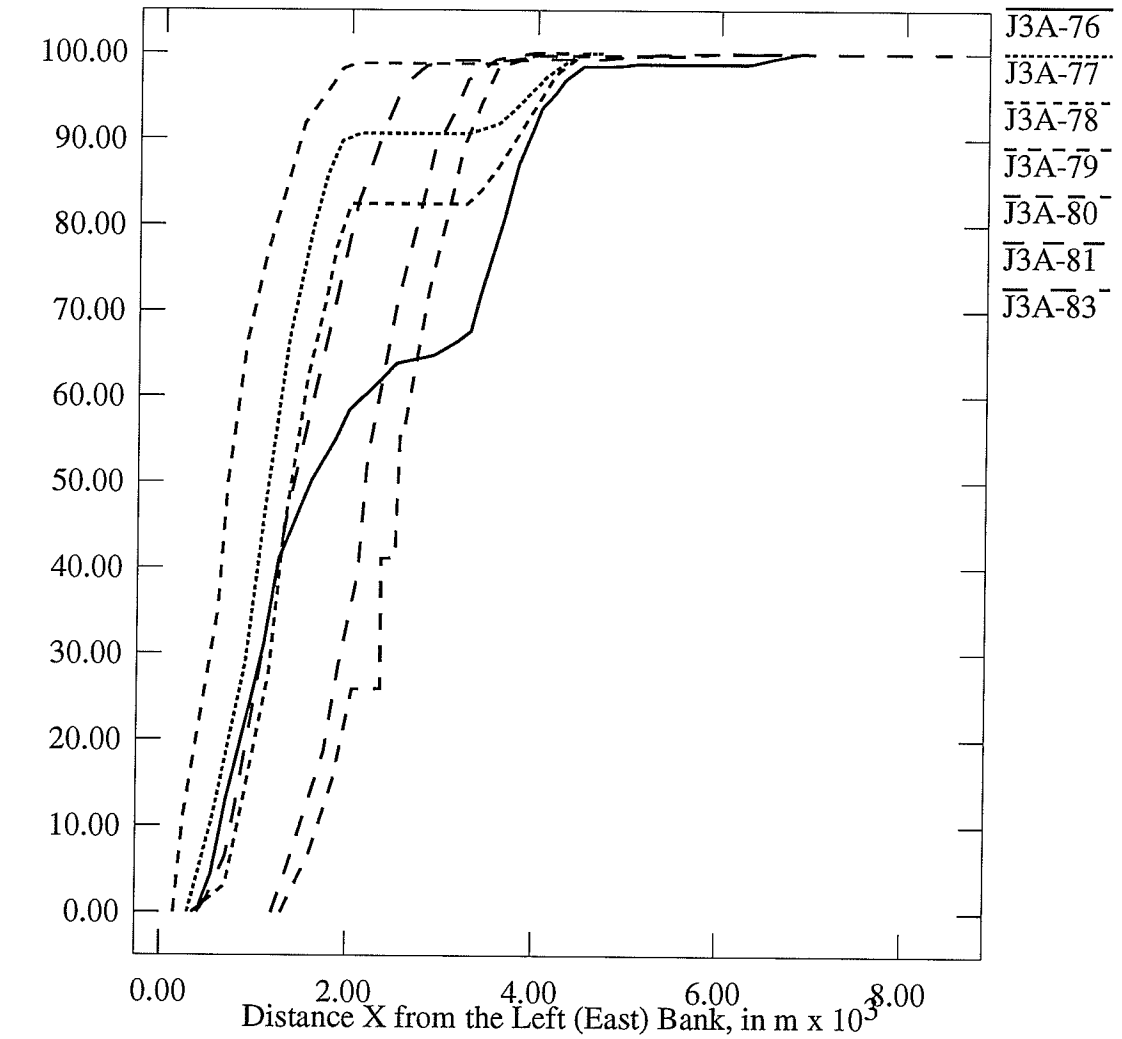

Cumulative of Relative Conveyance Curve of Section J-4

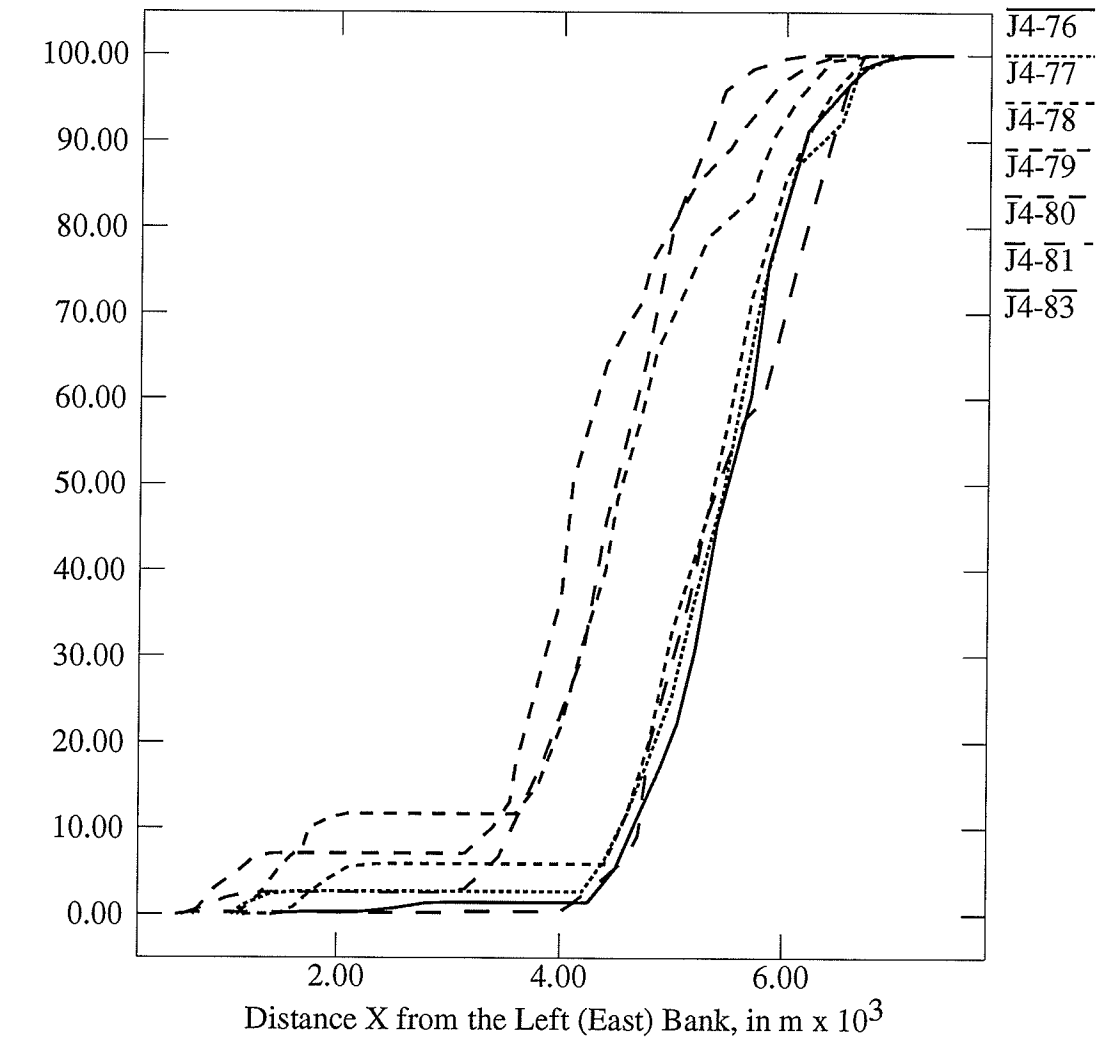

Cumulative of Relative Conveyance Curve of Section J-4A

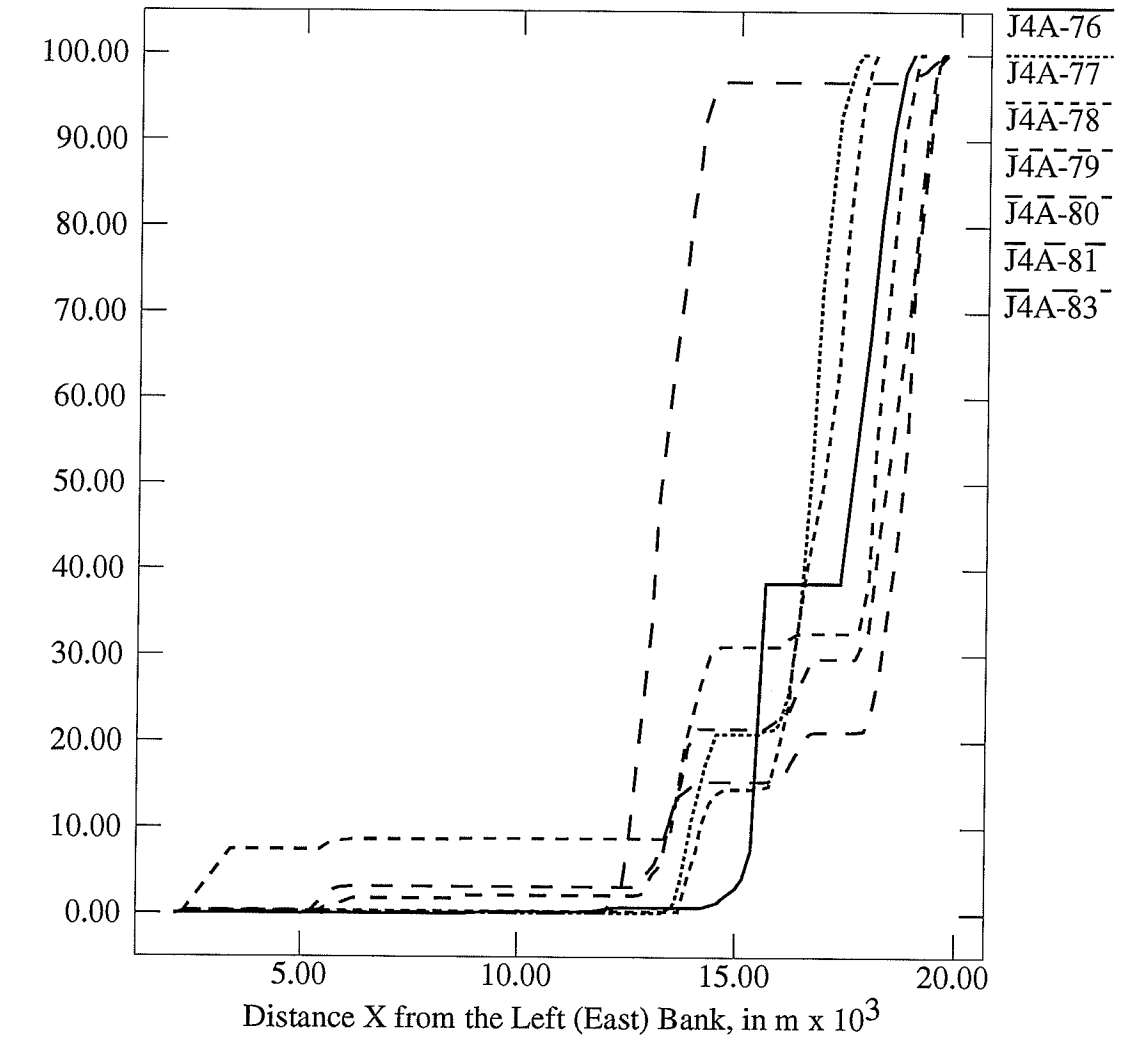

Cumulative of Relative Conveyance Curve of Section J-5

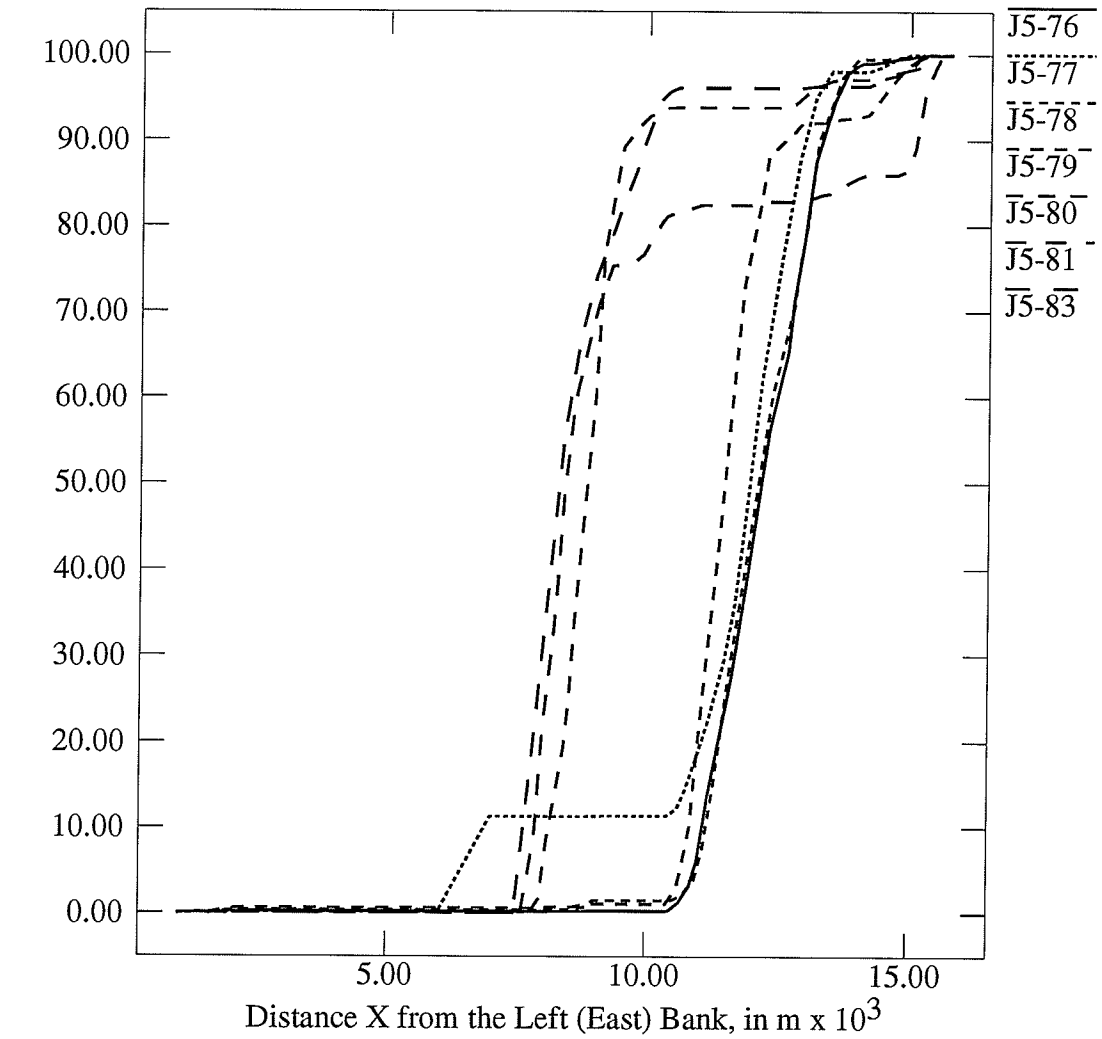

Cumulative of Relative Conveyance Curve of Section J-5A

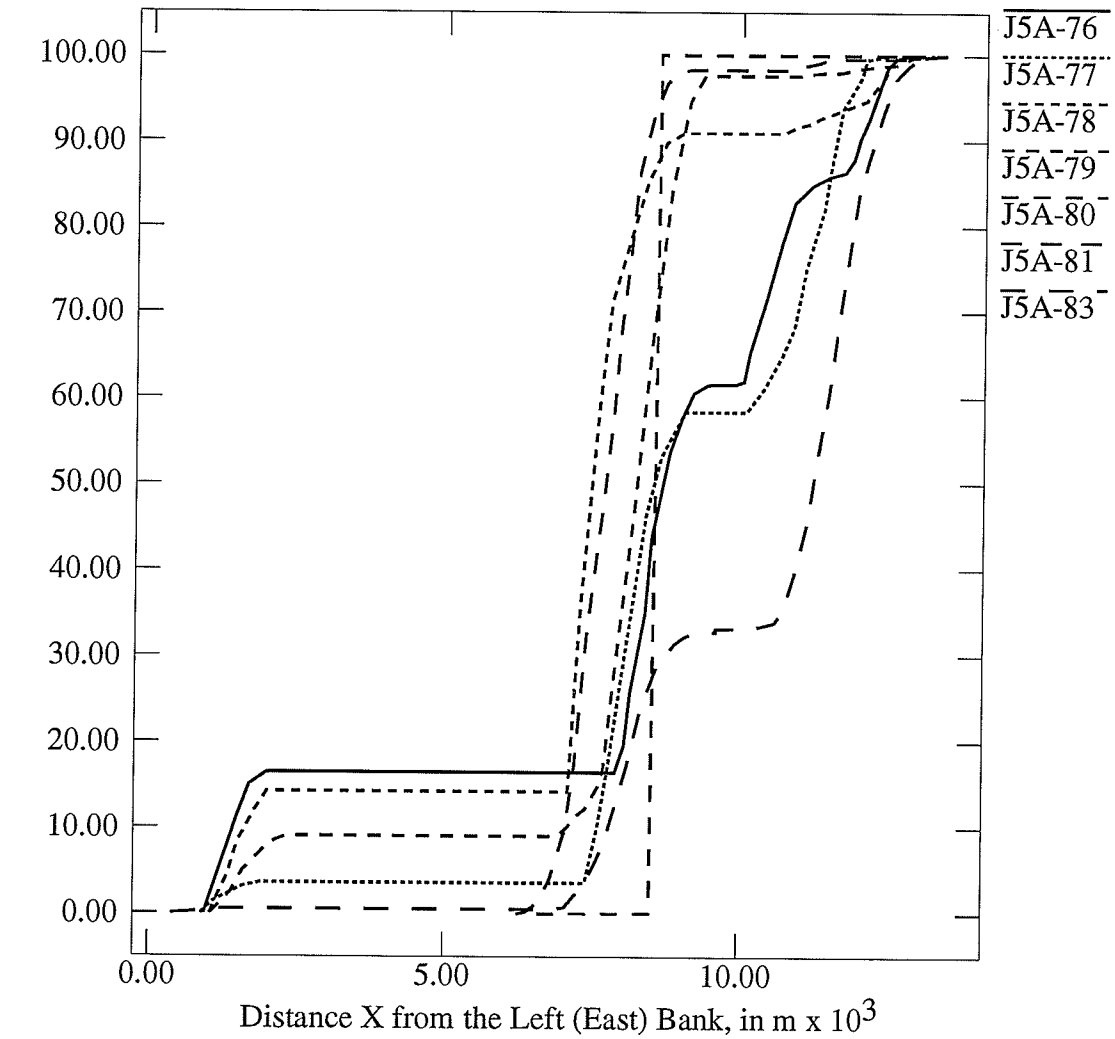

Cumulative of Relative Conveyance Curve of Section J-6

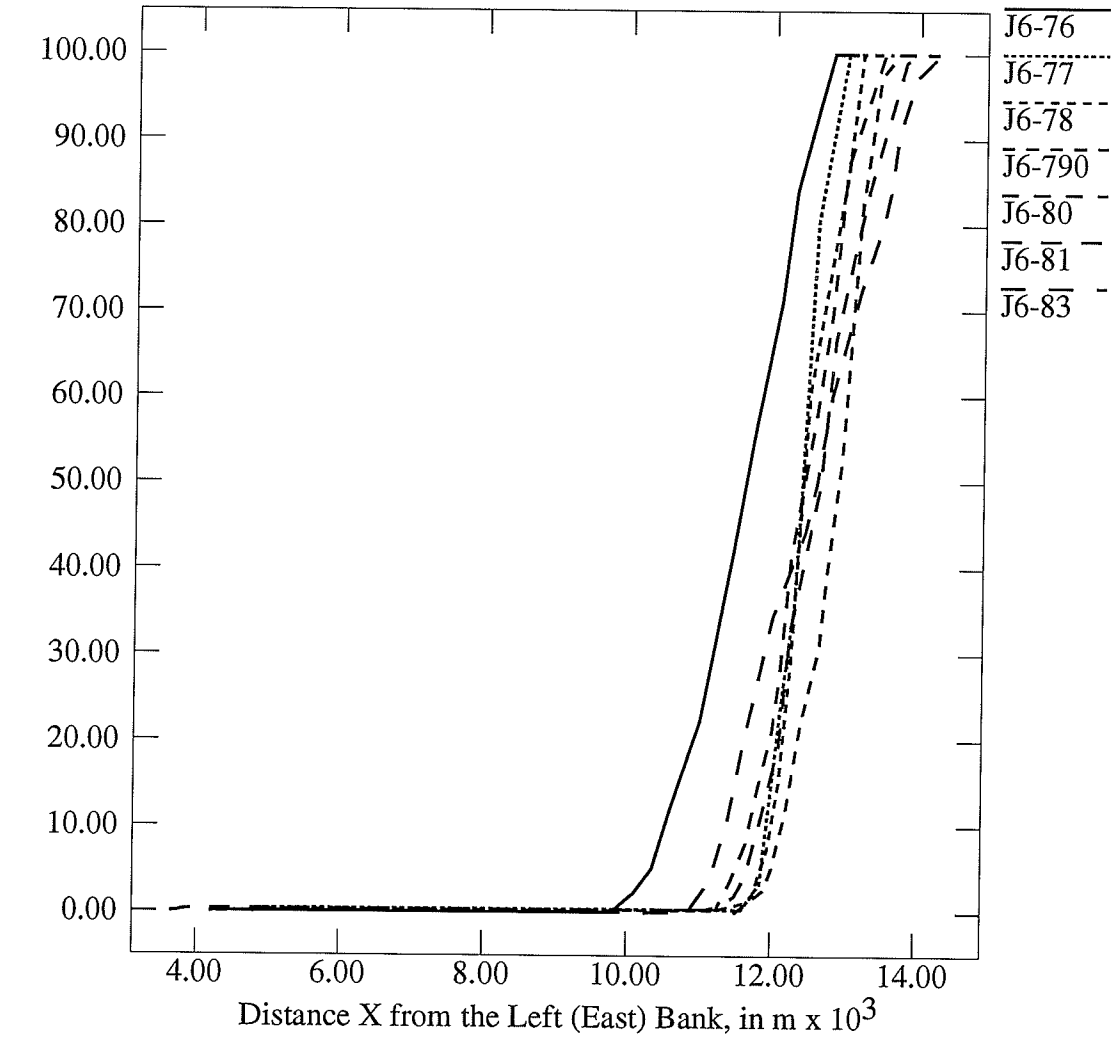

Cumulative of Relative Conveyance Curve of Section J-6A

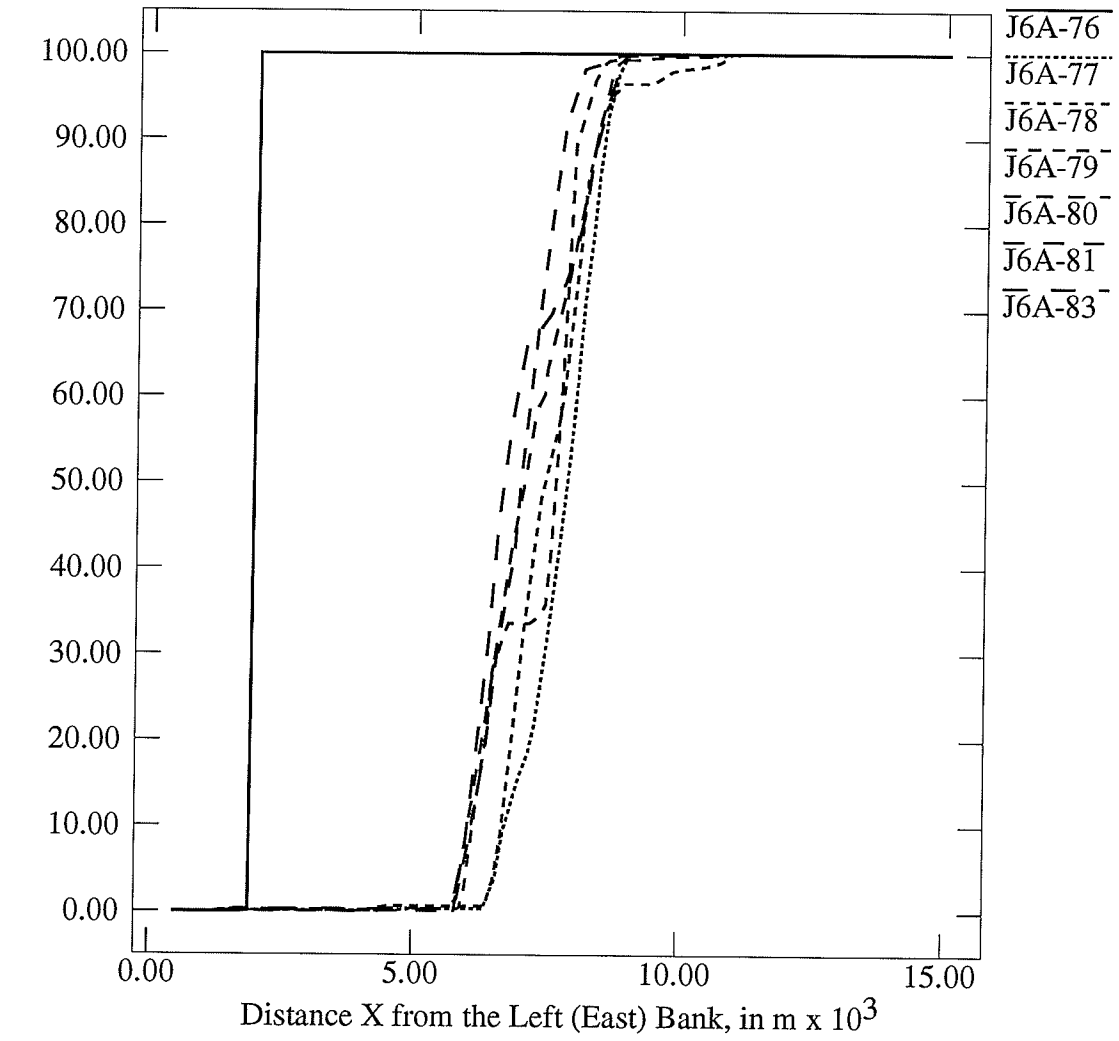

Cumulative of Relative Conveyance Curve of Section J-7

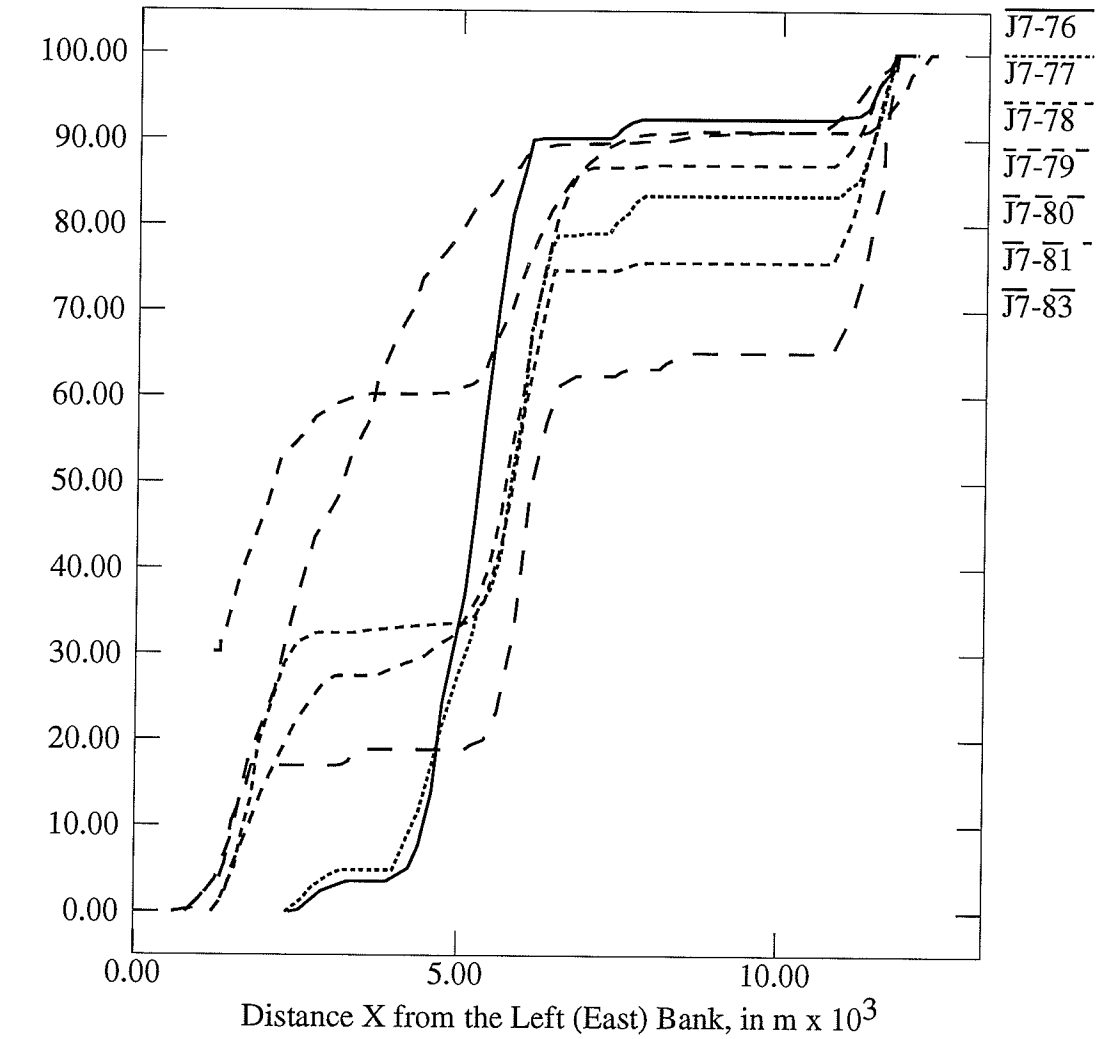

Cumulative of Relative Conveyance Curve of Section J-7A

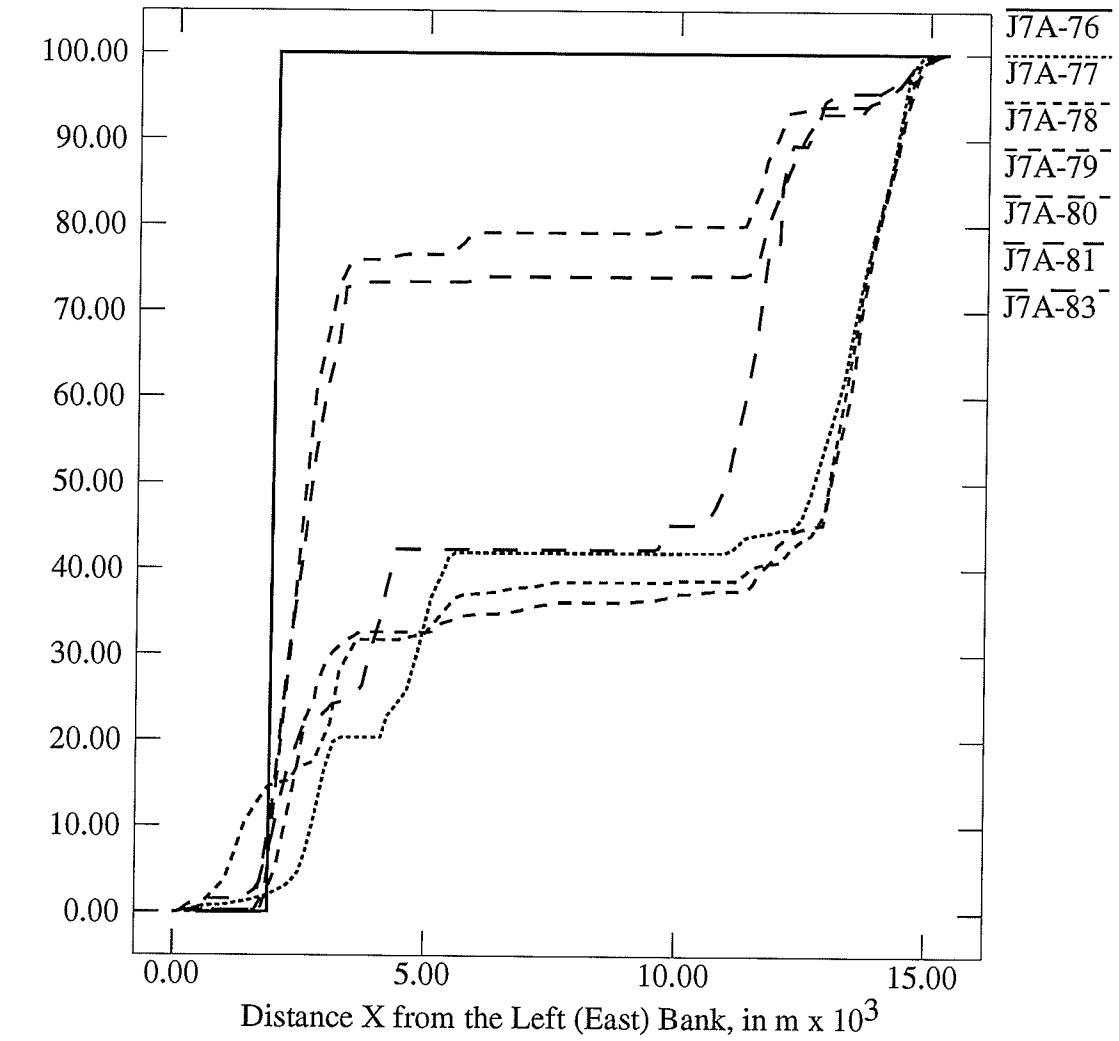

Cumulative of Relative Conveyance Curve of Section J-8

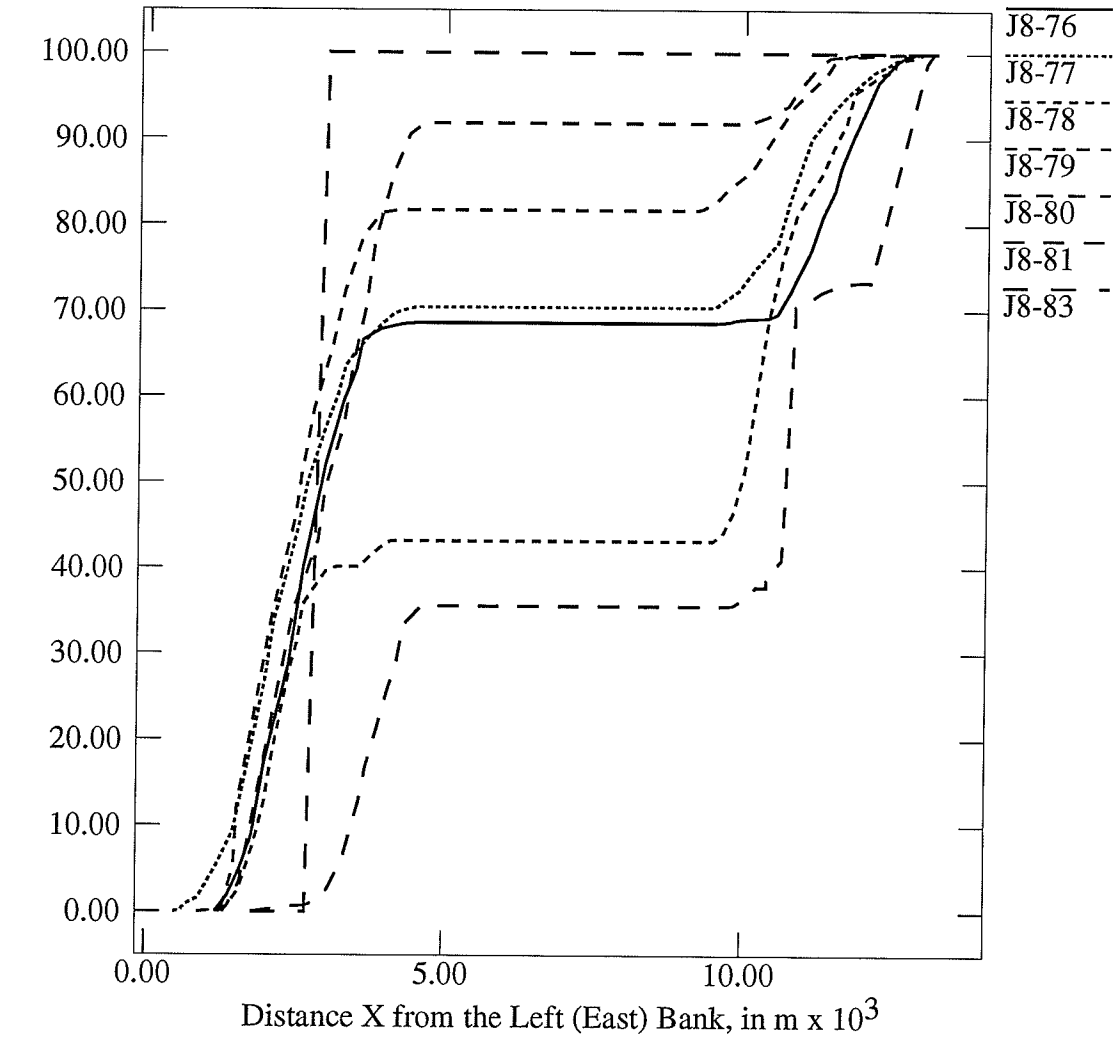

Cumulative of Relative Conveyance Curve of Section J-8A

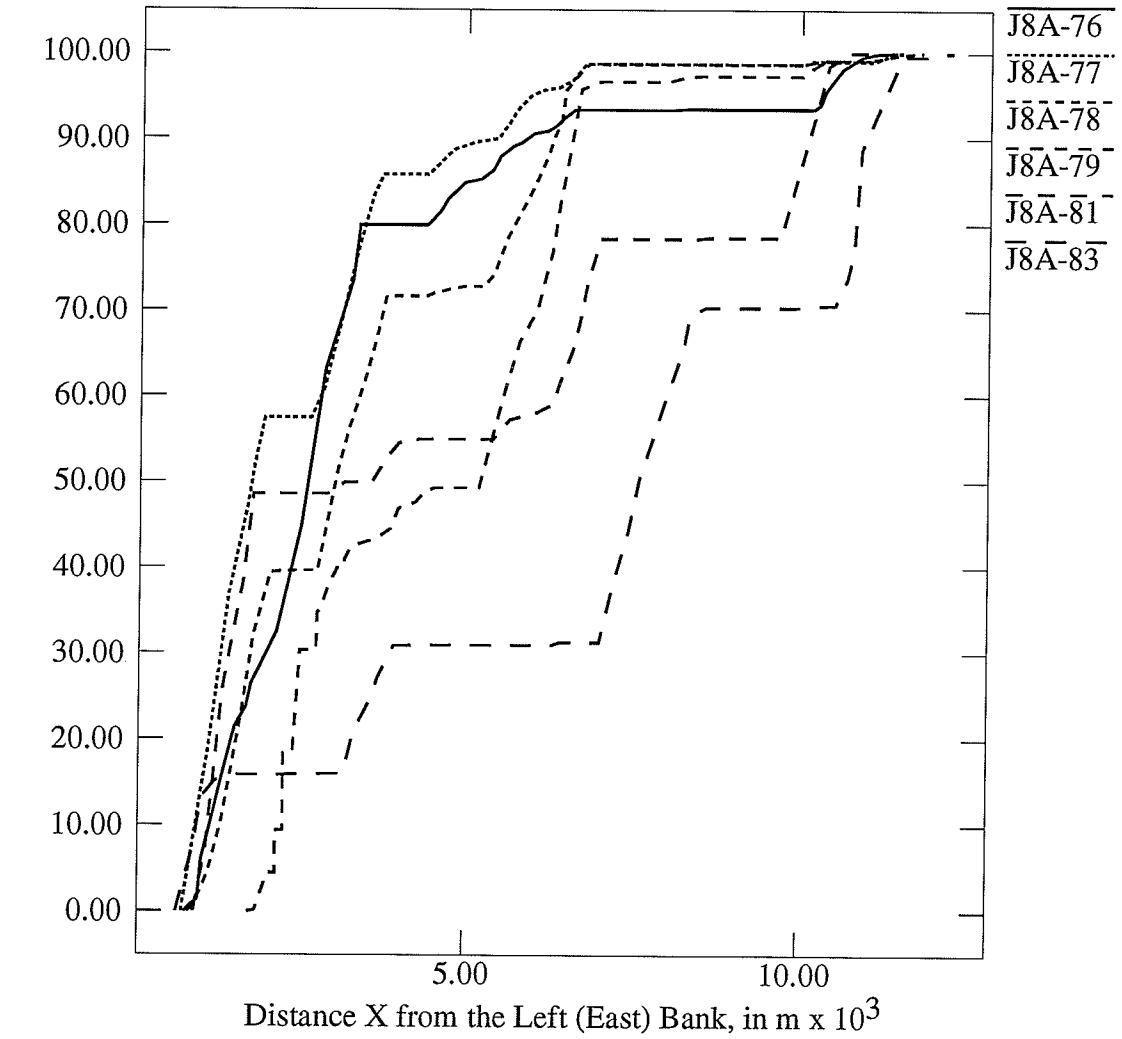

Cumulative of Relative Conveyance Curve of Section J-9

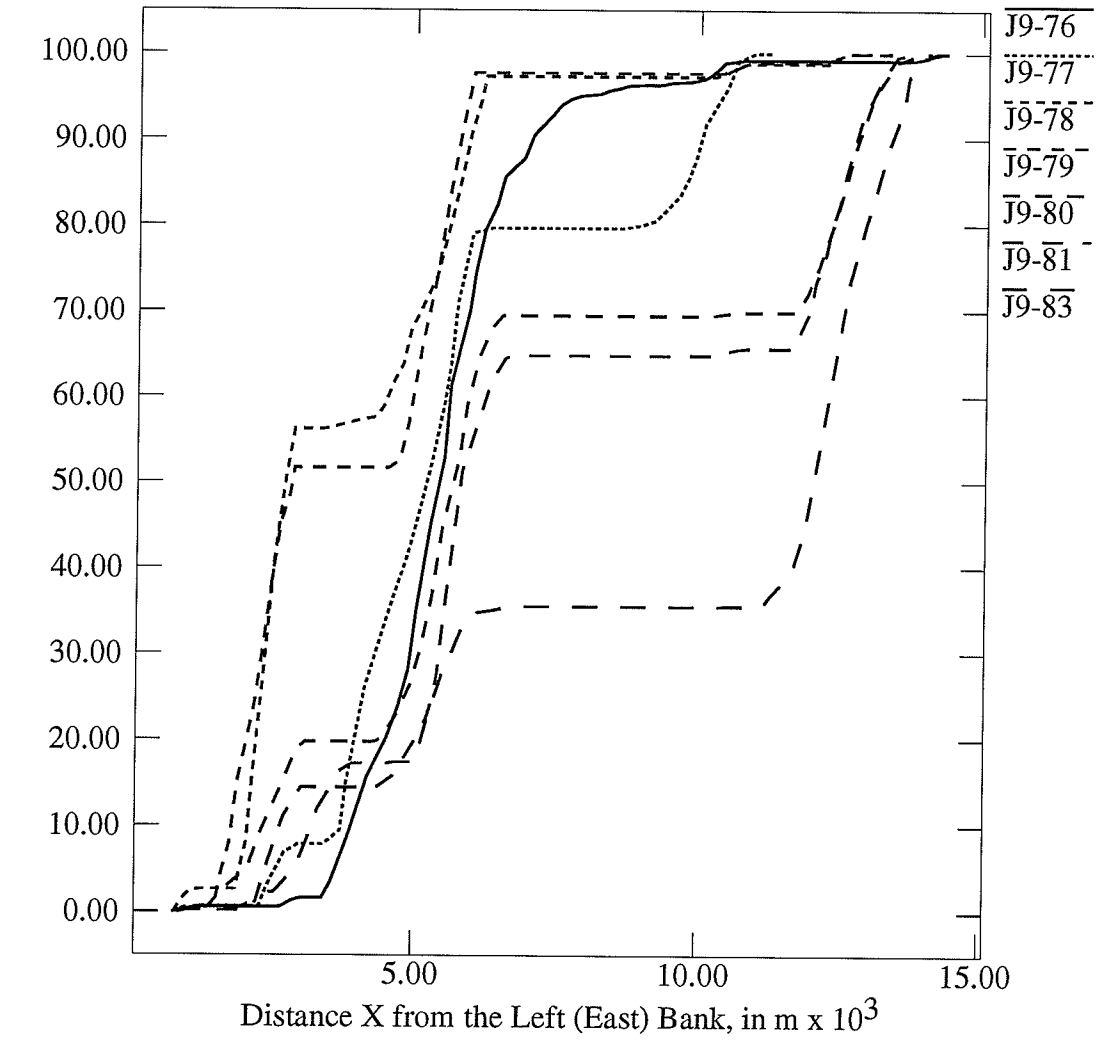

Cumulative of Relative Conveyance Curve of Section J-9A

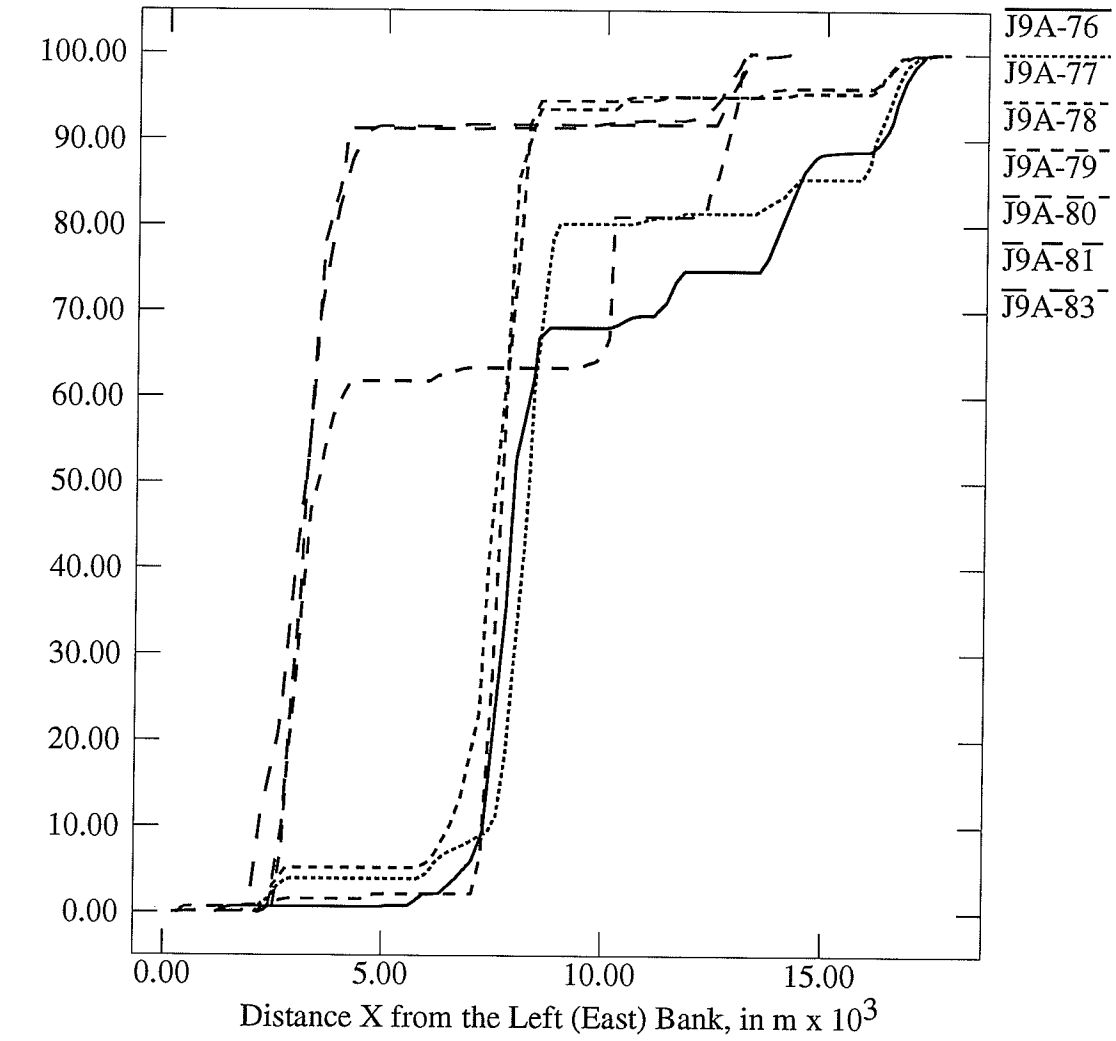

Cumulative of Relative Conveyance Curve of Section J-10

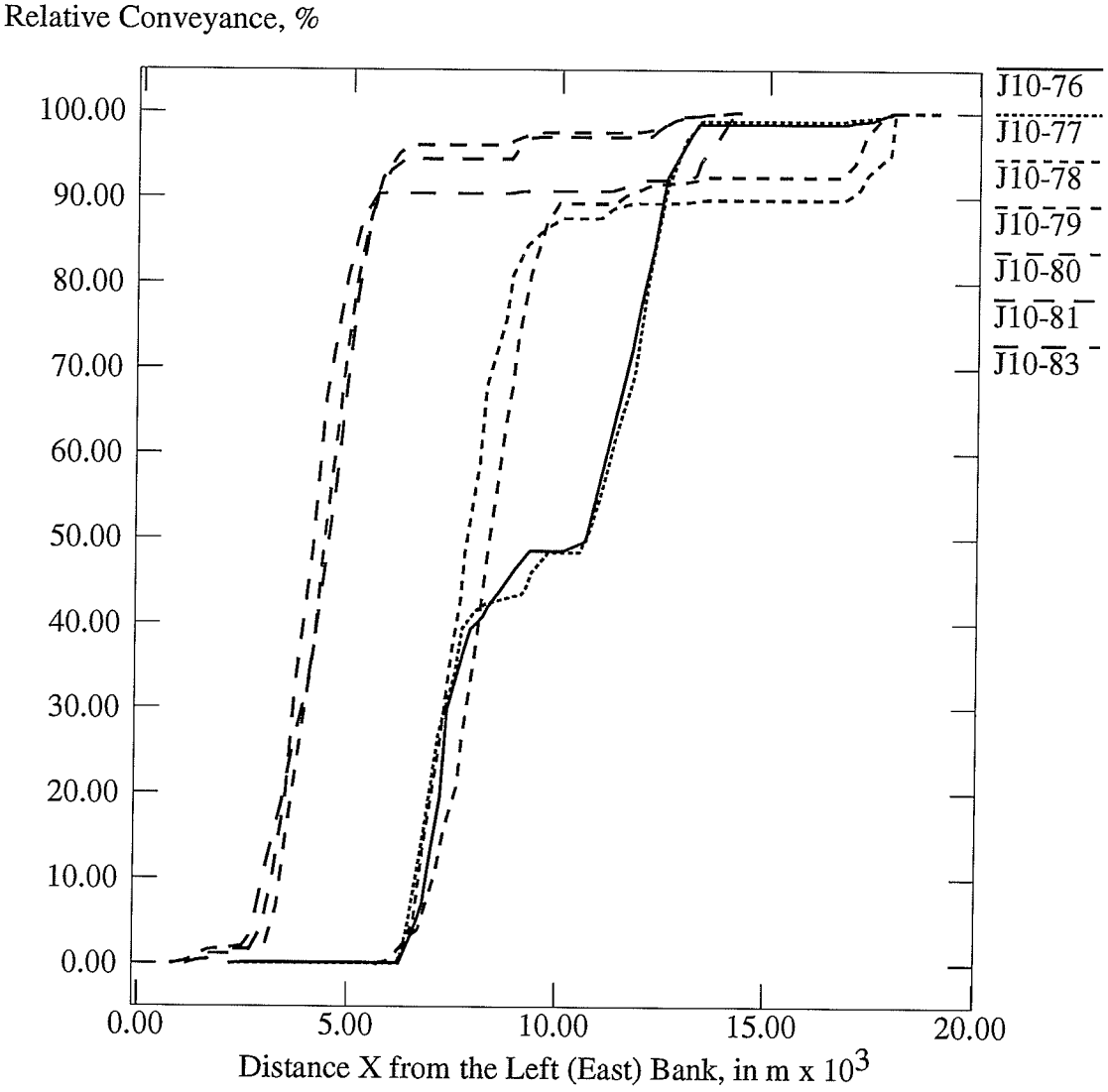

Cumulative of Relative Conveyance Curve of Section J-10A

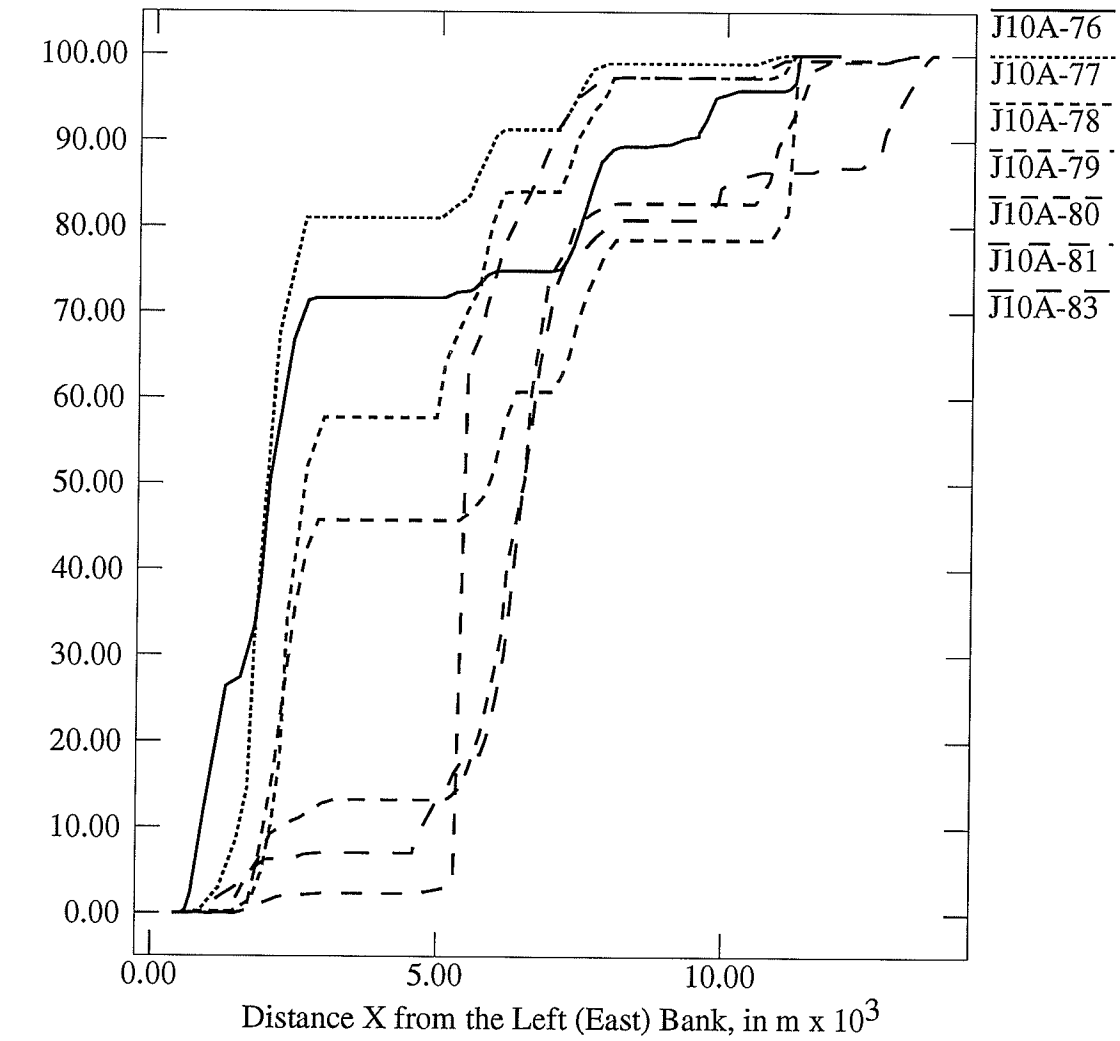

Cumulative of Relative Conveyance Curve of Section J-11

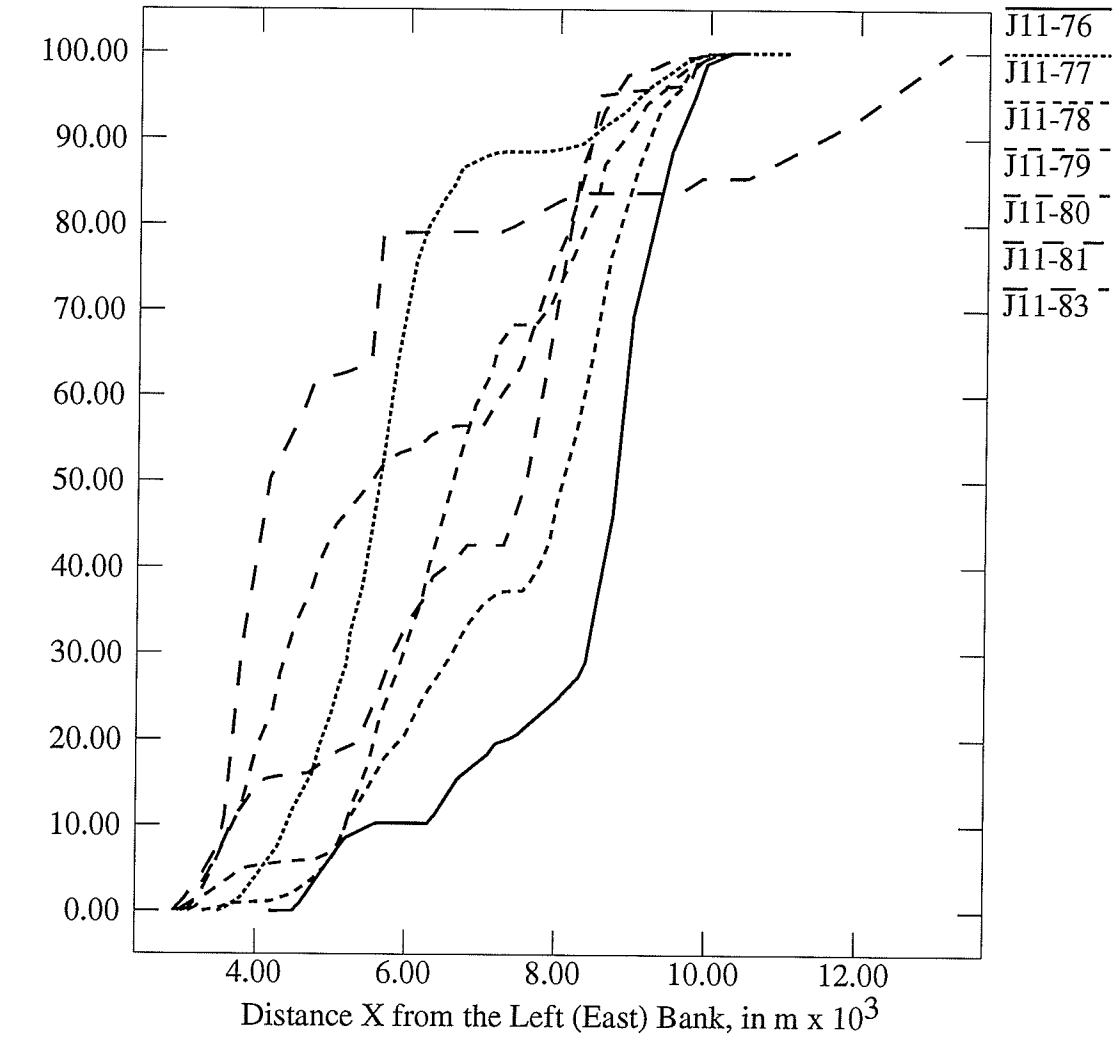

Cumulative of Relative Conveyance Curve of Section J-11A

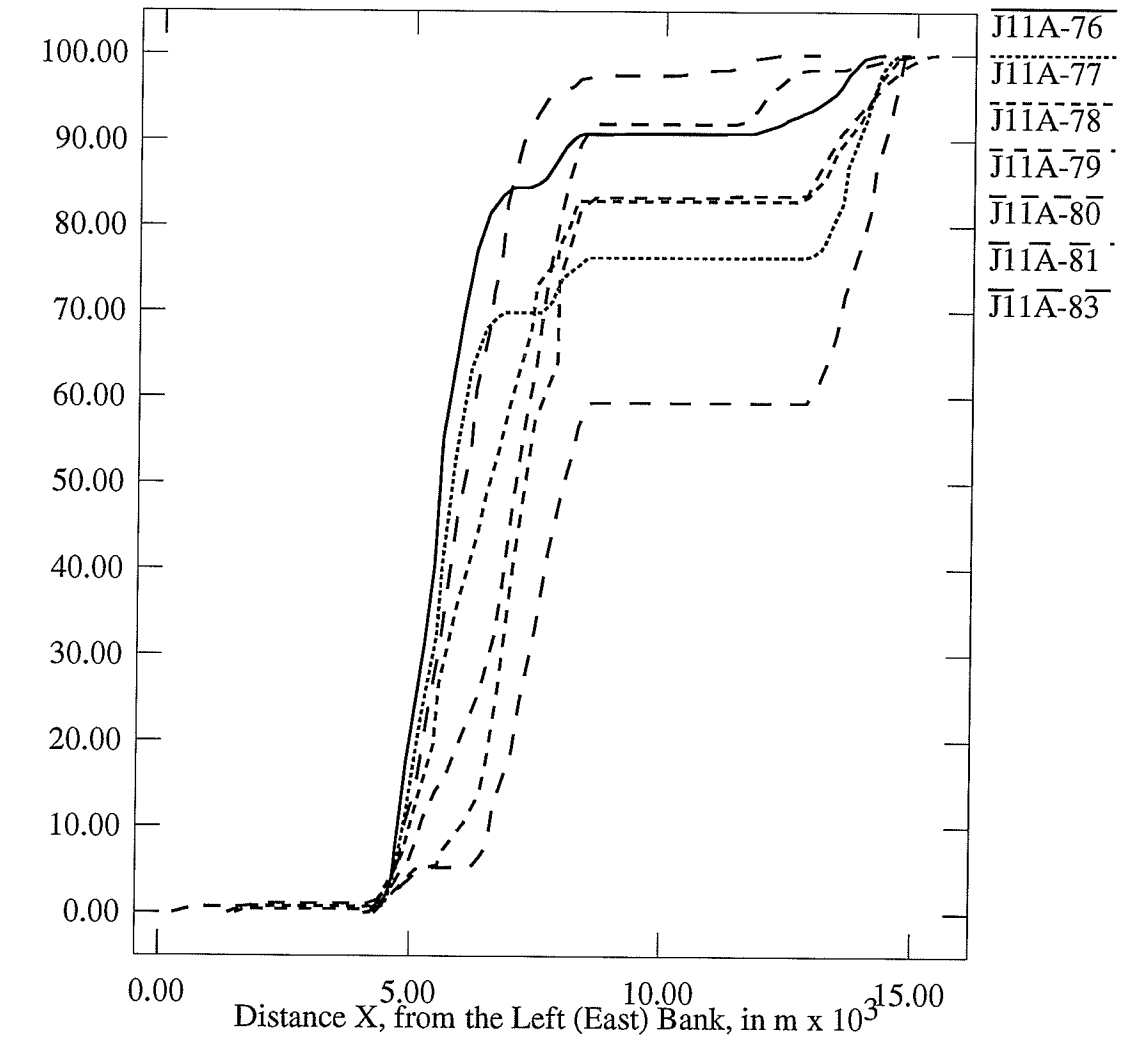

Cumulative of Relative Conveyance Curve of Section J-12

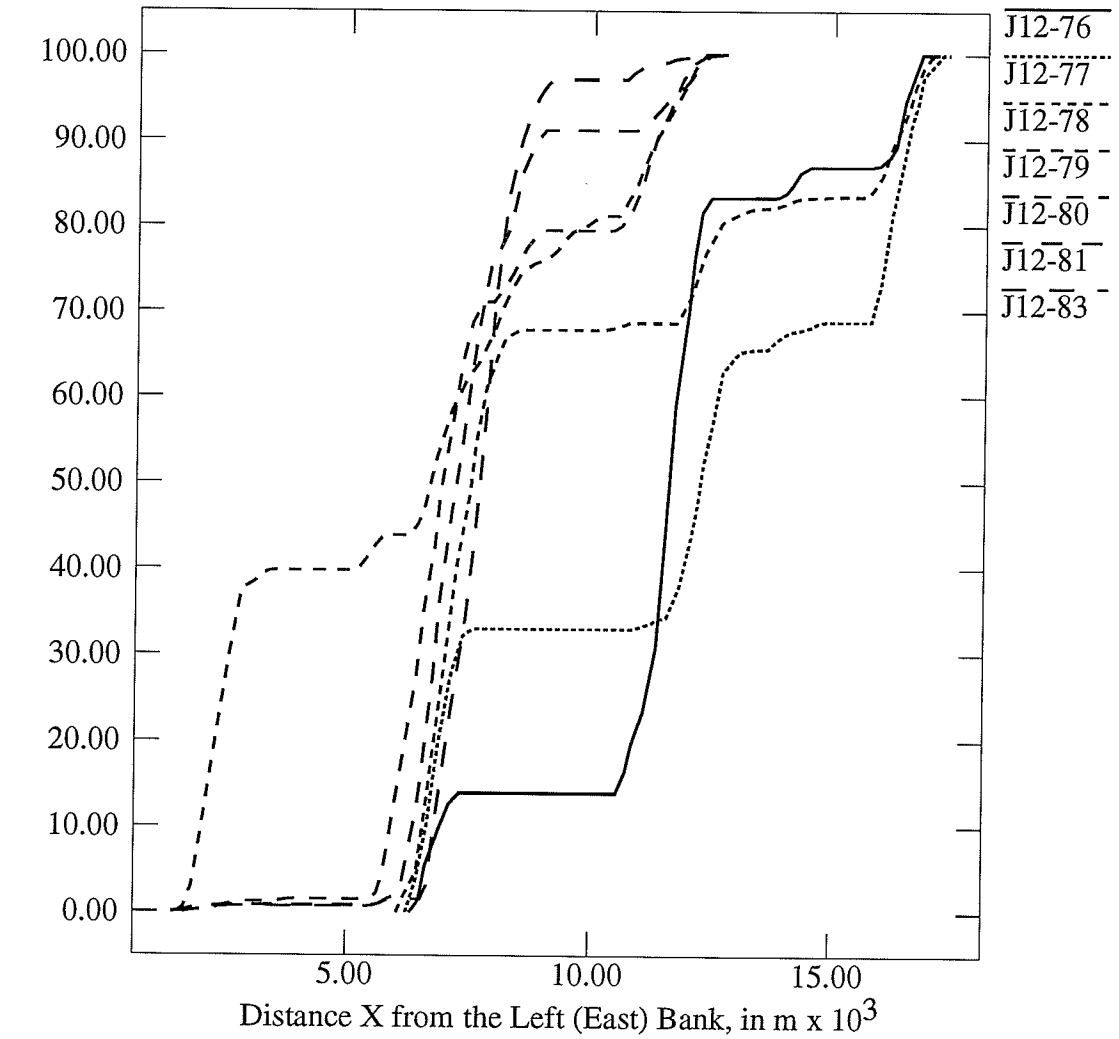

Cumulative of Relative Conveyance Curve of Section J-12A

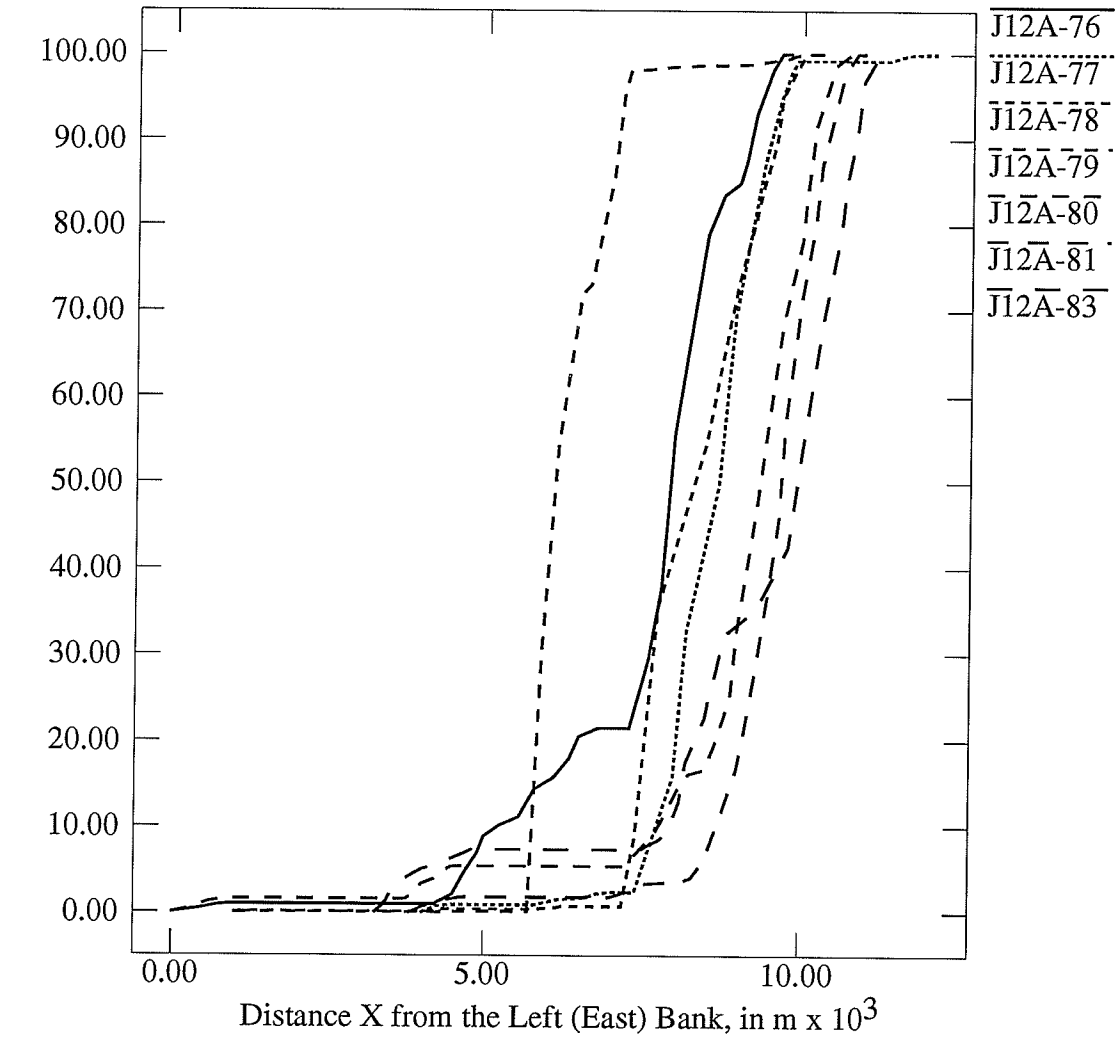

Cumulative of Relative Conveyance Curve of Section J-13

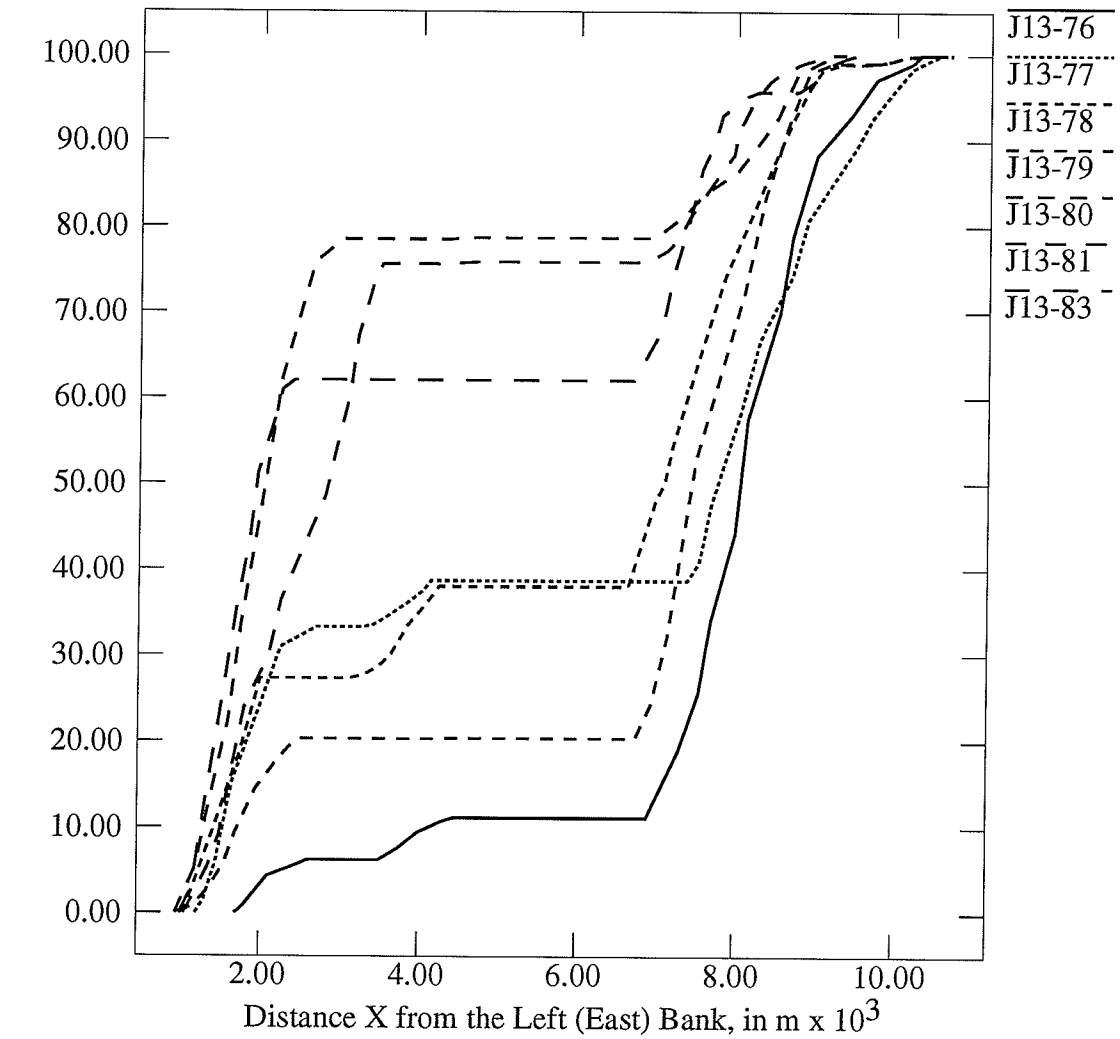

Cumulative of Relative Conveyance Curve of Section J-13A

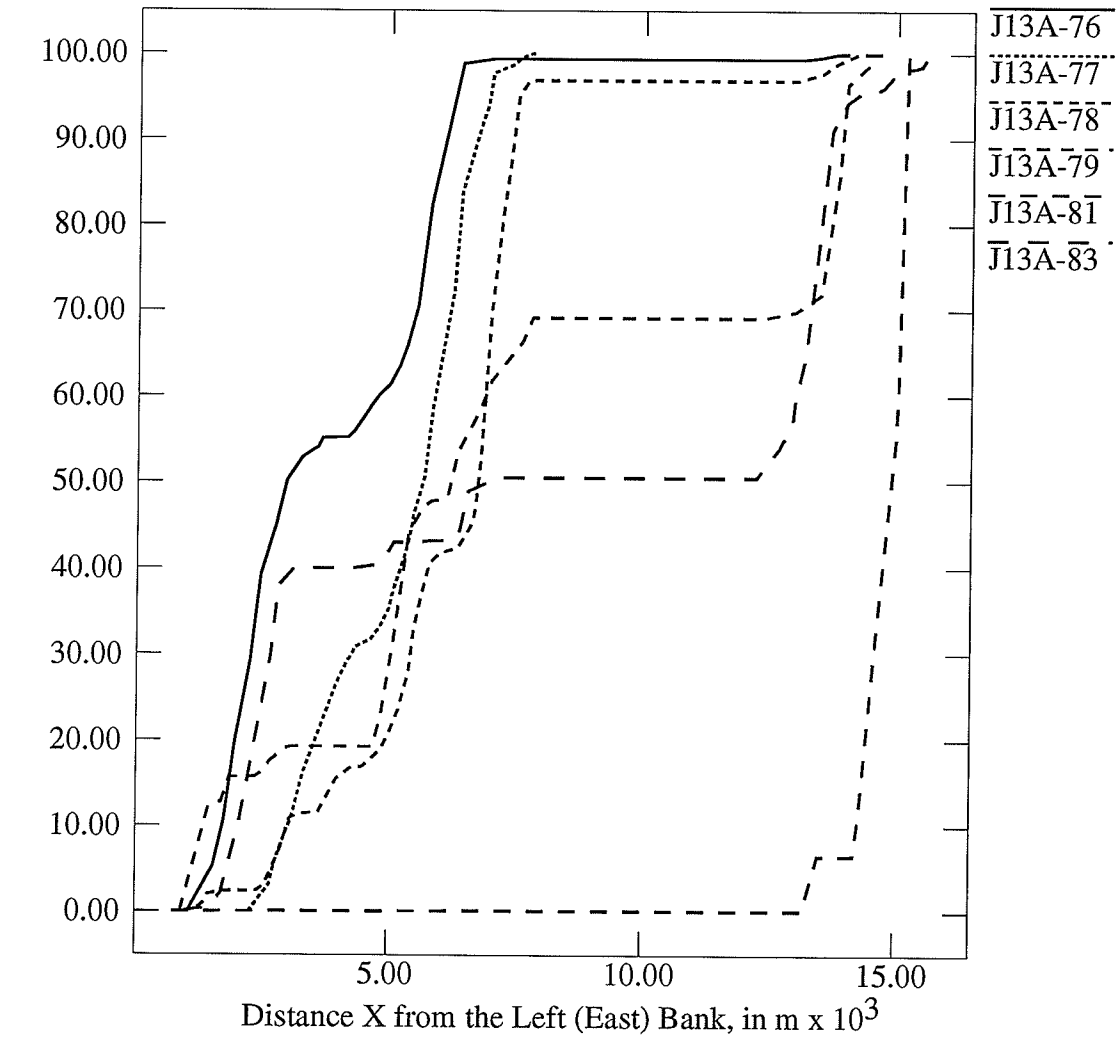

Cumulative of Relative Conveyance Curve of Section J-14

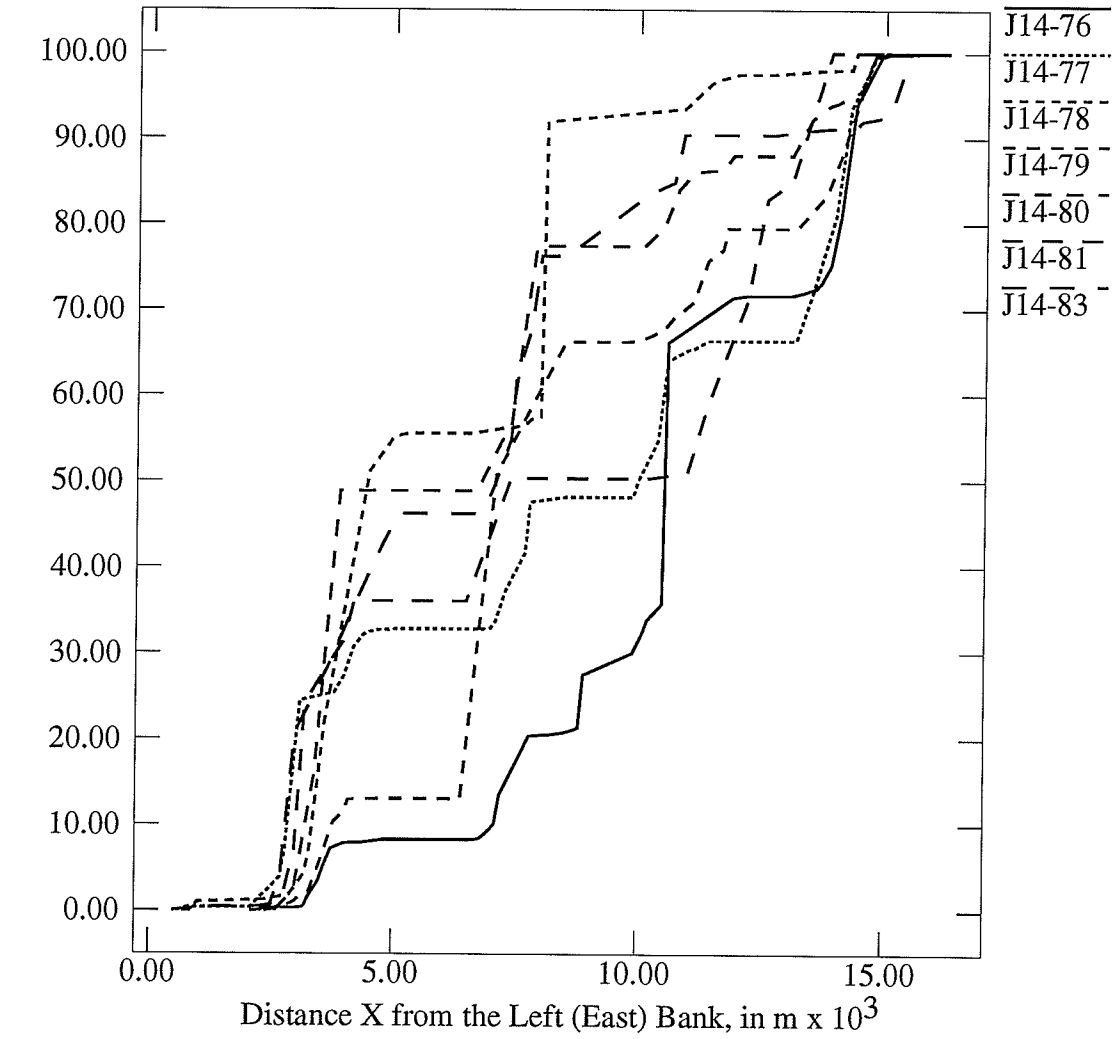

Cumulative of Relative Conveyance Curve of J-14A

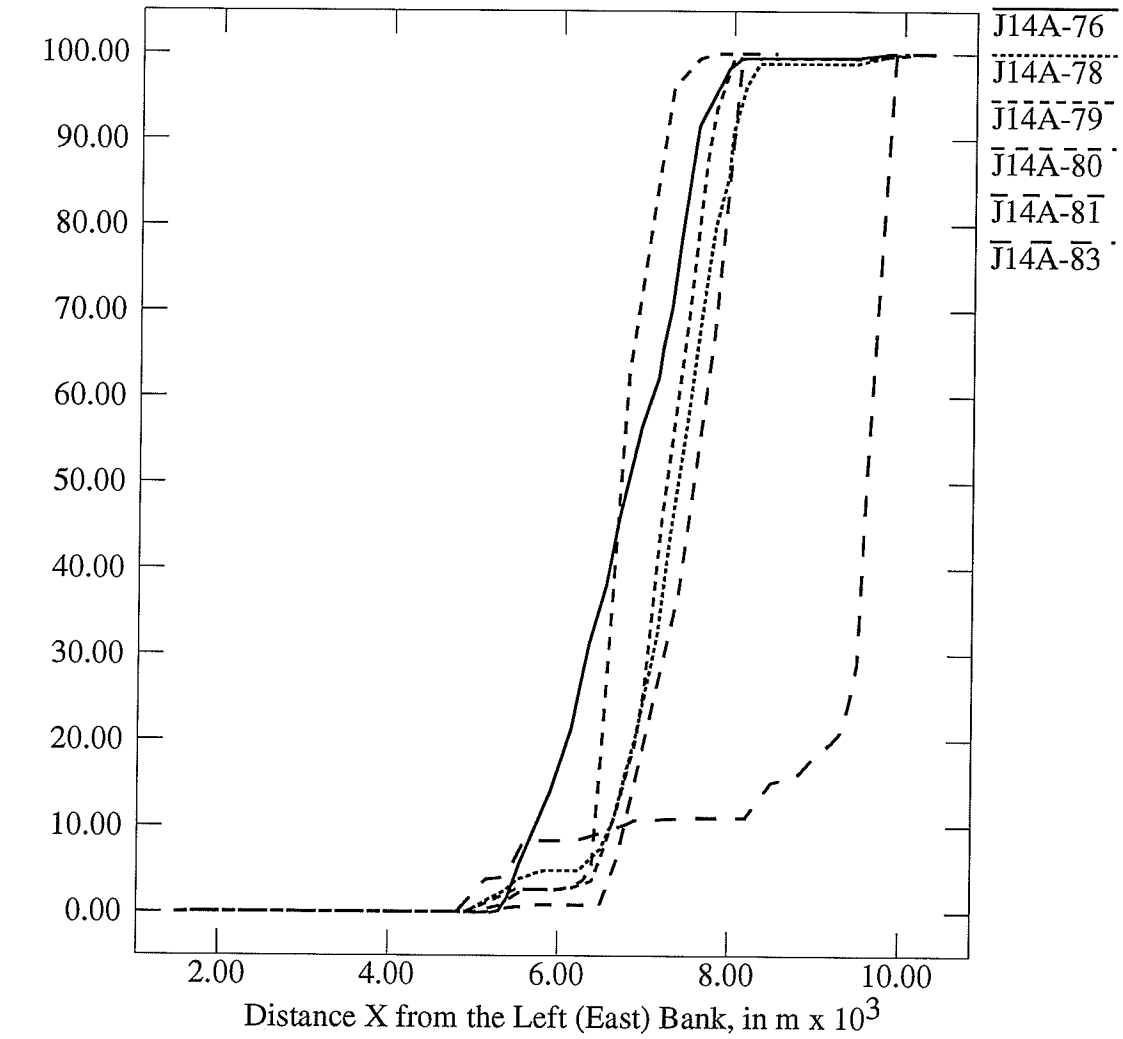

Cumulative of Relative Conveyance Curve of Section J-15

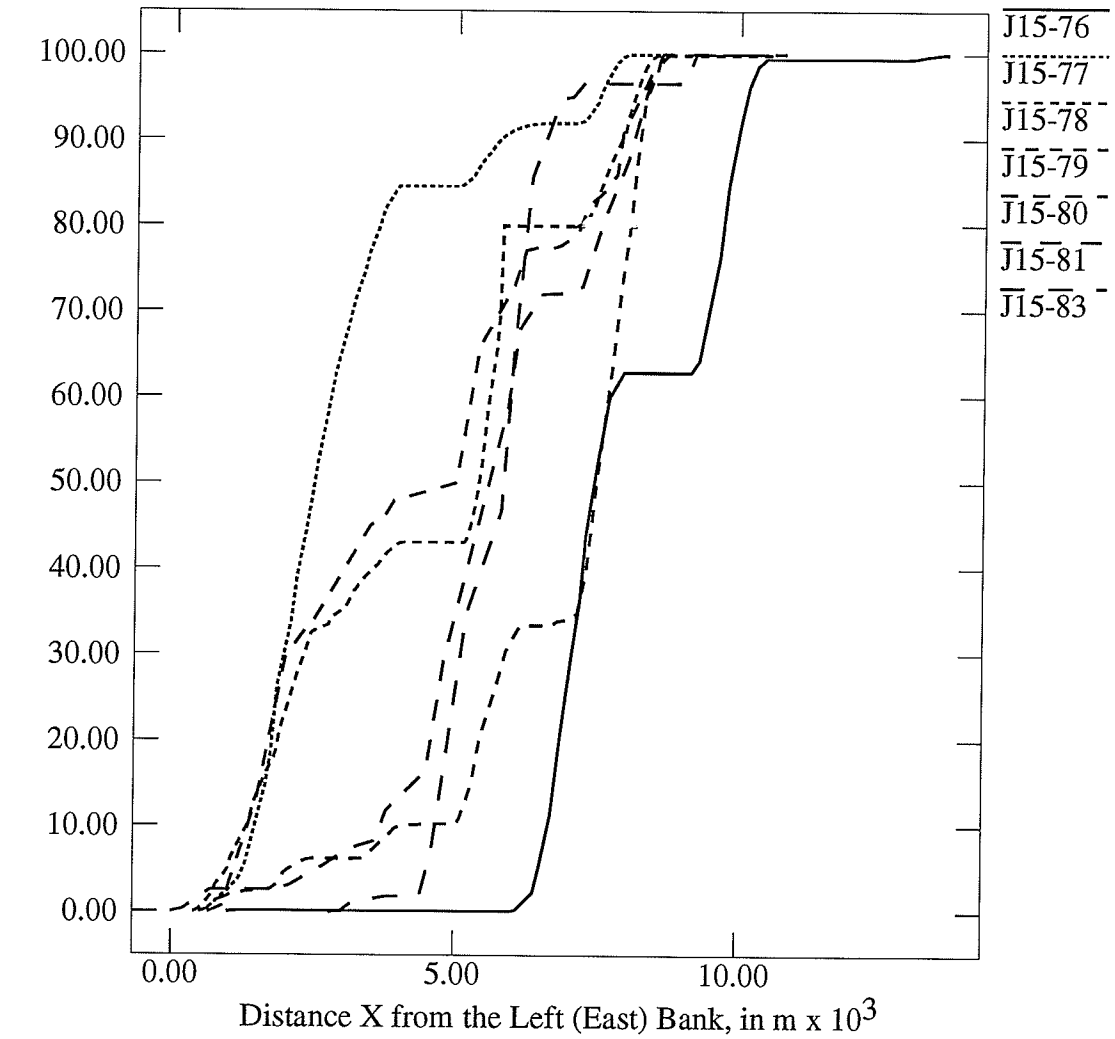

Cumulative of Relative Conveyance Curve of Section J-15A

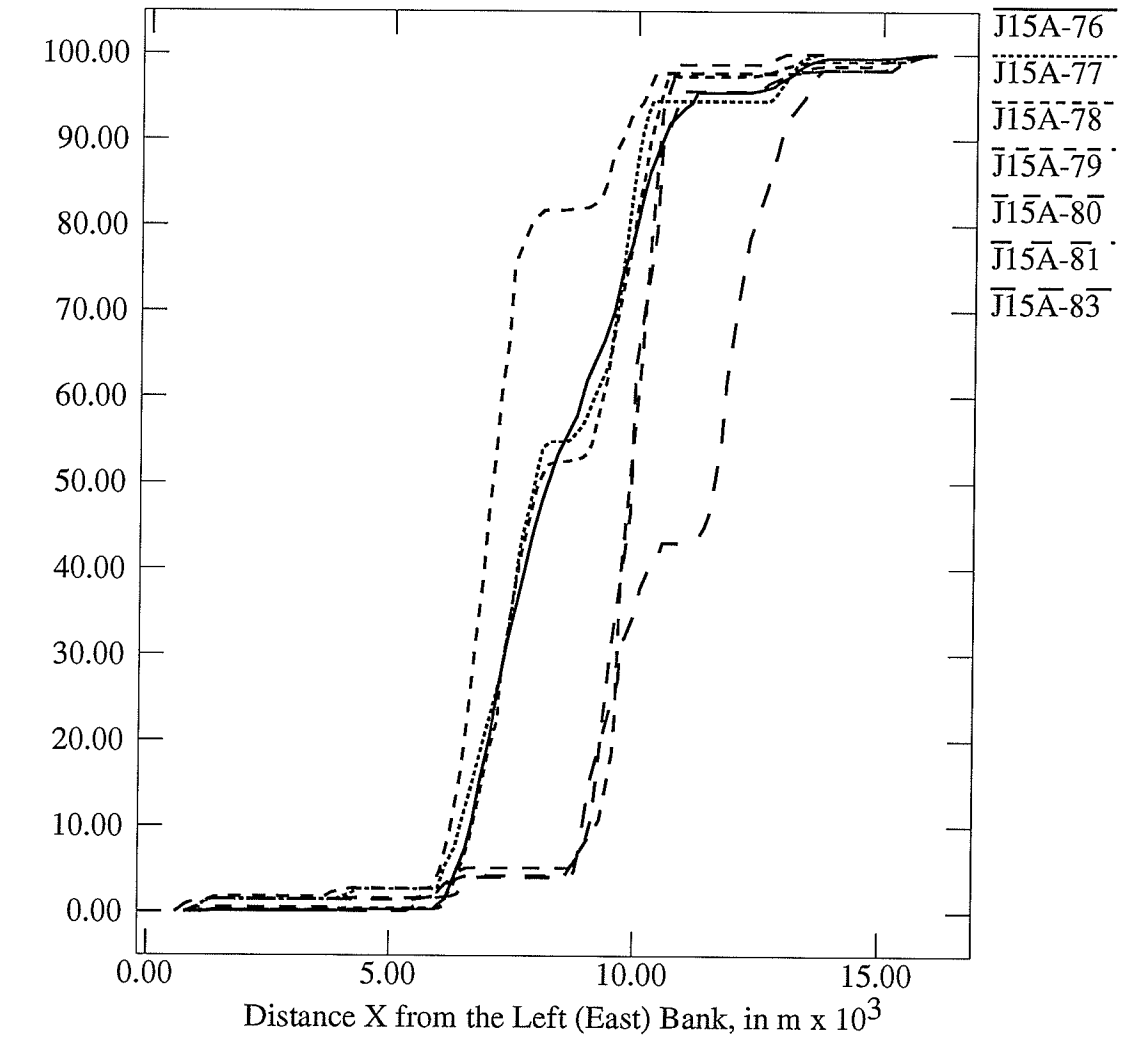

Cumulative of Relative Conveyance Curve of Section J-16

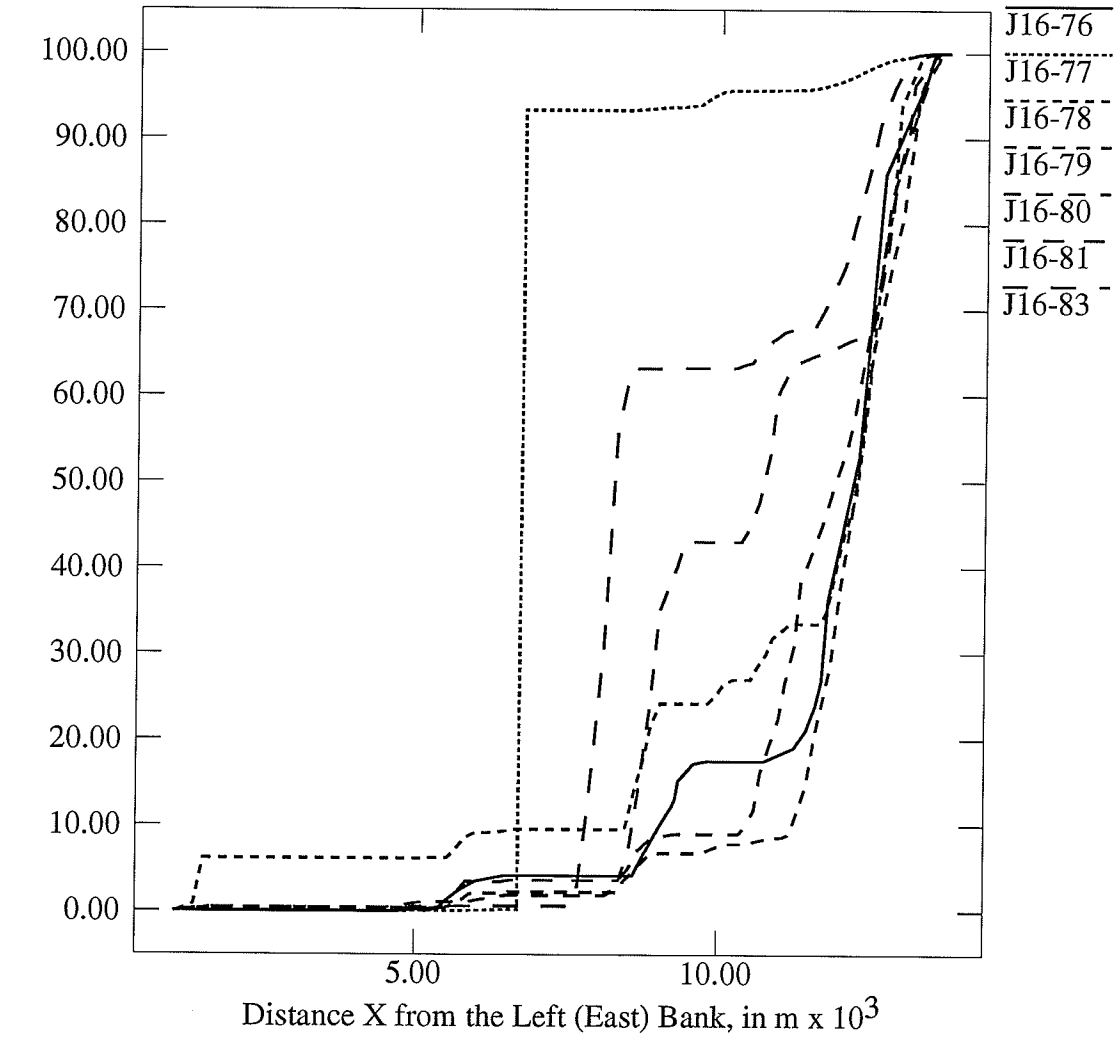

Cumulative of Relative Conveyance Curve of J-16A

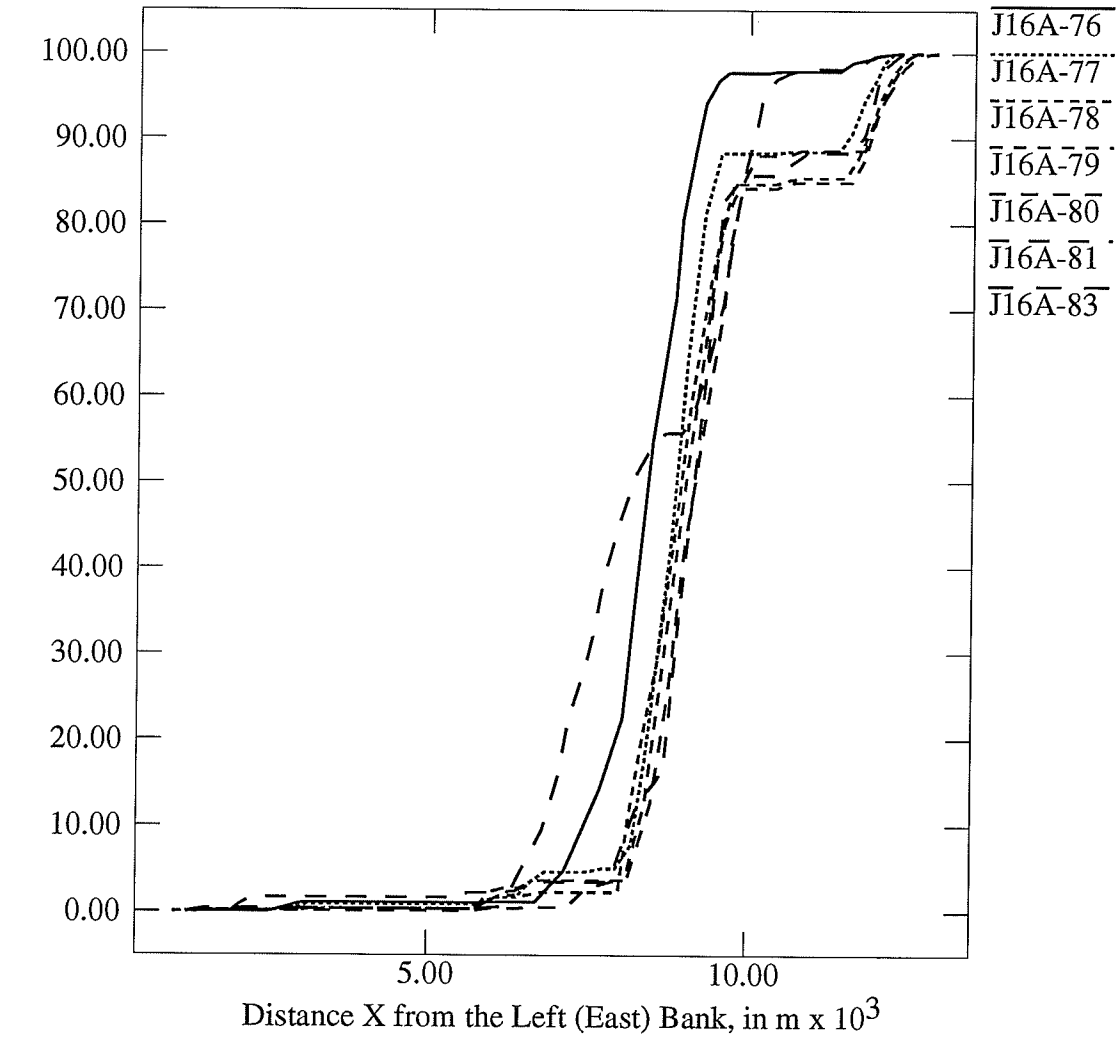

Cumulative of Relative Conveyance Curve of Section J-17